

Summer 5-2014

# NATURAL RADIOACTIVITY IN GROUNDWATER, ROCKS AND SEDIMENTS FROM SOME AREAS IN THE UAE: DISTRIBUTION, SOURCES AND ENVIRONMENTAL IMPACT

Dalal Matar Al Shamsi

Follow this and additional works at: [https://scholarworks.uaeu.ac.ae/all\\_dissertations](https://scholarworks.uaeu.ac.ae/all_dissertations)

Part of the [Geology Commons](#)

---

## Recommended Citation

Al Shamsi, Dalal Matar, "NATURAL RADIOACTIVITY IN GROUNDWATER, ROCKS AND SEDIMENTS FROM SOME AREAS IN THE UAE: DISTRIBUTION, SOURCES AND ENVIRONMENTAL IMPACT" (2014). *Dissertations*. 22.  
[https://scholarworks.uaeu.ac.ae/all\\_dissertations/22](https://scholarworks.uaeu.ac.ae/all_dissertations/22)

This Dissertation is brought to you for free and open access by the Electronic Theses and Dissertations at Scholarworks@UAEU. It has been accepted for inclusion in Dissertations by an authorized administrator of Scholarworks@UAEU. For more information, please contact [fadl.musa@uaeu.ac.ae](mailto:fadl.musa@uaeu.ac.ae).

United Arab Emirates University  
College of Science

**NATURAL RADIOACTIVITY IN GROUNDWATER, ROCKS  
AND SEDIMENTS FROM SOME AREAS IN THE UAE:  
DISTRIBUTION, SOURCES AND ENVIRONMENTAL IMPACT**

Dalal Matar Al Shamsi

This dissertation is submitted in partial fulfillment of the requirements  
for the degree of Doctor of Philosophy

Under the direction of  
Dr. Ahmed Murad

May 2014

## **DECLARATION OF ORIGINAL WORK**

I, Dalal Matar Al Shamsi, the undersigned, a graduate student at the United Arab Emirates University (UAEU) and the author of the dissertation entitled “Natural Radioactivity in Groundwater, Rocks and Sediments from some Areas in the UAE: Distribution, Sources and Environmental Impact”, hereby solemnly declare that this dissertation is an original research work done and prepared by me under the guidance of Dr. Ahmed Murad in the College of Science at UAEU. This work has not previously formed the basis for the award of any academic degree, diploma or similar title at this or any other university. The materials borrowed from other sources and included in my thesis/dissertation have been properly cited and acknowledged.

Student’s Signature:

Date:

Copyright © 2014 by Dalal Matar Al Shamsi  
All Rights Reserved

## SIGNATURE PAGE

Approved by

PhD Examining Committee:

- 1) Advisor (Committee Chair): Ahmed Murad  
Title: Vice Dean, Associate Professor  
Department of Geology  
College of Science  
United Arab Emirates University  
Signature .....Date.....
  
- 2) Member: Mohamed El-Tokhi  
Title: Professor  
Department of Geology  
College of Science  
United Arab Emirates University  
Signature .....Date.....
  
- 3) Member: Sayed Marzouk  
Title: Professor  
Department of Chemistry  
College of Science  
United Arab Emirates University  
Signature .....Date.....
  
- 4) Member (External Examiner): Ihsan Al-Aasm  
Title: Professor  
Department of Earth and Environmental Sciences  
College of Science  
University of Windsor in Canada  
Signature .....Date.....

Accepted by

Dean of the college: Prof. Peter Werner

Signature .....Date.....

Dean of the College of Graduate Studies: Prof. Nagi Wakim

Signature .....Date.....

Copy \_\_\_\_\_ of \_\_\_\_\_

## ABSTRACT

Groundwater contains a certain amount of natural radioactivity that generally results from the decay of uranium, thorium and  $^{40}\text{K}$  isotopes. Knowledge of concentration levels, spatial distribution and sources of these isotopes in groundwater is crucial for environmentally safe and sustainable groundwater resources in the United Arab Emirates (UAE). This dissertation focuses on investigating the distribution, environmental impact and sources of  $^{235}\text{U}$ ,  $^{238}\text{U}$ ,  $^{232}\text{Th}$ , as well as the activity of gross  $\beta$  and  $\alpha$  in groundwater in some locations in the UAE. Additionally, groundwater samples from Oman and selected aquifer rocks and sediments from the UAE were analyzed for comparison. A variety of techniques including liquid scintillation counter, ICP-MS, ICP-OES and ICP-SFMS, were used for the analyses. The results reveal considerable differences in radioactivity in terms of spatial and local variability and show relatively high concentrations of  $^{238}\text{U}$  in some locations. Most of the  $^{238}\text{U}$  concentrations in the groundwater are below the World Health Organization permissible limit for drinking water. The relatively high uranium concentrations in some aquifers suggest a long period of geochemical interactions between rocks, sediments and water as well as possible contribution from fertilizers. In coastal aquifers, however, seawater intrusion is expected to be an additional source of uranium. The  $^{232}\text{Th}$  concentrations were generally comparable and relatively low in all groundwater samples due to the low solubility of thorium in water. Results of the uranium distribution in the rocks and sediments indicate higher concentration in the sediments and further support the possible effect of fertilizers

as an additional source of uranium. The activity of gross  $\beta$  and gross  $\alpha$  were found to exceed the WHO permissible limits for drinking water in 77% and 13% of the groundwater samples, respectively. The most likely reason for this phenomenon is occurrence of  $^{40}\text{K}$ ,  $^{228}\text{Ra}$  and  $^{226}\text{Ra}$  in the aquifer body. The results of groundwater samples from Oman indicate low levels of  $^{235}\text{U}$ ,  $^{238}\text{U}$  and  $^{232}\text{Th}$ , and the activity of  $^{222}\text{Rn}$  and  $^{226}\text{Ra}$  were lower than the WHO permissible limits for drinking water. Dilution of groundwater by relatively high rainfall can be a possible cause of the relatively low activity of the radionuclides in Oman and other regions in the world.

*Keywords:* radioactivity, aquifer, uranium, thorium, arid region, UAE.



## ABSTRACT IN ARABIC

تحتوي المياه الجوفية على بعض النشاط الإشعاعي الناتج عن انحلال النظائر المشعة لعناصر اليورانيوم والثوريوم والبوتاسيوم. إن الدراسة المفصلة لهذه الإشعاعات وخواصها وتوزيعها المكاني ومصادرها تعد ضرورية للمحافظة على استدامة جودة موارد المياه الجوفية في دولة الإمارات العربية المتحدة. تهدف هذه الدراسة إلى استكشاف التوزيع المكاني و التأثير البيئي للنشاط الإشعاعي الطبيعي في المياه الجوفية، و المنبعث تحديداً من نظير اليورانيوم-238، ونظير اليورانيوم-235 ونظير الثوريوم-232، إضافة إلى قياسات انبعاثات إشعاعات ألفا وبيتا في المياه الجوفية في بعض مناطق دولة الإمارات. ولوجودها في نفس المنطقة الجغرافية والظروف المناخية الجافة، تم أخذ عينات مياه جوفية من سلطنة عمان لدراستها ومقارنتها بالمياه الجوفية في الإمارات. كما تم أخذ عينات من صخور أحد الخزانات المائية للمياه الجوفية ودراسة العلاقة بين نسبة العناصر المشعة في مياه الخزان الجوفي وصخوره والتربة الزراعية التي تروى بهذه المياه. استخدمت مجموعة من الأجهزة التحليلية الكتلية في قياسات النشاطات الإشعاعية المتنوعة في المياه الجوفية، كل عنصر حسب ما يتناسب مع خصائصه، للحصول على نتائج دقيقة. أظهرت نتائج التحاليل تراكيز متفاوتة للإشعاع من ناحية التوزيع المكاني، وقد أكدت الدراسة أن أسباب هذه الاختلافات يعود إلى مجموعة من العوامل التالية: الفترة الزمنية الطويلة للتفاعل بين المياه الجوفية و صخور الخزان الجوفي، وارتفاع ملوحة صخور الخزان، وغزو مياه البحر لخزانات المياه الجوفية القريبة من الساحل، إضافة إلى تسرب المكونات الفوسفاتية للأسمدة خلال التربة الزراعية و منها إلى الخزانات الجوفية الضحلة. ويعتبر ما ذكر من أسباب مرتبطاً بنسب اليورانيوم، أما الثوريوم فتراكيزه منخفضة نسبياً في المياه الجوفية بسبب قلة ذوبانه في المياه. وبالمقارنة مع توصيات منظمة الصحة العالمية، وجدنا أن معظم عينات المياه الجوفية تحتوى على تراكيز اليورانيوم والثوريوم أقل من الحد الأعلى المسموح به في مياه الشرب، أما بالنسبة إلى انبعاثات ألفا وبيتا فقد تجاوز عدد كبير منها الحد المسموح به، ونعتقد أن ذلك يعود إلى النظائر المشعة الأخرى التي لم يتم قياسها تفصيلاً مثل الراديوم و الرادون والبوتاسيوم. أما بالنسبة لسلطنة عمان، فجميع عيناتها تحتوى على نشاط إشعاعي أقل بكثير من

الحد الأعلى الذي أقرته منظمة الصحة العالمية في عام 2011، و يعود ذلك إلى زيادة معدل الأمطار السنوي في السلطنة، والذي يقوم بدوره بقليل تراكيز النشاط الإشعاعي في المياه. وقد تم تأكيد هذا الاستنتاج بمقارنة بين مجموعة دول من مناطق مناخية مختلفة حول العالم، حيث تبين أن الدول ذات المناخ المطير تحوي تراكيز أقل من نظائر اليورانيوم المشع في مياهها، باستثناء تلك الدول التي يطغى فيها التكوين الصخري الغني باليورانيوم والفسفات.

*الكلمات المفتاحية: نشاط إشعاعي، خزان جوفي، يورانيوم، ثوريوم، مناطق مناخية جافة، دولة الإمارات العربية المتحدة.*

## ACKNOWLEDGMENTS

I would like to offer my gratitude to my three supervisors Dr. Ahmed Murad, Prof. Ala Aldahan and Prof. Xiaolin Hou for continuous support, advice, patience and guidance.

Professor Ala Aldahan and Dr. Ahmed have given me incredible opportunities for publishing papers, sharing ideas and they have made a great effort toward providing me with self-confidence in the field of scientific research. Difficult times were smoother with Aldahan and Murad's support. They always consider me as a part of research team rather than a young non-experienced student. I appreciate all the uncounted kindness they provided to me. I am indebted to my third supervisor, Prof. Xiaolin Hou, for my experimental work in Denmark. He patiently helped me and explained everything, even the smallest details and always responded with great input to the scientific problems.

I also thank all the people in the Denmark Technical University (DTU) for their support for me in that period. It was an enriching experience in Roskilde.

I am thankful to the Head, faculty members and staff of the Geology Department, for their continuous support during my research period. I thank Dr. Khalid Al Bloushi for his support and wise decisions. Special thanks are extended to Dr. Ayman Elsayi, Dr. Osman Abdelghany and Dr. Saber Hussein for continuous help in many aspects of science and life. My thanks are also for Mr. Omar Albashir, Miss. Aysha Hader, Mrs. Shaheera Bahwan and Mr. Wajeih Kittana, for their unlimited technical help.

This research would not have been possible without the generous funding from the UAEU, which I gratefully appreciate.

## Dedication

*To my parents.*

*To my sister Yusra.*

*To all my teachers from the kindergarten stage in 1988 to PhD level in 2014.*

*To my husband Abdulla and my daughters Haya and Shamma.*

*To Dr. Abdulmajeed AlKhajeh, Assistant Dean for Research in the College of Sciences.*

*To Dr. Rasheed Al Hammadi (Assistant Professor in Biology).*

*To the Academic Advisor in the Advising Unit Mrs. Jawaher Al Shamsi.*

*And beloved supportive friends.*

## Table of Contents

TITLE PAGE.....	i
DECLARATION OF ORIGINAL WORK.....	ii
COPYRIGHT PAGE.....	iii
SIGNATURE PAGE.....	iv
ABSTRACT.....	vi
ABSTRACT IN ARABIC.....	viii
ACKNOWLEDGMENTS.....	x
DEDICATION.....	xi
LIST OF TABLES.....	xv
LIST OF FIGURES.....	xvii
LIST OF ABBREVIATIONS.....	xx
1 INTRODUCTION.....	1
1.1 Background.....	1
1.2 Research Objectives.....	4
1.3 Isotopes in nature.....	5
1.4 Radioactive decay modes.....	7
1.5 Gross beta and alpha activity.....	11
1.6 Uranium isotopes in the environment.....	12
1.6.1 Uranium speciation in water system with respect to pH and redox conditions.....	16
1.7 Thorium isotopes in the environment.....	19
1.8 Natural radium isotopes in the environment.....	21
1.9 Natural radon isotopes.....	22
1.10 Environmental impact of radioactivity.....	25

2 SAMPLING SITES AND ANALYTICAL TECHNIQUES.....	28
2.1 Brief regional geological and hydrogeological settings in the UAE.....	28
2.2 Groundwater sampling wells.....	34
2.3 Rocks and sediments sampling sites.....	41
2.4 Analytical procedures.....	50
2.4.1 Gross alpha and gross beta measurements in groundwater samples.....	50
2.4.2 $^{226}\text{Ra}$ measurements in groundwater samples.....	51
2.4.3 $^{222}\text{Rn}$ measurements in groundwater samples.....	51
2.4.4 $^{235}\text{U}$ , $^{238}\text{U}$ , $^{232}\text{Th}$ and $\text{Cl}^-$ measurements in groundwater samples.....	52
2.4.5 $\text{Na}^+$ and $\text{K}^+$ measurements in groundwater samples.....	54
2.4.6 $^{235}\text{U}$ , $^{238}\text{U}$ and $^{232}\text{Th}$ measurements in rock samples.....	54
2.4.7 $^{235}\text{U}$ , $^{238}\text{U}$ and $^{232}\text{Th}$ measurements in sediment samples.....	55
2.4.8 Major cations measurements in rocks and sediments.....	56
2.5 Statistical analyses and mapping.....	56
3 RESULTS.....	58
3.1 General properties of groundwater.....	58
3.2 $^{235}\text{U}$ and $^{238}\text{U}$ in groundwater.....	65
3.3 $^{232}\text{Th}$ in the groundwater.....	74
3.4 Gross $\beta$ and gross $\alpha$ in groundwater.....	74
3.5 Major element chemistry of rocks and sediments.....	78
3.6 $^{235}\text{U}$ , $^{238}\text{U}$ and $^{232}\text{Th}$ in rocks and sediments.....	81
3.7 Groundwater in Oman.....	87
4 DISCUSSION.....	89
4.1 Uranium and thorium variations in groundwater and environmental impact.....	89

4.2 Groundwater discharge inventory for uranium and thorium.....	107
4.3 Factors affecting the concentrations of $^{235}\text{U}$ , $^{238}\text{U}$ and $^{232}\text{Th}$ in groundwater.....	110
4.4 Groundwater in Oman.....	121
5 CONCLUSIONS AND RECOMMENDATIONS.....	124
5.1 Concluding summary.....	124
5.2 Prospect for future research.....	126
6 REFERENCES.....	127
7 APPENDICES.....	141
Appendix-A.....	141
Appendix-B.....	142
Appendix-C.....	143

## LIST OF TABLES

Table 1.1 Average concentrations of total U and Th in different types of rocks (in parts per million: ppm) (Faure, 1998; Dinh Chau et al., 2011)

Table 1.2 Average concentrations of total U and Th in different types of water (in microgram per gram) (ATSDR, 2014; EPA, 2012; Dinh Chau et al., 2011; HPS, 2011; Martin, 2003; Taylor and McLennan, 1985).

Table 2.1 Visual description of rocks depending on apparent texture and HCl test. Age and formation name: (O. Abdelghany, personal communication, April, 2014; Maurer et al., 2008).

Table 3.1 Location and groundwater data including pH, temperature, TDS, Cl, Na and K.

Table 3.2 Uranium, thorium, gross  $\beta$  and gross  $\alpha$  concentrations in groundwater samples.

Table 3.3 Major elemental composition of rocks and sediments samples.

Table 3.4 Uranium and thorium concentrations in rocks and sediments samples.

Table 3.5 Groundwater properties and radioactivity in Oman. All samples were taken from wells except sample 13.

Table 4.1 Permissible limits for radioactivity level in groundwater recommended by the World Health Organization (WHO) and US Environmental Protection Agency (EPA).

Table 4.2 Comparison of uranium concentration (in  $\text{Bq L}^{-1}$  and in  $\text{ng L}^{-1}$ ), measured in UAE and Oman with those in other regions reported the literatures.

Table 4.3 Comparison of thorium concentration in groundwater measured in this work with those in other regions reported in the literatures.

Table 4.4 Data used to build up Fig. 4.3; countries' abbreviations and radionuclide concentrations.

Table 4.5 Ranges and averages of dose contribution estimated by applying the additive formula on all samples by including  $^{235}\text{U}$ ,  $^{238}\text{U}$  and  $^{232}\text{Th}$  and their permissible limit in equation (1).

Table 4.6 Accumulation of uranium and thorium in soil loaded from groundwater by irrigation in the cases of  $5 \text{ m}^3$  or  $10 \text{ m}^3$  daily irrigation.



Table 4.7 A comparison between the uranium concentrations and average annual rainfall in the study areas and other countries. The rainfall averages in the study areas in the UAE are taken from the website of National Center of Meteorology and Seismology as averages from 2003 to 2011. Rainfall in the other regions obtained from the US National Oceanographic and Atmospheric Agency (NOAA) and World Meteorological Organization (Retrieved in October, 2013).

## LIST OF FIGURES

Fig. 1.1 The  $^{238}\text{U}$  decay chain, including  $\alpha$  and  $\beta$  decays. The decay series ends with the stable isotope  $^{206}\text{Pb}$  (Adamiec & Aitken,1998).

Fig. 1.2 The  $^{235}\text{U}$  decay chain, including  $\alpha$  and  $\beta$  decays. The decay series ends with the stable isotope  $^{207}\text{Pb}$  (Adamiec & Aitken,1998).

Fig. 1.3 Uranium speciation in carbonate solution with respect to Eh and pH (modified after Puigdomenech, 2010): The solid lines symbolize the equilibrium conditions where the activities are equal -for the species on each side of that line-. The dashed green lines show the stability limits of water in the system. The red dashed rectangle represents the general range of the groundwater in the world where the water are of oxidizing conditions and pH ranges between 6 and 9. At oxidizing conditions the Uranyl ion ( $\text{UO}_2^{2+}$ ) and its complexes are formed, and so uranium can migrate long distances from its source (Finch & Murakami, 1999).

Fig. 1.4 The  $^{232}\text{Th}$  decay chain, including  $\alpha$  and  $\beta$  decays. The decay series ends with the stable isotope  $^{208}\text{Pb}$  (Adamiec & Aitken,1998).

Fig. 1.5 Distribution of average natural radiation exposure (modified after WHO, 2011).

Fig. 1.6 Radon (Rn) distribution worldwide in  $\text{Bq/m}^3$  (after Zielinski and Jiang, 2007).

Fig 2.1 Surface geology of the UAE (Modified after the Ministry of Energy, Petroleum and Minerals sector). The sampling sites of this study were added to the map.

Fig. 2.2 Water table map across Abu Dhabi area (after Dawoud, 2008). The sampling sites of this study were added to the map.

Fig 2.3 Groundwater salinity map in the UAE including the distribution in Abu Dhabi area only (after Dawoud, 2008). The sampling sites of this study were added to the map.

Fig 2.4 Groundwater sampling wells sites.

Fig. 2.5 Location map of sampling wells and spring in Oman.

Fig. 2.6 Some of the groundwater in area A-2 is used for recreational activities and landscaping.

Fig. 2.7 Satellite image of Wadi Al Bih (A-4) showing the locations of rocks samples: r-1 to r-30, and sediment/soil samples: F1 to F3. The yellow lines illustrates the roads.

Fig. 2.8 Sampling location of rocks in Jabel Hafit (A-2) along a fault plane.

Plate 2.1 Rocks samples: JH-1 and JH-3 from A-2, and r-4 from A-4.

Plate 2.2 Rocks samples: r-5, r-8 and r-19 from A-4.

Fig. 2.9 The ICP-MS instrument used for uranium and thorium mass concentrations at the Technical University of Denmark (Center for Nuclear Technologies, Risø campus).

Fig. 2.10 The rock sample with no residue (looks like dry salt) after 3 times repetition of HF and HNO<sub>3</sub> addition.

Fig. 3.1 The TDS distribution in the investigated areas.

Fig. 3.2 The distribution of <sup>235</sup>U concentration in groundwater of the investigated areas.

Fig. 3.3 The distribution of <sup>238</sup>U concentration in groundwater of the investigated areas.

Fig. 3.4 The distribution of the <sup>232</sup>Th concentration in groundwater from A-2, A-4 and A-5.

Fig. 3.5 Gross β distribution in the study areas.

Fig. 3.6 Gross α distribution in the study areas.

Fig. 4.1 Correlations between <sup>238</sup>U and TDS in each study area.

Fig. 4.2 Average concentrations of (a) <sup>238</sup>U (b) <sup>232</sup>Th in the different climatic regions, details are in Table 4.2 and Table 4.3 compared with the WHO (2011) permissible limit (dashed line).

Fig. 4.3 The concentration of (a) <sup>238</sup>U and (b) <sup>232</sup>Th in some arid and semi-arid countries compared with WHO (2011) permissible limits (dashed line). The countries abbreviations and <sup>238</sup>U and <sup>232</sup>Th concentrations are illustrated in Table 4.4.

Fig. 4.4 The concentration of uranium in groundwater over the world.

Fig. 4.5 The uranium concentration in groundwater all over the world.

Fig. 4.6 The <sup>232</sup>Th concentration in groundwater in some areas in the world.

Fig. 4.7 Annual rainfall average versus total uranium <sup>T</sup>U (a) in the study areas in the UAE (b) in the study areas in the UAE and other regions mentioned in Table 4.7.

Fig. 4.8 Loading plot of factor analysis using the parameters of uranium in rocks, uranium in water and TDS in water.

Fig. 4.9 Correlation between total uranium and chloride anion among the 30 groundwater samples, showing moderate linear relationship ( $R=0.84$ )

Fig. 4.10 Factor analysis using  $^{235}\text{U}$ ,  $^{238}\text{U}$ , TDS and  $\text{Cl}^-$  as loadings.

Fig. 4.11 The correlation between thorium in rocks and in groundwater versus iron oxides has the values of  $R = 0.85$  and  $0.92$  respectively.

## LIST OF ABBREVIATIONS

A-1	Abu Dhabi-Al Ain road Area.
A-2	Jabel Hafit Area.
A-3	Al Ain-Dubai road Area.
A-4	Wadi Al Bih Area.
A-5	Liwa Oasis Area.
Bq	Becquerel.
Ci	Curie.
EAD	Environment Agency-Abu Dhabi.
EC	Electrical Conductivity.
EPA	Environmental Protection Agency-USA.
ICP-MS	Inductively Coupled Plasma Mass Spectrometry.
ICP-OES	Inductively Coupled Plasma Optical Emission Spectrometry.
ICP-SFMS	Inductively Coupled Plasma Sector Field Mass.
IDC	Individual Dose Criterion.
ISL	In Situ Leaching.
KeV	Kilo electron Volt.
lb	Pound (mass).
LET	Linear Energy Transfer.
LOI	Loss Of Ignition.
LSC	Liquid Scintillation Counter.
MeV	Milli electron Volt.
mSv	milli Sieverts.
R	Pearson correlation coefficient.
Sv	Sieverts.
T <sub>1/2</sub>	Half life time.
TDI	Tolerable Daily Intake.
TDS	Total Dissolved Solids.
Th	Thorium.
<sup>T</sup> U	Total uranium including uranium-235 and uranium-238.
U	Uranium.
UAE	United Arab Emirates.
UTM	Universal Transverse Mercator coordinate system.
WHO	World Health Organization.

# 1 INTRODUCTION

## 1.1 Background

Radionuclides exist everywhere on the Earth's surface and can generally be grouped into four classes according to their origin: primordial radionuclides, cosmogenic radionuclides, natural decay series daughters and anthropogenic radionuclides (Dinh Chau et al., 2011). Primordial radionuclides have existed on earth since its creation during the formation of the Earth and are distinguished by their extreme long half-lives compared to the life of the Earth, such as  $^{40}\text{K}$  ( $T_{1/2} = 1.248 \times 10^9$  years),  $^{232}\text{Th}$  ( $T_{1/2} = 1.405 \times 10^{10}$  years) and  $^{238}\text{U}$  ( $T_{1/2} = 4.468 \times 10^9$  years). Cosmogenic radionuclides are produced by the interaction of cosmic radiation with the Earth's atmosphere and surface. Examples of commonly used cosmogenic radionuclides in chronology are  $^{14}\text{C}$  and  $^{10}\text{Be}$  (Aldahan and Possnert 2003). Natural decay series radionuclides are generated from the continuous decay of primordial radioactive isotopes (e.g.  $^{232}\text{Th}$ ,  $^{235}\text{U}$  and  $^{238}\text{U}$ ). The decay processes comprise nuclear transformation associated with emission of different types of subatomic particles (Faure & Mensing, 2005). The decay of these daughters' nuclides induce more than 80% of the total effective radiation dose to the environment and are a major source of radiation hazards. Some of short lived radionuclides, such as  $^{131}\text{I}$  and  $^{137}\text{Cs}$ , are introduced to the environment through human activities including nuclear weapon testing, accidental releases from nuclear power plants, nuclear fuel reprocessing and many other industrial and medical uses, these radionuclides are called anthropogenic radionuclides whereas the other three origins of radionuclides are natural occurring.

Natural and anthropogenic radionuclides in the environment may enter the human body through inhalation and ingestion (WHO, 2011). It is, therefore, vital to study these radionuclides in each environmental compartment (atmosphere, hydrosphere, lithosphere and biosphere) worldwide and to evaluate the risk hazards on human health. Among the many investigations concerning naturally occurring isotopes, attention has been paid to the isotopes of uranium, thorium, radon and radium because they are most commonly found in the environment. Furthermore, measurements of gross beta and gross alpha activities were commonly implemented as the first screen for assessment of environmental radioactivity.

In many parts of the world, the isotopes of uranium have gained a lot of interest because of the operation of nuclear power reactors. Uranium-235 is commonly used in generating energy in nuclear power plants, which need to be enriched from natural uranium by a process called uranium-235 enrichment. This means increasing the occurrence of  $^{235}\text{U}$  from an abundance of 0.72% to about 5%, and thus the  $^{235}\text{U}$  after this process is called enriched uranium. The remaining uranium contains less  $^{235}\text{U}$  and is called depleted uranium (OECD Nuclear Energy Agency, 2003). Due to its very high density ( $19.1 \text{ g/cm}^3$ ), the depleted uranium could be used as a radiation shield, a counter weight in aircrafts and a stabilizer in some industries. Depleted uranium is less radiation hazardous than that of natural uranium because it is less radioactive due to its lower content of both  $^{235}\text{U}$  and  $^{234}\text{U}$ .

The most common occurrence of natural uranium is in the lithosphere in different minerals of rocks which are mined (uranium ores) for the separation of uranium. In 2009, uranium ore production across the world was about 50,572 tones (World Nuclear Association, 2014). Uranium ore exists in different forms: vein type in hydrothermal precipitations, igneous intrusions, phosphate deposits (Dahlkamp, 1993), unconformity-related deposits, hematite breccia complex deposits, sandstone deposits, surficial deposits, volcanic and caldera-related deposits, metasomatite deposits, collapse breccia pipe deposits, metamorphic deposits, lignite deposits, black shale deposits and quartz-pebble conglomerate deposits (World Nuclear Association, 2010). Uranium is extracted from ore by different processes; the most popular one is *in situ* leaching (ISL) which stands for 45% of uranium yearly extraction (World Nuclear Association, 2014). This method depends on using chemical solutions to dissolve the uranium and recover it while the ore is in its original position in the ground and thus is environmentally highly hazardous.

The natural leaching of uranium, thorium and their decay products from rocks can transfer the elements into water systems and also occur as weathered rock particles in soil, sediments and dust. Plants and animals may uptake these elements into their bodies and thereby the isotopes constitute a source of environmental hazard when exceeding particular levels. As the subject of radioactivity and radionuclides distribution in the UAE has not yet been well investigated, the dissertation work presented here considers some aspects of this issue as described below.



## 1.2 Research objectives

This study aims at establishing data about the distribution of  $^{232}\text{Th}$ ,  $^{235}\text{U}$  and  $^{238}\text{U}$  as well as gross beta and gross alpha in groundwater in the UAE. Furthermore, selected rocks, sediments and soil samples will be analyzed for the content of uranium and thorium isotopes. Analyses of groundwater from Oman will be also conducted with measurements of  $^{222}\text{Rn}$  and  $^{226}\text{Ra}$  in addition to uranium and thorium isotopes.

All these data shall be used to achieve the following objectives:

- 1) Contribute to the UAE radioactivity baseline data which are absent in groundwater, rocks and soil. Hence, the radioactivity level in the environment could be monitored in the future, particularly after the opening of the Barakah nuclear power plant in western UAE.
- 2) Provide the first spatial distribution of natural radioactivity in groundwater of the UAE as well as some data in Oman as a comparison. This will lead to know more about the rock-water interaction between the recharge area in Oman Mountains and discharge in the UAE aquifers.
- 3) Identify levels of groundwater radioactivity with respect to international standards in drinking water and possible environmental impact and contamination risk upon agricultural and domestic use.
- 4) Explore the levels of natural radioactivity in some soils, sediments and rocks and possible impact on groundwater radioactivity.

- 5) Recognize factors controlling the spatial distribution of radioactivity in the UAE groundwater and specify the main natural and anthropogenic sources.

Before describing details of the dissertation work, a summary of natural radioactivity and radioactive isotopes distribution in the environment is given below.

### 1.3 Isotopes in nature

Isotopes of elements have the same number of protons but different number of neutrons and hence a different number of atomic masses.

Isotopes might be stable or unstable, i.e. radioactive. Some of these stable isotopes are the end products of the decay series, for instance,  $^{206}\text{Pb}$  is a stable isotope and the end product of the  $^{238}\text{U}$  decay series and the stable isotope  $^{208}\text{Pb}$  is the end product of the  $^{232}\text{Th}$  decay series. Similarly,  $^{40}\text{K}$  decays to the stable isotopes of the  $^{40}\text{Ca}$  and  $^{40}\text{Ar}$  by beta and electron capture decay, respectively. Radioactive isotopes decay to its daughter products by emitting radiation until reaching a stable isotope. Natural occurring isotopes are the radionuclides occurring naturally in the environment rather than being a product of human activities. Some of the well-known radioactive isotopes in the environment are:  $^{234}\text{U}$  ( $T_{1/2} = 2.45 \times 10^5$  years),  $^{235}\text{U}$  ( $T_{1/2} = 7.04 \times 10^8$  years),  $^{238}\text{U}$  ( $T_{1/2} = 4.468 \times 10^9$  years),  $^{232}\text{Th}$  ( $T_{1/2} = 1.405 \times 10^{10}$  years),  $^3\text{H}$  ( $T_{1/2} = 12.32$  years),  $^{14}\text{C}$  ( $T_{1/2} = 5700$  years),  $^{40}\text{K}$  ( $T_{1/2} = 1.248 \times 10^9$  years),  $^{210}\text{Pb}$  ( $T_{1/2} = 22.23$  years),  $^{210}\text{Po}$  ( $T_{1/2} = 138.376$  days),  $^{226}\text{Ra}$  ( $T_{1/2} = 1600$  years),  $^{228}\text{Ra}$  ( $T_{1/2} = 5.75$  years),  $^{222}\text{Rn}$

( $T_{1/2} = 3.823$  days). The half-life ( $T_{1/2}$ ) is a specific feature of a radionuclide meaning the time the radionuclide decays to the half of its initial value. The initial value is the radionuclide concentration when it was first produced (formed) or captured in a isolated system, for example the radioactive isotopes of an igneous rock, are at their initial concentration when the lava starts to flow, while the initial concentrations in the metamorphic rocks exist at the metamorphosing moment and then starts to decay. The decay rate decides the emission rate of certain particles and associated radiation from the nucleus, and is expressed as radionuclide activity. The radionuclide activity could be measured as Bq (Becquerel) or Ci (Curie) and  $1 \text{ Ci} = 3.7 \times 10^{10} \text{ Bq}$ . The shorter half-life a radionuclide has, the high specific activity it is and so the more radioactivity it emits per unite mass of the radionuclide.

Referring to the wide abundance of radionuclides in nature, their mass concentration calculation has been of great interest to the geochemists. Therefore, many studies have been conducted to perform these calculations in different types of rocks and water (Tables 1.1 and 1.2).

Table 1.1 Average concentrations of total U and Th in different types of rocks (in parts per million: ppm) (Faure, 1998; Dinh Chau et al., 2011)

Rock type	Th	U
<b>Ultrabasic (ultramafic)</b>	$4.5 \times 10^{-3}$	$(2.0 - 3.0) \times 10^{-3}$
<b>Basalt</b>	2.2 - 3.5	0.6 - 0.7
<b>High-Ca granites</b>	8.5	3.0
<b>Low-Ca granites</b>	17.0	3.0
<b>Shale</b>	12.0	3.7
<b>Sandstone</b>	1.7	0.5 - 5.1
<b>Carbonate rocks</b>	1.7	2.2
<b>Deep sea clay</b>	7.0	1.3

Table 1.2 Average concentrations of total U and Th in different types of water (in microgram per gram) (ATSDR, 2014; EPA, 2012; Dinh Chau et al., 2011; HPS, 2011; Martin, 2003; Taylor and McLennan, 1985).

Water type	Th	U
<b>Stream water</b>	$<10^{-4}$	$4.0 \times 10^{-5}$
<b>Seawater</b>	$6.0 \times 10^{-8}$	$3.1 \times 10^{-3}$
<b>Groundwater</b>	$<4.0 \times 10^{-4}$	$3.0 \times 10^{-3}$
<b>Precipitation</b>	$<0.5 \times 10^{-4}$	$<8.0 \times 10^{-4}$

#### 1.4 Radioactive decay modes

Decay of a radioactive isotope is defined as the natural disintegration of a radionuclide associated with the emission of ionizing radiation in the form of alpha and/or beta particles and/or gamma rays (Hanks et al., 2003). The decay

mode is distinguished through the emitted radiation. Alpha decay mode ( $\alpha$ -decay) occurs if the radionuclide emits an  $\alpha$  particle and transforms into another element which has an atomic number less by two and mass number less by four. This is because an  $\alpha$  particle is similar to helium atom consisting of two protons, two neutrons and an atomic mass equal to four. The  $^{238}\text{U}$  (atomic number = 92) is an example of a radionuclide going through  $\alpha$  decay and transforms to  $^{234}\text{Th}$  (atomic number = 90). In beta decay mode ( $\beta$ -decay), the radionuclide emits a beta particle, either an electron or a positron. Electron emission (negatron emission) results in negative beta decay ( $\beta^-$ ), while positron emission processes a positive beta decay ( $\beta^+$ ). In electron emission, a neutron is converted to a proton and both an electron and antineutrino are emitted. Thus the atomic number is increased by one, producing a different element and the atomic mass is not changed after the electron emission. The  $^{14}\text{C}$  (atomic number = 6) undergoes  $\beta^-$  decay and produces  $^{14}\text{N}$  (atomic number = 7). In contrast, in the positron emission ( $\beta^+$ ) a proton is converted to a neutron accompanied by the emission of a positron (anti-electron) and a neutrino; therefore the atomic number is decreased by one producing different element and the atomic mass is unchanged. The  $^{18}\text{F}$  (atomic number = 9) goes over  $\beta^+$  decay and produces  $^{18}\text{O}$  (atomic number = 8). Decay by electron capture mode is similar to the  $\beta^+$  decay in decreasing the atomic number by one and keeping the atomic mass, but it emits a neutrino without emitting a positron (anti-electron). The electron capture decay mode usually exists in rich-proton nuclides, where the nuclide captures an inner shell, thereby transforming a proton to a neutron causing the emission of neutrino. An example of electron capture is

the transformation of  $^{83}\text{Rb}$  (atomic number = 37) to  $^{83}\text{Kr}$  (atomic number = 36). In the gamma decay mode ( $\gamma$ -decay), electromagnetic radiations with enormous frequencies and energies are emitted from the nucleus when it undergoes a transition from high to low energy state. In fact, gamma radiation is associated commonly with  $\alpha$  and  $\beta$  decays. The  $\alpha$ -decay and  $\beta$ -decay, produce a nucleus with excessive energy (at excited state), and instead of emitting another  $\beta$  or  $\alpha$  particle, the excessive energy is lost by emitting electromagnetic radiation, named gamma radiation. Similar to all electromagnetic radiation types, the gamma radiation has neither mass nor charge (Erhard, 2013). Therefore, gamma radiation is secondary radiation of  $\alpha$  and  $\beta$  decays. During gamma decay, the atomic number and neutrons are unchanged; only the energy transits to lower state. An example of an element which undergoes gamma decay is the  $^{137}\text{Cs}$ , which first decays in  $\beta$ -decay mode to  $^{137\text{m}}\text{Ba}$ , i.e. an excited state of  $^{137}\text{Ba}$ ,  $^{137\text{m}}\text{Ba}$  excited to  $^{137}\text{Ba}$  by emitting gamma radiation. In general, all decay modes cause ionizing radiation, which consists of particles carrying sufficient kinetic energy to liberate an electron from an atom and ionize it (Satake, 1997). The ionizing radiation alters the chemical bonds and creates ions which are chemically reactive, and thereby these reactive ions cause significant damage to biological cells, causing health defects, cancer and death. The major difference between the radiation energy of  $\alpha$ ,  $\beta$  and gamma decay modes is the amount of Linear Energy Transfer (LET). The LET is the measure of the conservative force acting on a charged ionizing particle penetrating the matter (International Commission on Radiation Units and Measurements, 1970), and is expressed as the amount of deposited

kinetic energy per unit path length crossed by the charged particles emitted by radiation interaction, given by keV/ $\mu\text{m}$  or MeV/cm. The LET is more reliable and extensively high for  $\alpha$  particles, because of their heavy mass relative to the atoms they ionize. Thus,  $\alpha$  particles travel for very short distances and deposit all the released total kinetic energy of the charged particles within this short traveling path length from the emission point (often within tens of micrometers).

Therefore,  $\alpha$  emitting radionuclides commonly do not cause an external radiation risk. They are risky if taken within body (Stellman, 1998). Conversely,  $\beta$  particles have much lower mass weight so can traverse longer paths and deposit less energy per unit path length. Despite its having no mass and charge, gamma radiations has an associated LET (but this LET is low) , due to the energy transfer through electrons track (Alpen, 1998). LET is greatly lower for  $\beta$  particles and gamma rays than it is in  $\alpha$  particles.

The different LET values cause differences in biological impacts such as tissue damage and cells affinity to cancer. The radiation dose delivered to certain tissue in the human body is proportional to the deposited kinetic energy in the tissue mass. The absorbed dose in the tissue is equal to the total energy divided by the tissue mass. Hence, the LET concept is useful to determine the biological effectiveness when the radiation source is inside the body; however, when the radiation source is external it is more reliable to recognize which radiation is more penetrating. Reversal to the internal source case, if the radiation is external then  $\alpha$  particles have the least bio-impact on the body because they are the least penetrating as they are relatively large and have the highest charge (Bleise et al.,

2003). The high charge of  $\alpha$  particles encourages strong repulsion via electrostaticity and so decreases the particles' ability to penetrate the human body (Fano, 1964). The  $\beta$  particles are more penetrating than  $\alpha$  due to their smaller size and lower charge. The gamma rays are the most penetrating, because they are massless with no charge so there are no electrostatic forces to resist them. This means that gamma radiations can pass through the living body without interferences with the body's nuclides (Burchfield, 2009). Broadly,  $\alpha$  emitters are the most hazardous to living body if ingested or inhaled, while gamma and  $\beta$  emitters are the riskiest if they are from external source.

### **1.5 Gross $\beta$ and alpha activity**

Gross  $\beta$  is defined as the measurement of all  $\beta$  activity occurring in the sample, without considering specific radionuclide (Gundersen & Wanty, 1993). Similarly, gross  $\alpha$  is the measurement of all  $\alpha$  activity despite their particular radionuclide source. Gross measurements are performed for the purpose of screening samples and determining which samples shall go for further measurement. The gross  $\alpha$  and  $\beta$  activity in groundwater samples are first measured to check the concession with international guidance levels and to establish the data which can be used as a baseline for verifying possible changes in environment over human activities or natural changes (Turhan et al., 2013). Comparing gross  $\beta$  to gross  $\alpha$  activities in measured samples would lead to identifying the dominant decay mode and thus define the major radionuclides as either  $\beta$



or  $\alpha$  emitters. These measurements provide a general evaluation of the radioactivity in groundwater in a study area and give preliminary information on the suitability of water for drinking. Practically, gross  $\alpha$  is more significant than gross  $\beta$  for natural radioactivity in water as it refers to the radioactivity of uranium, thorium, radium and radon, which are the most abundant natural radionuclides in water (Garba et al., 2013). Also,  $\alpha$  emitters are more harming in case of intake than being an external radiation.

### 1.6 Uranium isotopes in the environment

Uranium occurs generally in low concentrations in all rocks, soil and water. Uranium also exists in the Earth's crust in concentration averages at 2-4 ppm (Emsley & John, 2001). Uranium might be found either as a trace element in nature or in ore, in for example phosphate rocks. Uranium is a metallic solid in the actinide series in the periodic table and is weakly radioactive with atomic number of 92 and has three natural isotopes:  $^{238}\text{U}$  ( $T_{1/2} = 4.468 \times 10^9$  years),  $^{235}\text{U}$  ( $T_{1/2} = 7.04 \times 10^8$  years) and  $^{234}\text{U}$  ( $T_{1/2} = 245500$  years). It is worth mentioning that the half-life of  $^{238}\text{U}$  is nearly equal to the earth's age which is  $4.54 \times 10^9$  years. This makes  $^{238}\text{U}$  useful in dating earth's processes (Dalrymple, 2001). All uranium isotopes are  $\alpha$  emitters, and both  $^{238}\text{U}$  and  $^{235}\text{U}$  are primordial radionuclides having their own decay series (Figs. 1.1 and 1.2). However,  $^{234}\text{U}$  is a daughter product of the  $^{238}\text{U}$  decay series. There are many other uranium isotopes such as  $^{232}\text{U}$ ,  $^{233}\text{U}$ ,  $^{236}\text{U}$  and  $^{239}\text{U}$ , which are rare products of activation reaction as well as those used in nuclear power reactors as nuclear fuel as well as

to produce medical isotopes such as  $^{225}\text{Ac}$  and  $^{213}\text{Bi}$  (Forsburg & Lewis, 1999).

The occurrence and distribution of these uranium isotopes in the environment is still poorly investigated. Certain minerals are rich in uranium and called uranium minerals such as: uraninite, coffinite and davidite (Merkel et al., 2005).

### The Uranium-238 decay chain

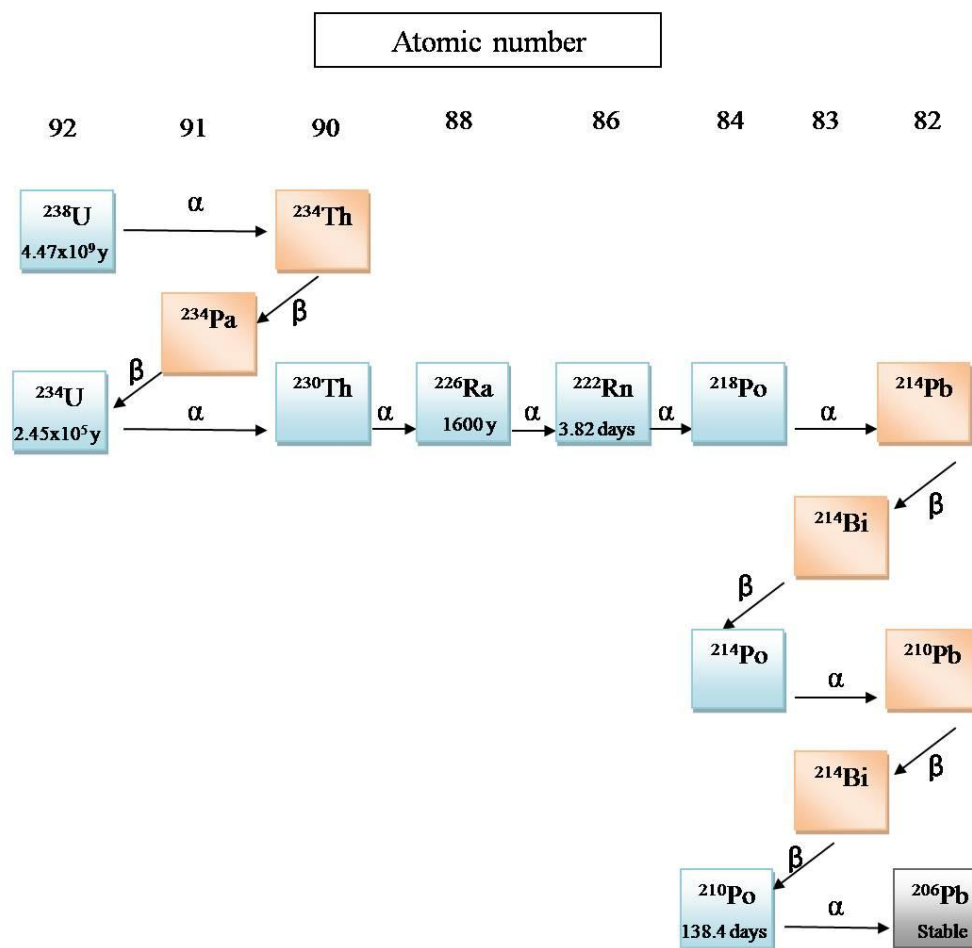


Fig. 1.1 The  $^{238}\text{U}$  decay chain, including  $\alpha$  and  $\beta$  decays. The decay series ends with the stable isotope  $^{206}\text{Pb}$  (Adamic& Aitken,1998).

### The Uranium-235 decay chain

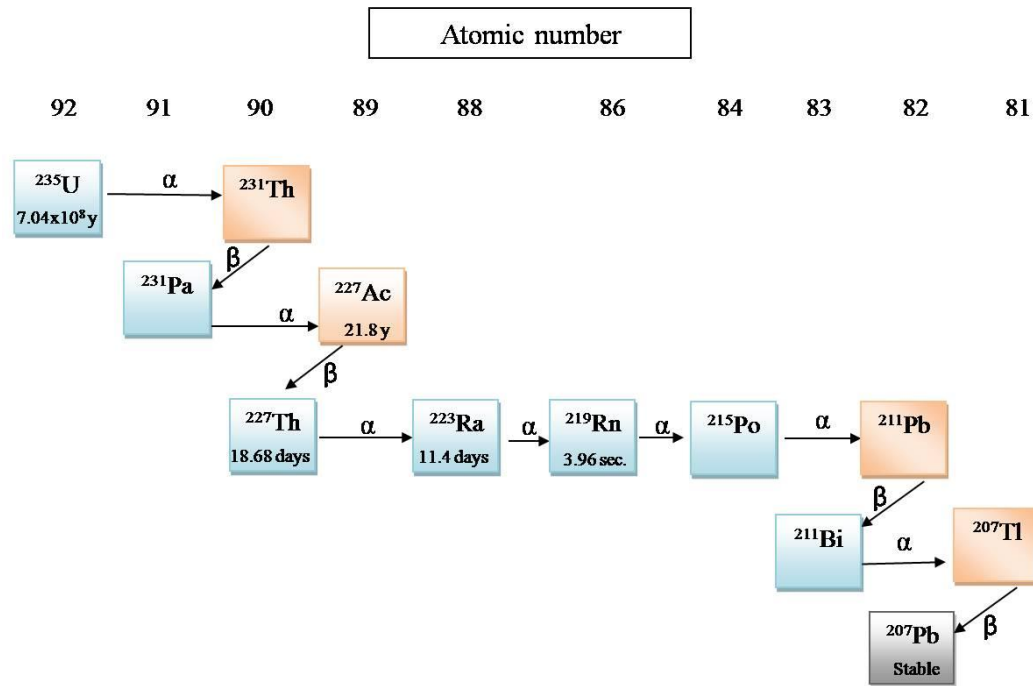


Fig. 1.2 The  $^{235}\text{U}$  decay chain, including  $\alpha$  and  $\beta$  decays. The decay series ends with the stable isotope  $^{207}\text{Pb}$  (Adamic & Aitken, 1998).

The natural abundances of  $^{238}\text{U}$ ,  $^{235}\text{U}$  and  $^{234}\text{U}$  are 99.27%, 0.72% and 0.005% respectively. In the natural occurring uranium isotopes, it was found that  $^{238}\text{U}/^{235}\text{U}$  atomic ratio has not been deviated in  $137.5\pm 0.5$  in environmental samples (Rogers & Adams, 1969; Fried et al., 1985). When this ratio exists constantly in any environment, then it is an indication of the natural sources of uranium (i.e. If the uranium is naturally occurring, then correlation coefficient (R) between concentration measurements of  $^{238}\text{U}$  and  $^{235}\text{U}$  must approximately equal unity). On the other hand, the unity of the activity ratio  $^{238}\text{U}/^{234}\text{U}$  proves the secular equilibrium of the uranium in the tested environment. Broadly, in closed systems the activity ratio of  $^{238}\text{U}/^{234}\text{U} = 1$  (Titayeva, 1994). Secular equilibrium means that production rate equals decay rate, so the quantity of the radionuclide remains steady (US Environmental Protection Agency, 2012).

### **1.6.1 Uranium speciation in water system with respect to pH and redox conditions**

Uranium may migrate long distances from its source and may be incorporated in groundwater because of its high solubility in alkaline conditions, where it forms complexes particularly in the presence of phosphates or carbonates. These complexes are produced mainly in a pH range of 6 and 8. The majority of groundwater in the world falls in this pH range. Solubility is generally controlled by some physical and

chemical conditions such as oxidation-reduction potential, pH and temperature (Zhongbo et al., 2007). In particular, the pH and oxidation state have strong effect on uranium solubility. Dissolved uranium occurs principally in the hexavalent state (U (VI)), whilst uranium in the tetravalent state (U (IV)) forms insoluble compounds. Uranium often exists in the hexavalent state under oxidizing to slightly reducing environments. The tetravalent state of uranium occurs mainly under reducing conditions and is almost insoluble (Krupka and Serne, 2002); however, tetravalent uranium occurs under oxidizing condition only if  $\text{pH} < 4$  (Dinh Chau et al., 2011). The oxidation state is controlled by reduction potential (Eh, measured in volts or millivolts) of the aqueous environment. The more positive is the Eh of the aqueous environment, the more affinity of the occurred element to be oxidized (Vanloon & Duffy, 2011).

Chemical speciation is the distribution of a chemical element through its possible compounds (species) in a certain system (Templeton et al., 2000). Usually, chemical speciation is represented with respect to pH and Eh (called Pourbaix diagram), to illustrate the effect of both pH and redox conditions on the available species of certain element. In the Pourbaix diagram, the vertical axis is Eh with respect to the standard hydrogen electrode (SHE), and the horizontal axis show the pH (activity of hydrogen ions or protons) (Drissi et al., 1995). The lines in the Pourbaix diagram represent the equilibrium conditions, i.e. where the

activities are equal, of two or more species on each side of that line. Away from the line, one type of species is predominant (Vanloon et al., 2011).

The Pourbaix diagram for uranium in carbonate solution is presented in Fig. 1.3 (modified after Puigdomenech, 2010). The uranium species in the carbonate system might include: uranyl dioxide ion ( $\text{UO}_2^{2+}$ ), uranyl carbonate ions with different oxidation states ( $\text{UO}_2(\text{CO}_3)$ ) and mixed-valent uranium oxide ( $\text{U}_4\text{O}_9$ ).

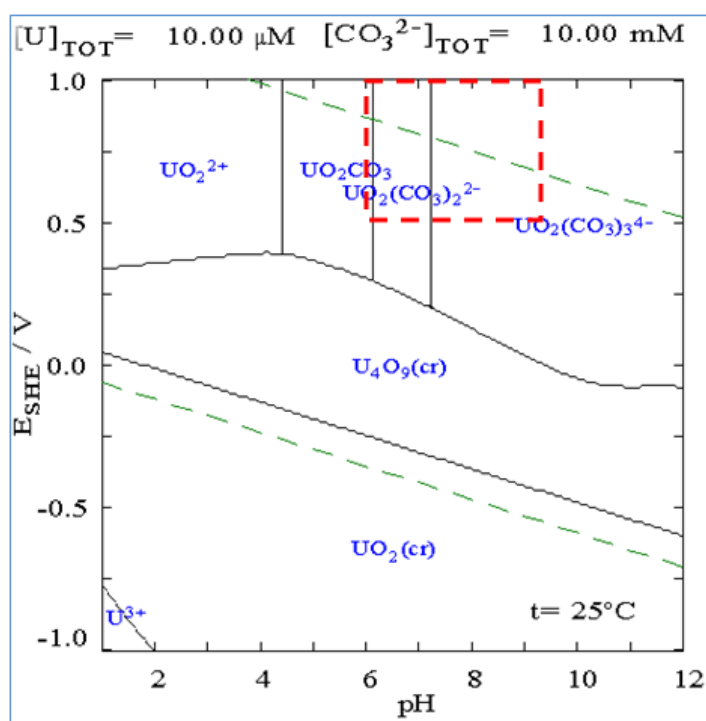


Fig. 1.3 Uranium speciation in carbonate solution with respect to Eh and pH (modified after Puigdomenech, 2010): The solid lines symbolize the equilibrium conditions where the activities are equal -for the species on each side of that line-. The dashed green lines show the stability limits of water in the system. The red dashed rectangle represents the general range of the groundwater in the world where the water are of oxidizing conditions and pH ranges between 6 and 9. At oxidizing conditions the Uranyl ion ( $\text{UO}_2^{2+}$ ) and its complexes are formed, and so uranium can migrate long distances from its source (Finch & Murakami, 1999).

## 1.7 Thorium isotopes in the environment

Thorium has 6 naturally occurring isotopes:  $^{232}\text{Th}$  ( $T_{1/2} = 1.405 \times 10^{10}$  years),  $^{234}\text{Th}$  ( $T_{1/2} = 24.1$  days),  $^{230}\text{Th}$  ( $T_{1/2} = 75380$  years),  $^{231}\text{Th}$  ( $T_{1/2} = 25.5$  hours),  $^{228}\text{Th}$  ( $T_{1/2} = 1.91$  years) and  $^{227}\text{Th}$  ( $T_{1/2} = 18.68$  days).  $^{232}\text{Th}$  has the longest half-life and produces its own daughter nuclides through  $^{232}\text{Th}$  decay chain (Fig. 1.4), where  $^{228}\text{Th}$  is progeny of  $^{232}\text{Th}$ . Both  $^{234}\text{Th}$  and  $^{230}\text{Th}$  are daughters of  $^{238}\text{U}$  decay chain, while both  $^{231}\text{Th}$  and  $^{227}\text{Th}$  are progenies of  $^{235}\text{U}$  decay chain. The half-life of  $^{232}\text{Th}$  is comparable to the age of the universe, which made it low specifically radioactive with natural abundance near to 100%. The  $^{232}\text{Th}$  is also much more common in the Earth's crust than uranium (Hammond, 2004). Thorium exists in rocks (Table 1.1) and it may comprise up to 2.5 wt. % oxide in monazite and around 12% in thorianite (Wickleder et al., 2006). Unlike uranium, thorium is generally insoluble and tends to be adsorbed on iron hydroxides; however there are few soluble thorium compounds. These soluble compounds consist of the chloride, fluoride, nitrate, and sulfate salts (Weast, 1988). Moreover, thorium solubility is independent of redox conditions (Hyde, 1960) and thus, thorium is rarely found in water and is widely recognized in sediments.



### The Thorium-232 decay chain

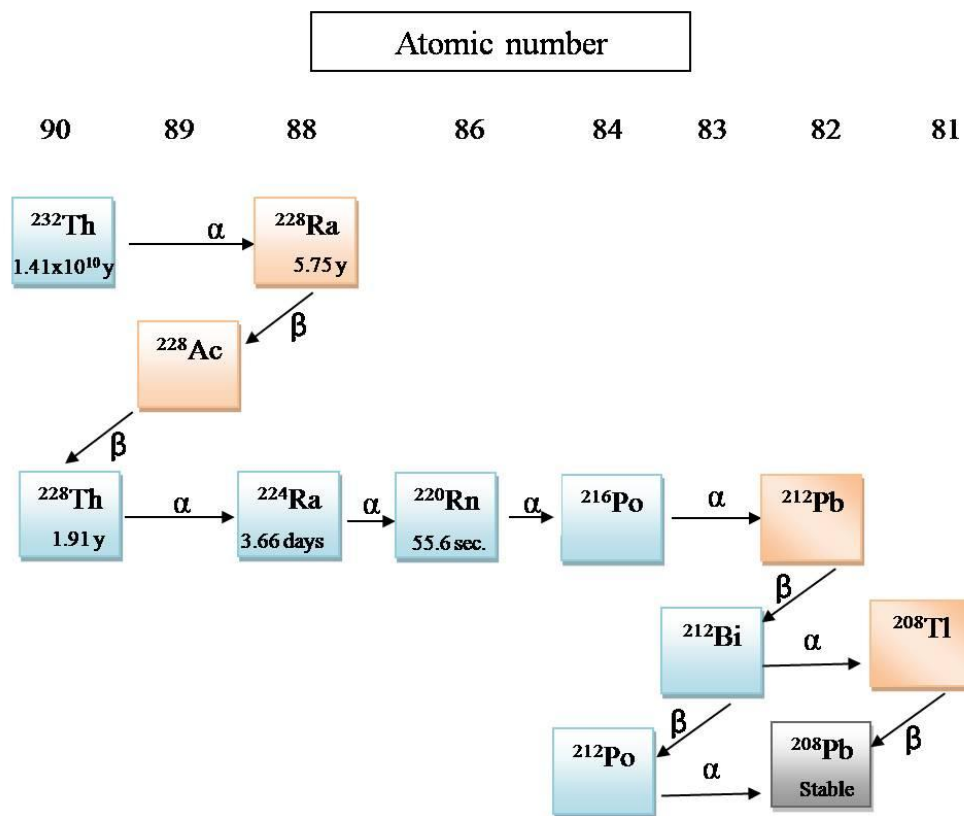


Fig. 1.4 The  $^{232}\text{Th}$  decay chain, including  $\alpha$  and  $\beta$  decays. The decay series ends with the stable isotope  $^{208}\text{Pb}$  (Adamicc & Aitken, 1998).

## 1.8 Natural radium isotopes in the environment

Radium is a radioactive element without any stable isotope, has an atomic number of 88 and it was first recognized in the form of radium chloride by Marie Curie and Pierre Curie in 1898. Radium is found in uranium ores in trace quantity, and has four naturally occurring isotopes:  $^{226}\text{Ra}$  ( $T_{1/2} = 1600$  years),  $^{228}\text{Ra}$  ( $T_{1/2} = 5.75$  years),  $^{224}\text{Ra}$  ( $T_{1/2} = 3.63$  days) and  $^{223}\text{Ra}$  ( $T_{1/2} = 11.43$  days) (National Nuclear Data Center, 2009). The  $^{226}\text{Ra}$  is a daughter in  $^{238}\text{U}$  decay chain, and  $^{223}\text{Ra}$  is a daughter of  $^{235}\text{U}$  decay chain, and both  $^{228}\text{Ra}$  and  $^{224}\text{Ra}$  are daughters in  $^{232}\text{Th}$  decay chain. The  $^{223}\text{Ra}$ ,  $^{224}\text{Ra}$  and  $^{226}\text{Ra}$  are  $\alpha$  emitters and decay straightforwardly to radon, while  $^{228}\text{Ra}$  decay to radon after two  $\beta$  decays and two  $\alpha$  decays. Although radium is moderately soluble in water (Zapeczka & Szabo, 1988), it can enter the groundwater system by leaching from the aquifer (hosting rocks) or desorption (releasing the adsorbed substance from the surface). The solubility of radium salts in water is proportional to pH levels but it is independent on redox conditions (US Environmental Protection Agency, 2012). The known soluble radium salts are chloride, bromide, nitrate, and hydroxide, and the common sparingly soluble radium salts are carbonate and phosphate. The least soluble radium salt in water is radium sulfate (US National Library of Medicine, 2014). The  $^{226}\text{Ra}$  and  $^{228}\text{Ra}$  are the most abundant isotopes in water because of their relative higher half-lives, and so they are of more concern in groundwater.

## 1.9 Natural radon isotopes

Radon is also a radioactive element with an atomic number of 86 and is a noble gas and occurs naturally as progeny in the uranium and thorium decay series. Radon has three naturally occurring isotopes and all are gaseous, thus they are highly contributing (approximately 50%) to the total radiation effective dose received globally from natural sources of radiation (Fig. 1.5). Since the radon is an  $\alpha$  emitter, it is worth finding how much the human body absorbs radon. The quantity of absorption is measured in Sieverts (Sv) or milli Sieverts (mSv).

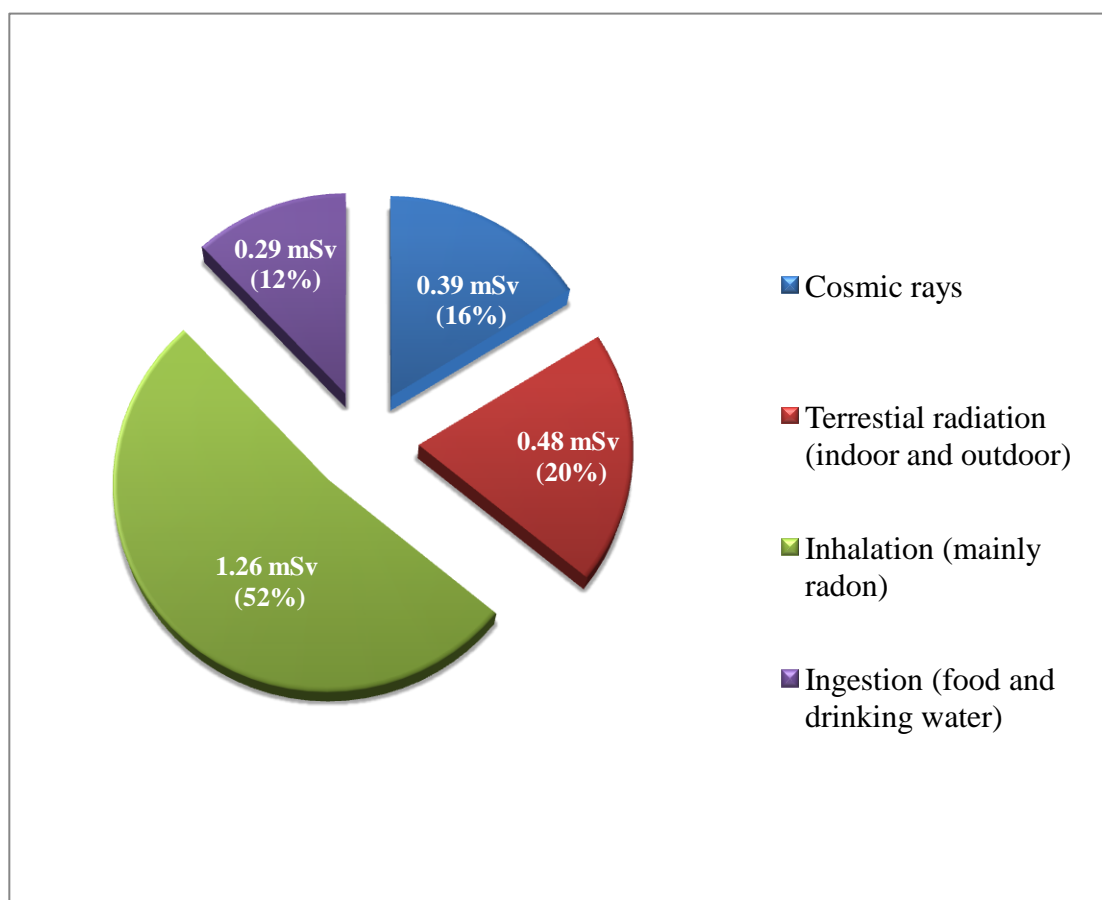


Fig. 1.5 Distribution of average natural radiation exposure (modified after WHO, 2011).

The natural isotopes of radon are:  $^{222}\text{Rn}$  ( $T_{1/2} = 3.82$  days),  $^{220}\text{Rn}$  ( $T_{1/2} = 55.6$  seconds) and  $^{219}\text{Rn}$  ( $T_{1/2} = 3.96$  seconds).  $^{222}\text{Rn}$ ,  $^{220}\text{Rn}$  and  $^{219}\text{Rn}$  are progenies of  $^{238}\text{U}$ ,  $^{232}\text{Th}$  and  $^{235}\text{U}$  decay chains respectively. The relative high solubility in water makes radon existence in groundwater of interest for researchers although radon will decay rather rapidly (O'Neil et al., 2006). However, continuous generation of radon from the aquifer provides rather high amounts in some areas. Radon is more generated in igneous fractured aquifers, like the case in Nordic countries (Asikainen, 1982; Akerblom, 1994; Banks et al., 1995), due to the availability of uranium in the aquifer rock (Fig. 1.6). Since radon gas is a product of uranium, it is available in high concentrations near uranium mines and could affect the health of workers especially in the case of open mines. The indoor radon gas is released from the water in showers, building materials and soil seeps through cracks in building, however, average radon in home air in general is about 0.048 Bq/L (US Environmental Protection Agency, 2013).

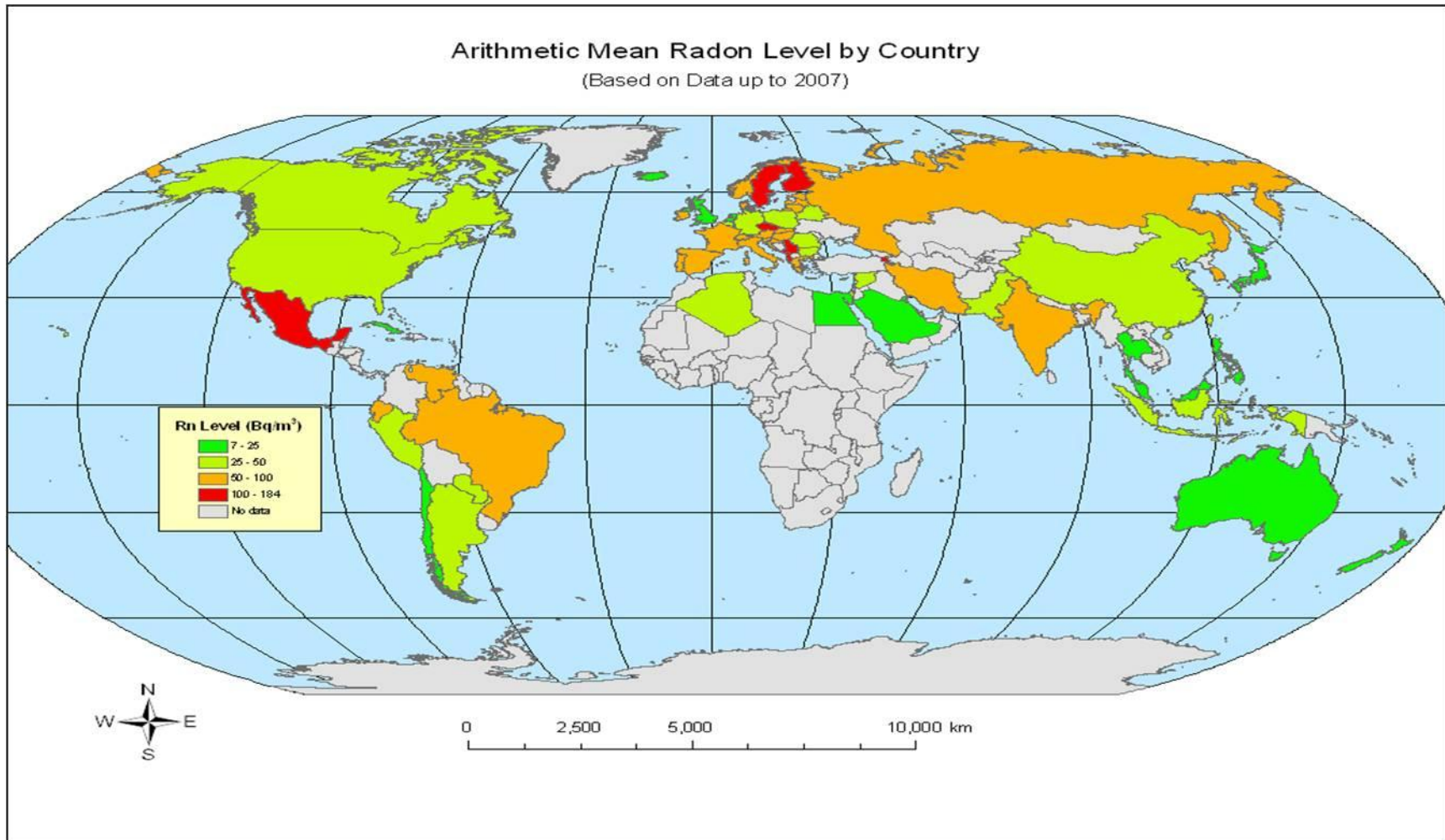


Fig. 1.6 Radon (Rn) distribution worldwide in Bq/m<sup>3</sup> (after Zielinski & Jiang, 2007).

### **1.10 Environmental impact of radioactivity**

Uranium, thorium, radium and radon may exist in groundwater as a result of interaction with aquifer rocks, nearby uranium tailings, absorption from soils and leaching of fertilizers (Flynn & MacGregor, 2002; Taylor & Taylor, 1997). Once in the groundwater, these radionuclides can be further transported to the environment through drinking, domestic, farming and industrial uses. Within the environmental compartment, the radionuclides can then enter the human body through direct or indirect pathways. The direct pathway means use of groundwater for drinking or eating vegetables polluted with radionuclides fallout, while indirect pathway encompasses the intake of harvests irrigated with polluted water or cattle fed by polluted fodder. However, the indirect consumption is believed to be non-risky to health in general due to low received dose (Cothorn, 1996).

Radon gas is easily released from water or uranium tailings and then inhaled by human. The radon isotopes emit radioactivity mainly in the form of  $\alpha$  radiation which cannot penetrate the outer layers of the skin. So, these radionuclides are risky only if taken into the body via ingestion or inhalation (see section 1.4 for details). The health risks might exist as accumulation of the radionuclide dust through mining, aggregation in kidneys and bones or cancer (Darby et al., 2001). Despite its weak radioactivity, uranium may harm the kidney as a heavy metal through long term accumulation. High radium exposure could cause lowering of the immune system, anemia, cataracts and teeth frailty. These health impacts are realized only through extreme exposure

to radium in the workplace (Department of Environmental services in New Hampshire, 2007; WHO, 2011). Uranium, radium and radon are classified as “carcinogenic to human” by the US Environmental Protection Agency (EPA). The risk of lung cancer might increase through the inhalation of uranium and radium dust as well as radon gas released from water or uranium tailings.

The EPA and the WHO have recommended (separately) guidelines for isotopes concentration in drinking water, relying on estimations of the annual radiation dose per person and the type of radiation. Dose is measured in Sieverts (Sv) or milliSieverts (mSv), where  $1 \text{ Sv} = 1 \text{ Joule/Kg}$ . The global average annual dose per person was estimated by the United Nations Scientific Committee on the Effects of Atomic Radiation (UNSCEAR, 2008) to be about 3.0 mSv/year. Eighty percent of the annual dose is derived from the naturally existing radionuclide, 19.6% from medical diagnosis and 0.4% from other anthropogenic sources. Increased cancer risk presents at doses greater than 100 mSv (Brenner, 2003), and below this dose serious risk was difficult to identify. The EPA and WHO guidance levels of selected radionuclides are represented in the discussion chapter (Table 4.5). These guidelines are not mandatory, but may be considered as a trigger for more investigations (WHO, 2011). WHO recommends measuring first the gross  $\beta$  and gross  $\alpha$  as screening measurements, then looking at specific radionuclides which contribute extremely in the radiations.

Exposure to radionuclides can be reduced (or limited), using either simple or complicated techniques, depending on the decay mode of the radionuclide.

Gamma emitters, for example, are highly penetrating and can be blocked by highly dense materials like thick concrete or lead. B emitters are medium penetrating and could be blocked by a piece of cloth or thin layer of a substance like wood. A emitters are completely safe if coming from an external source and stop at the dead layer of skin as well as they may be blocked by a piece of paper (explanation in section 1.4).

Some techniques have been developed to protect from the exposure to radionuclides in groundwater. These techniques work mainly with chemical alterations which make the radionuclide insoluble and so less available in drinking water.

For example, uranium concentration is lowered in the groundwater by injecting certain bacteria which are able to reduce uranium from its hexavalent state to its tetravalent state, and so make it insoluble (Veeramani et al., 2011). Dangerous levels of radionuclides need special cleanup methods regulated by the EPA. Polluted sites must be monitored periodically and sample should be collected with documented date and time. It is also obligatory to communicate to the audience and clarify the risk severity in the different situations in clear language for the public (WHO, 2011).



## **2 SAMPLING SITES AND ANALYTICAL TECHNIQUES**

Before going into details of the sampling and analytical techniques, a brief description of the surface geology and hydrogeology of the UAE is presented.

### **2.1 Brief regional geological and hydrogeological settings in the UAE**

The UAE lies between latitudes 22°50' and 26° north and longitudes 51° and 56°25' east and is located in the southeast of the Arabian Peninsula on the Arabian Gulf, bordering with Oman to the east and Saudi Arabia to the south, and also sharing sea borders with Qatar and Iran. The tropic of cancer (lies at ~ 23.5° N) passes through the UAE where it crosses Al Ain city. The UAE, surface area of 83600 km<sup>2</sup>, is considered within the arid climate zone having an average annual rainfall of about 120 mm (Ministry of Energy in the United Arab Emirates, 2006). This rainfall was averaged from 1974 to 2005.

The hydrogeological conditions in the UAE are strongly related to the topographic features that are dominated by a mountain range in Oman at the eastern margin of the Arabian Platform that extends as a chain (about 650 km long and 30-130 km wide) between the Musandam Peninsula in the Northwest and the Indian Ocean in the Southeast (Fig. 2.1). These mountains contain a variety of exposed rocks extending from the Paleozoic era (about 490 million years ago) to the Neogene era (about 20 million years ago) (El-Siay & Jordan, 2007). The lithology of these rocks varies between sedimentary, igneous and

metamorphic. The high topography of the mountainous region, together with relatively higher rainfall, represents the main recharge pathways for groundwater in the UAE. Aside from the mountainous region, most of the UAE surface geology is represented by sand dunes and wadi alluvials of the Quaternary age. These sediments, in addition to the rocks, are the aquifers in the UAE.

A comprehensive map of groundwater level that covers the whole UAE is lacking, but maps are available on local scales (Fig 2.2). The deepest groundwater level in the Emirate of Abu Dhabi Emirate is found in the eastern and northeastern UAE and the shallow level in the central and western UAE. However, the regional groundwater level and salinity maps of the Abu Dhabi indicate complex patterns. When it comes to salinity (Fig. 2.3), then groundwater is apparently most saline in the coastal plain, inland sabkhas and interdunal sabkhas. The enormous exploitation of groundwater in some areas in addition to the anthropogenic recharge in others, has a strong spatial and temporal impact on groundwater level and salinity. Therefore, cautions should be taken when considering the data from one year to another. Regardless of these generalizations, topography still has a strong impact on groundwater flow (mountains to plain areas) and the variation caused by natural recharge conditions should be more effective in areas outside large metropolitan and farming localities. As shown in Fig. 2.1, the wells used in the designated investigation areas A-1 to A-5 spread along the sand dunes and wadi alluvial, in addition to the rocky mountains in the north and east. The subsurface geology of the sand dune areas mainly consists of both carbonates and clastics (sandstones and

conglomerates) which are the hosting rocks (aquifers) of the groundwater (Brook et al, 2006; Wood & Alsharhan, 2003). It is, however, important to mention that even the igneous (mainly ophiolite suit) and metamorphic rocks act as aquifers in the mountainous region.

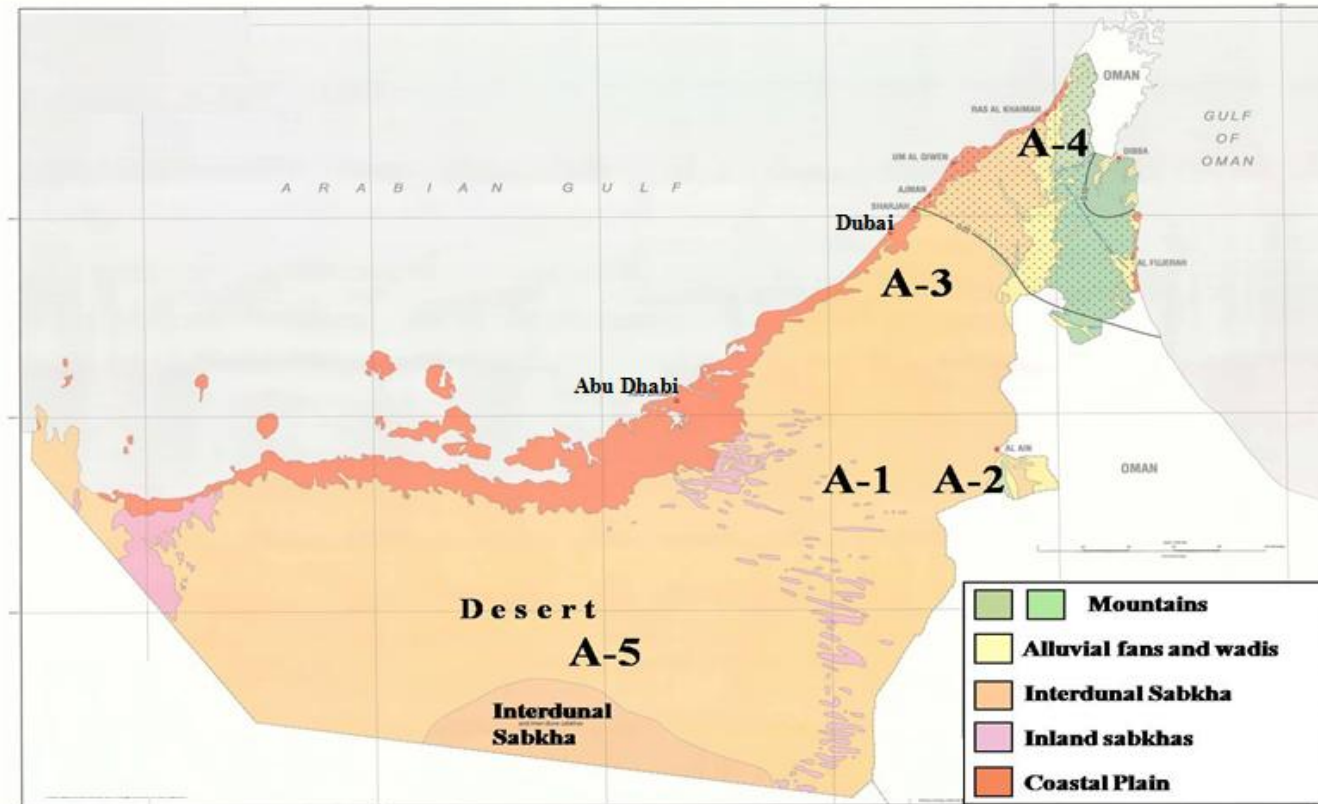


Fig. 2.1 Surface geology of the UAE (Modified after the Ministry of Energy, Petroleum and Minerals sector). The sampling sites of this study were added to the map, where A-1: Abu Dhabi-Al Ain road, A-2: Jebel Hafit, A-3: Al Ain- Dubai road, A-4: Wadi Al Bih and A-5: Liwa Oasis.

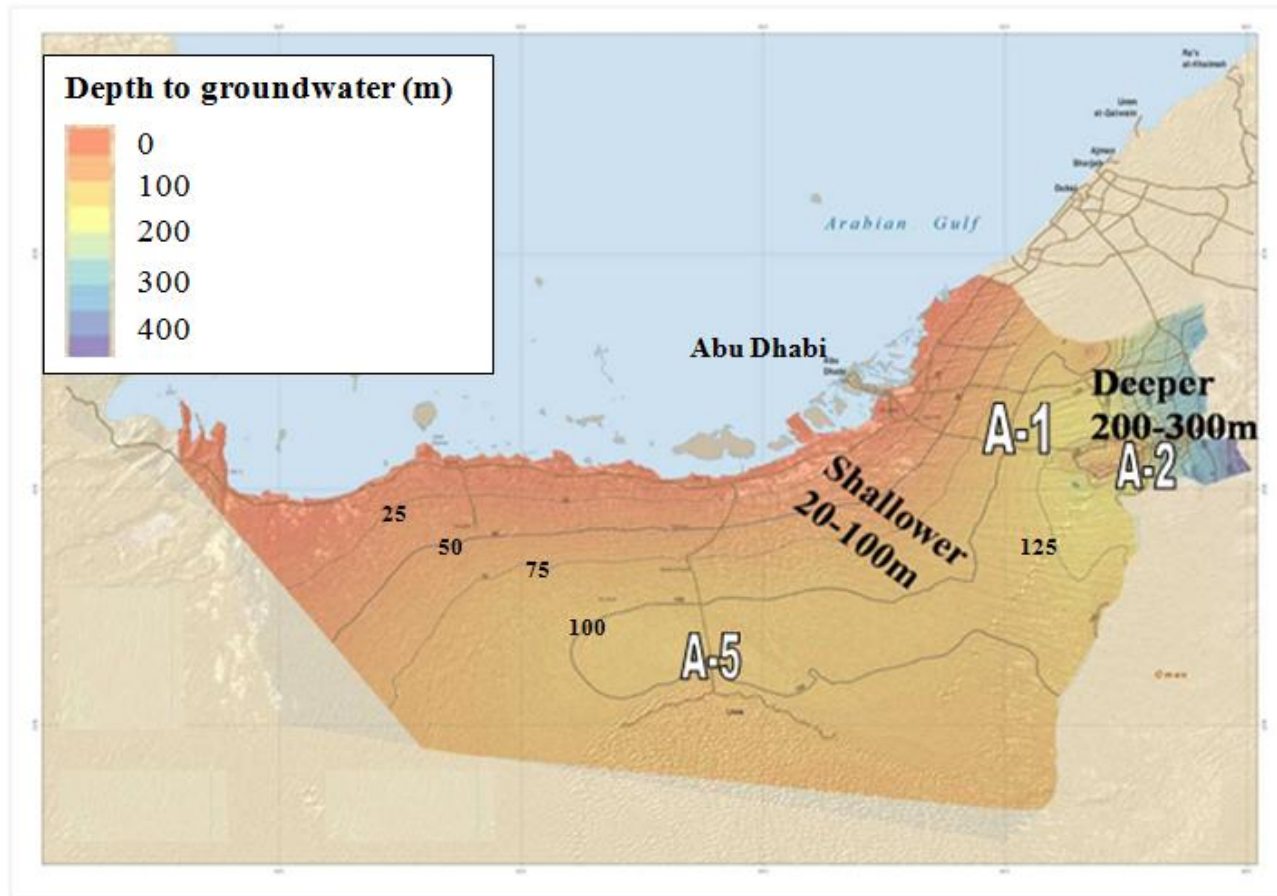


Fig. 2.2 Water table map across Abu Dhabi area (after Dawoud, 2008). The sampling sites of this study were added to the map.

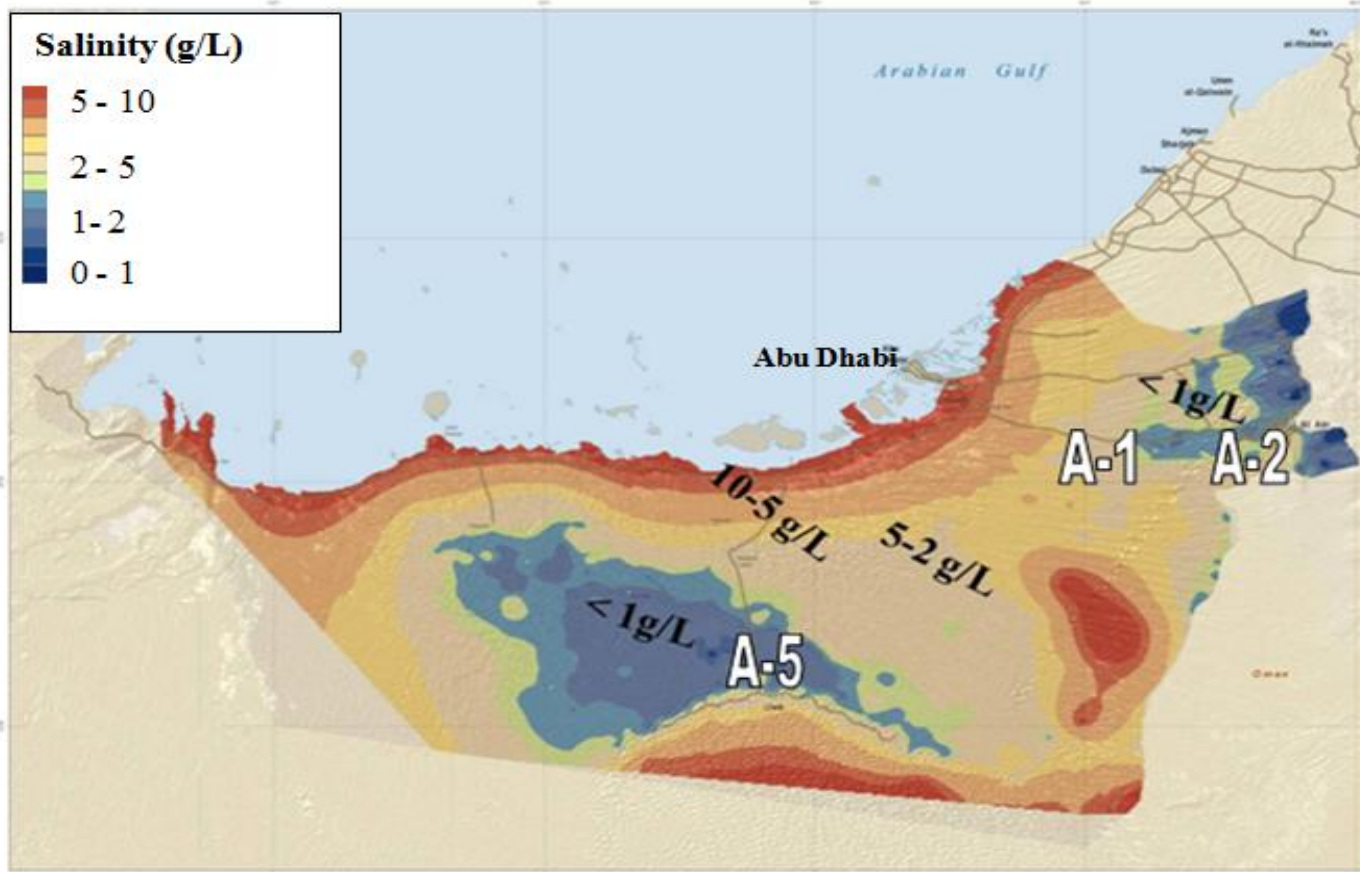


Fig. 2.3 Groundwater salinity map in the UAE including the distribution in Abu Dhabi area only (after Dawoud, 2008). The sampling sites of this study were added to the map.

## 2.2 Groundwater sampling wells

Sampling was performed once for each well, and so it is expected that if it was done more than one time, the results might differ due to the continuous changes in the aquifer system recharges and discharges. Periodic sampling is significant to observe the variations in the hydrological system. Groundwater samples from 67 different wells were spread into areas throughout the as shown in Fig. 2.4 in the UAE. These wells were selected because of availability and accessibility. Also, groundwater was sampled from Oman for comparison purposes from 12 wells and one spring (Fig. 2.5). The sampling time was in autumn, winter and spring seasons. The sampling locations are distributed as (Fig. 2.4):

1. Area (A-1), with 5 wells distributed along Abu Dhabi-Al Ain road, which is a farming rich area and is dominated by Neogene to Quaternary alluvial aquifers (younger than 20 million years) (Brook et al, 2006).
2. Area (A-2), with 20 wells along Jabel Hafit and neighboring area (Fig. 2.6), which is known as a recreational area and the main aquifers are Paleogene to Neogene (younger than 40 million years) carbonate rocks and are composed of nodular and partly dolomitic limestones with interlayers of marls, anhydrites and some shale (El-Saiy and Jordan, 2007).

3. Area (A-3), with 16 wells along the Al Ain-Dubai road, which contains many farms as well as several small towns with the main aquifers as Quaternary alluvial and sand dunes.
4. Area (A-4), with 20 wells along Wadi Al Bih in the Emirate of Ras Al Khaimah and near to Ras Al Khaimah city, which represents a farming strip having mainly Upper Triassic (230- 215 million years ago) to Lower Cretaceous (145- 140 million years ago) carbonate rock aquifers which vary in lithology from dolomitic, argillaceous carbonates to interbedded shale (Clarkson et al., 2012; Breesch et al., 2010; Rizk et al., 2007).
5. Area (A-5), with 6 wells in the Liwa Oasis along the Southern part of the Abu Dhabi Emirate, near to the border with the Kingdom of Saudi Arabia. The area is rich with farms as well as recreation and tourism with the main aquifers as Quaternary sandstone (Wood & Alsharhan, 2003).
6. Along the borders of UAE and Oman, 10 wells, from Quaternary alluvial deposits aquifer (silt, sand and gravel).
7. North-western Oman, 2 wells, of Cretaceous carbonate (140-65 million years old).
8. From Oman's capital, Muscat; near the coast of the Gulf of Oman, one sample was collected from the hot spring named as Ayn Al Hamam.



Groundwater sampling was limited by the availability of open wells and accessibility of the wells for direct sampling. Accordingly, only wells that were possible to pump for a certain time were sampled. All the wells are used for irrigation and occur either within a farm or the water is transported to the farm through a pipe system. The sampling was performed after allowing each well to pump for at least one hour to capture the aquifer original water. All samples were kept in dark and cold conditions (ice box in the field and during transport and refrigerator at 4°C in the lab) until analyses and a water sample was divided into portions for the different measurements as the following:

- Water for Na<sup>+</sup> and K<sup>+</sup> analyses in 1 liter plastic (HDPE wide mouth) bottle to which a few drops of concentrated nitric acid (HNO<sub>3</sub>; 65%) was added in the field after sampling.
- Water for Cl<sup>-</sup> analysis in 1 liter plastic (HDPE wide mouth) bottle.
- Water for gross β and α radioactivity, uranium, thorium and radium measurements was sampled in a 1 liter (HDPE wide mouth) bottles and shipped to Denmark by airplane.
- Water for radon (Rn-222) measurement, which was sampled in 20 ml low diffusion LSC (Liquid Scintillation Counting) vial prefilled with 10 mL Opti-Fluor O liquid scintillation cocktail (PerkinElmer). The samples were shipped to Denmark as quickly as possible and the time from sampling until measurement was 1-2 weeks.

Temperature, electrical conductivity (EC) and pH were measured in the field using WTW-COND-3301 instrument. The total dissolved solids (TDS) were calculated as EC multiplied by conversion factor that varies between 550 and 750 at a standard temperature of 23 °C (Freeze & Cherry, 1979).

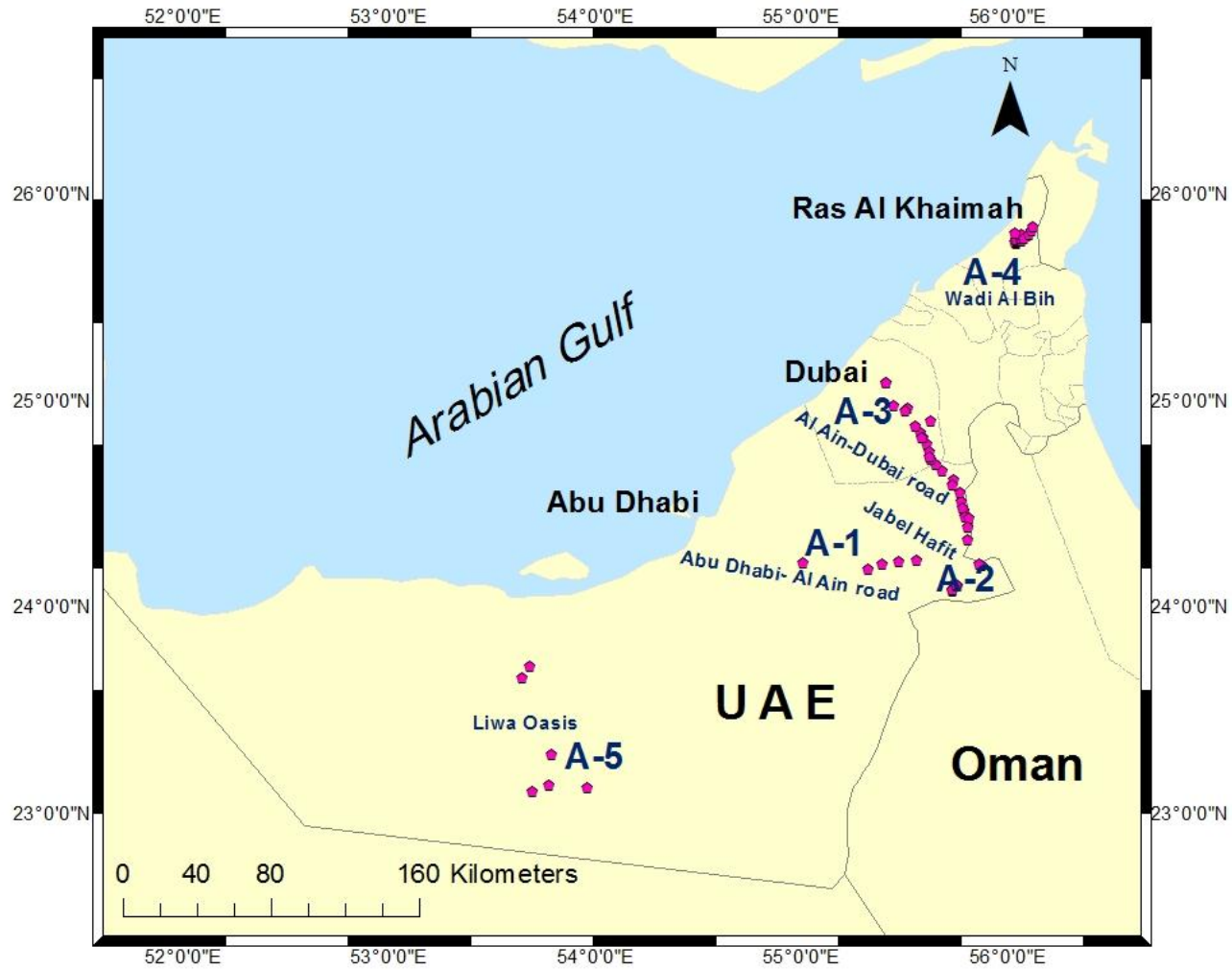


Fig. 2.4 Groundwater sampling wells sites.

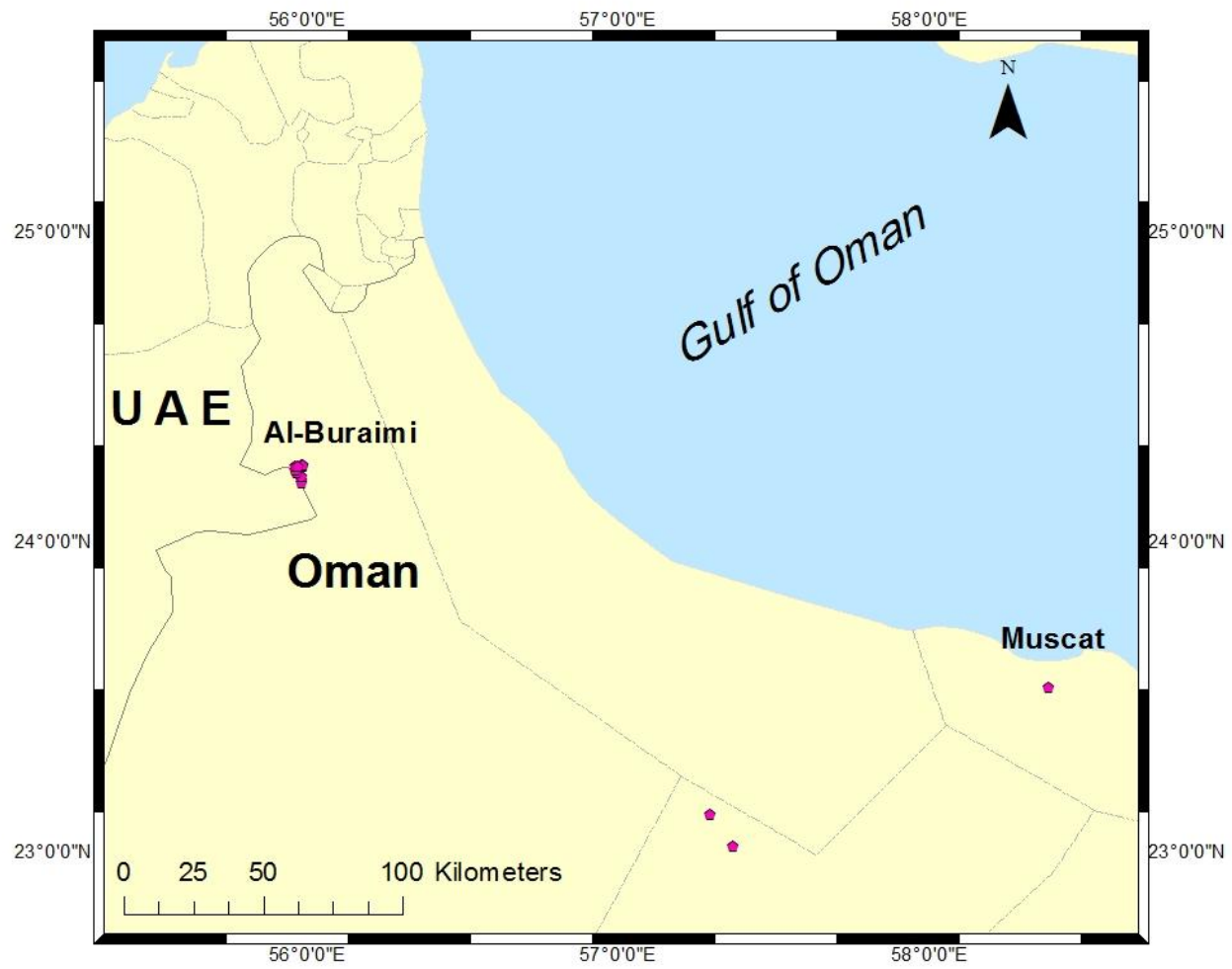


Fig. 2.5 Location map of sampling wells and spring in Oman.



Fig. 2.6 Some of the groundwater in Jabel Hafit area (A-2) is used for recreational activities and landscaping.

### **2.3 Rocks and sediments sampling sites**

As carbonate rocks and sediments represent the main aquifers of the groundwater in the investigated area and because of the relatively high concentration of radioactivity observed in the groundwater samples near to the carbonate aquifers, selected outcrop samples were collected in areas A-2 and A-4. There is no doubt that samples should have been selected from all the areas and at much higher sampling spatial density and even at depth. However, because of limitation in time and funding as well as large surface coverage of the investigated areas, only representative samples were analyzed to provide first results of natural radioactivity in the aquifers and their relation to the hosted groundwater. Thirty rock samples were collected from the carbonate rocks in A-4 and A-2 (Figs. 2.7, 2.8) and nine samples from sediment/soil layers in A-4. The rocks in A-4 are named: r-1 to r-30, and in A-2: JH-1 to JH-3. The carbonate rocks are generally composed of calcite and dolomite with different textures described generally in Table 2.1 and exemplified in Plates 2.1 and 2.2. The sediment/soil samples were collected from three different depths (0-10 cm, 10-20 cm and 20-30 cm) in three farms in A-4, named: F1, F2 and F3 (Fig 2.7). The sampling process was performed after making a small trench of 50 cm and excavation in each sampling depth range.



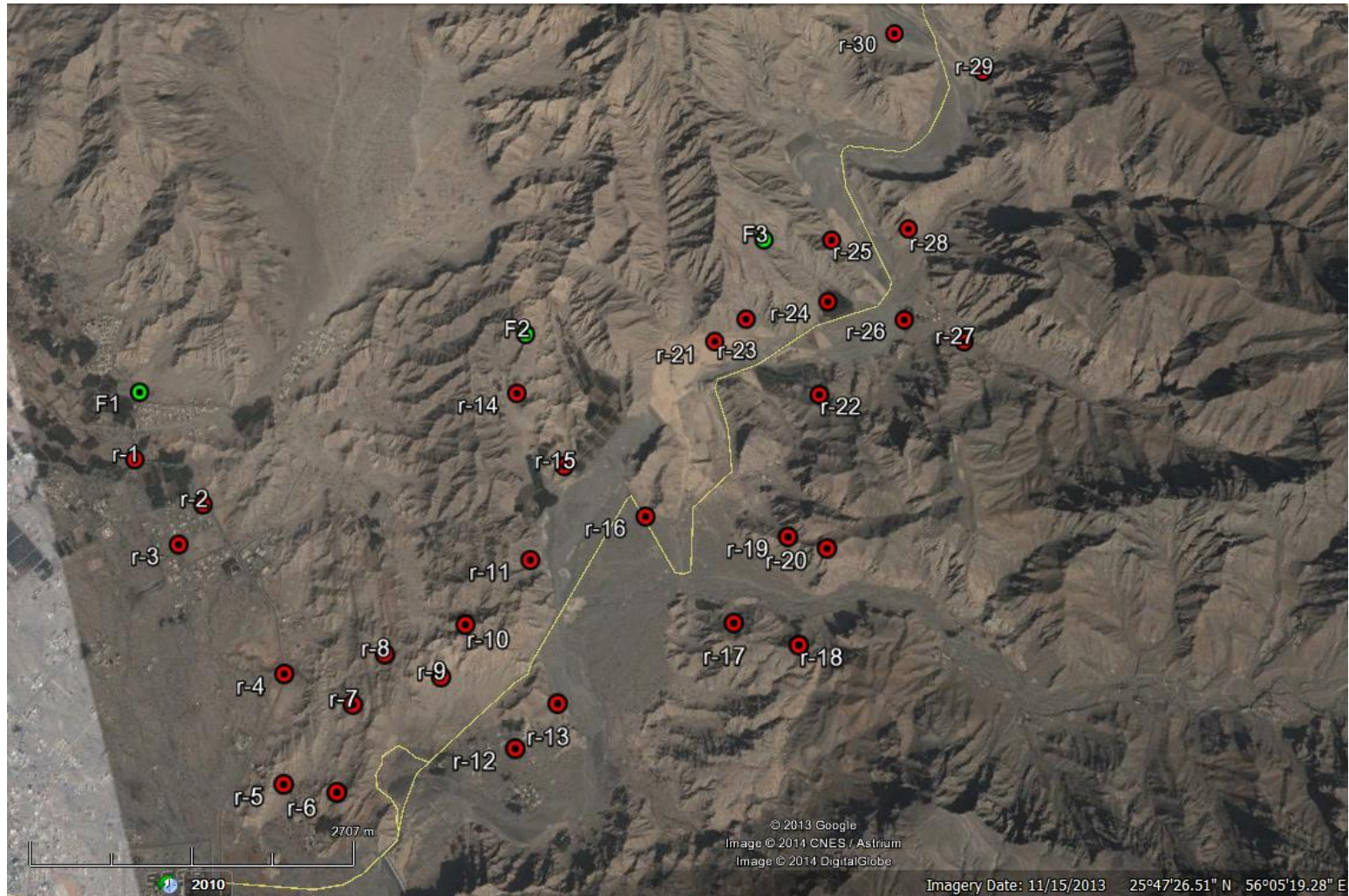


Fig. 2.7 Google satellite image of Wadi Al Bih (A-4) showing the locations of rocks samples: r-1 to r-30, and sediment/soil samples: F1 to F3. The yellow lines illustrates the roads



Fig. 2.8 Sampling location of rocks in Jabel Hafit (A-2) along a fault plane.



Table 2.1 Table 2.1 Visual description of rocks depending on apparent texture and HCl test. Age and formation name:  
(O. Abdelghany, personal communication, April, 2014; Maurer et al.,2008).

<b>Sample ID</b>	<b>General discription</b>	<b>Age and formation name</b>
<b>JH-1</b>	White colored faulted plane calcite with slicken side, fractured, and dolomitic partly	Lower Eocene; Rus Formation
<b>JH-2</b>	Grayish brown chertified granular limestone	Lower Eocene; Rus Formation
<b>JH-3</b>	White colored tabular calcite crystals up to several centimeters length	Lower Eocene; Rus Formation
<b>r-1</b>	Grayish brown dolomitic limestone	Lower Jurassic, Musandam Formation
<b>r-2</b>	Grayish brown crystalline limestone	Lower Jurassic, Musandam Formation
<b>r-3</b>	Grayish brown muddy limestone	Lower Jurassic, Musandam Formation
<b>r-4</b>	Red, strongly weathered limestone	Upper Triassic, Ghalilah Formation
<b>r-5</b>	Whitish grey chertified limestone	Lower Jurassic, Musandam Formation

<b>Sample ID</b>	<b>General discription</b>	<b>Age and formation name</b>
<b>r-6</b>	Black phosphatic limestone	Triassic/Jurassic boundary, Ghalilah Formation
<b>r-7</b>	Grayish brown chertified limestone	Middle Triassic, Milaha Formation
<b>r-8</b>	Grayish brown chertified limestone with some vugs	Middle Triassic, Milaha Formation
<b>r-9</b>	Grayish brown chertified microcrystalline limestone	Middle Triassic, Milaha Formation
<b>r-10</b>	Grayish brown chertified microcrystalline limestone	Lower Triassic, Ghail Formation
<b>r-11</b>	Grayish brown microcrystalline limestone	Lower Triassic, Ghail Formation
<b>r-12</b>	Grayish brown microcrystalline limestone	Lower Triassic, Ghail Formation
<b>r-13</b>	Gray lime-mudstone	Upper Permian, Hagil Formation
<b>r-14</b>	Gray lime-mudstone	Upper Permian, Hagil Formation

<b>Sample ID</b>	<b>General discription</b>	<b>Age and formation name</b>
<b>r-15</b>	Gray lime-mudstone	Upper Permian, Hagil Formation
<b>r-16</b>	Grayish brown microcrystalline limestone	Middle Triassic, Milaha Formation
<b>r-17</b>	Grayish brown microcrystalline limestone	Middle Triassic, Milaha Formation
<b>r-18</b>	Grayish brown microcrystalline limestone	Middle Triassic, Milaha Formation
<b>r-19</b>	Gray argillaceous limestone	Lower Triassic, Ghail Formation
<b>r-20</b>	Gray argillaceous limestone	Lower Triassic, Ghail Formation
<b>r-21</b>	Gray carbonate mudstone	Upper Permian, Hagil Formation
<b>r-22</b>	Greenish brown fractured mudstone	Upper Permian, Hagil Formation
<b>r-23</b>	Greenish brown mudstone	Upper Permian, Hagil Formation

<b>Sample ID</b>	<b>General discription</b>	<b>Age and formation name</b>
<b>r-24</b>	Greenish brown dolomitic mudstone	Upper Permian, Hagil Formation
<b>r-25</b>	Greenish brown dolomitic mudstone	Upper Permian, Hagil Formation
<b>r-26</b>	Greenish brown dolomitic mudstone	Upper Permian, Hagil Formation
<b>r-27</b>	Greenish brown lime-mudstone	Middele Permain, Bih Formation
<b>r-28</b>	Greenish brown lime- mudstone	Middele Permain, Bih Formation
<b>r-29</b>	Greenish brown lime-mudstone	Middele Permain, Bih Formation
<b>r-30</b>	Gray laminated siltstone	Middele Permain, Bih Formation



Plate 2.1 Rocks samples: JH-1 and JH-3 from A-2, and r-4 from A-4.



Plate 2.2 Rocks samples: r-5, r-8 and r-19 from A-4.

## **2.4 Analytical procedures**

### **2.4.1 Gross alpha and gross beta measurements in groundwater samples**

Gross alpha and gross beta measurements were performed in general for the purpose of samples screening. These measurements provide an overall estimate of radiation. The measurement procedures are as Lehto & Hou (2010). For these measurements, a 100 ml water sample was transferred to a glass beaker and then evaporated on a hot plate at 200 °C in the beginning and at 100 °C when the water volume was reduced to less than 20 ml to avoid any spattering. After evaporated to near dryness, the residue was dissolved with water to a final volume of 5-15 ml. A mixture of 4 ml of the concentrated solution and 16 ml of Ultima Gold LLT scintillation cocktail was added to the LSC vial. The mixing solution was placed in dark and cooled for 1 hour and the measurements were done using the Quantulus 1220 liquid scintillation counter for 60 minutes each sample for 3 cycles. Detection limits were 0.01 Bq/L for gross- $\alpha$  and 0.03 Bq/L for gross- $\beta$ . The principle of this instrument is based on measuring photons which result from the interaction between emitted radiations ( $\alpha$  or  $\beta$ ) and the scintillation cocktail (i.e. the function of cocktail is transferring the radiation of photons). The measured photons energy was then translated into counts and radiation through use of standards (Hou & Roos, 2008).

#### 2.4.2 $^{226}\text{Ra}$ measurements in groundwater samples

The measurements of  $^{226}\text{Ra}$  was performed after the precipitation as  $\text{Ba}(\text{Ra})\text{SO}_4$  from 500 ml water using  $\text{BaCl}_2$  carrier and 20 Bq  $^{133}\text{Ba}$  as chemical yield tracer (Lehto & Hou, 2010). The  $\text{Ba}(\text{Ra})\text{SO}_4$  precipitate was washed with water and then dissolved with 5 ml of 1M EDTA solution (pH=9) in a hot water bath, and the solution was then transferred to a low diffusion LSC vial. An amount of 10 ml of Opti-Flour O liquid scintillation cocktail was then added. The vial was kept for more than 7 days for ingrowth of  $^{222}\text{Rn}$  from  $^{226}\text{Ra}$  and then counted using Quantulus 1220 liquid scintillation counter for 60 minutes of each sample for 3 cycles. The result was corrected for blank count rate, in-growth of  $^{222}\text{Rn}$  from  $^{226}\text{Ra}$  between  $^{226}\text{Ra}$  separation and counting and quenching.

#### 2.4.3 $^{222}\text{Rn}$ measurements in groundwater samples

For  $^{222}\text{Rn}$  measurement, 10 ml of water was directly sampled into a 20 mL low diffusion LSC vial prefilled with 10 ml of Opti-Fluor O liquid scintillation cocktail (Perkin Elmer). After being mixed, the activity of  $^{222}\text{Rn}$  was measured by Quantulus 1220 liquid scintillation counter using  $\alpha/\beta$  discrimination function (Lehto & Hou, 2010). The  $^{222}\text{Rn}$  activity was calculated by summation of the counts of  $^{222}\text{Rn}$  and two of its short-lived progenies ( $^{218}\text{Po}+^{214}\text{Po}$ ) and then corrected for both blank and decay, as well as counting efficiency considering the counting of  $^{222}\text{Rn}$  and 2 of its daughter radionuclides.



#### 2.4.4 $^{235}\text{U}$ , $^{238}\text{U}$ , $^{232}\text{Th}$ and $\text{Cl}^-$ measurements in groundwater samples

The measurement of  $^{238}\text{U}$ ,  $^{235}\text{U}$ ,  $^{232}\text{Th}$  and  $\text{Cl}^-$  was performed after the addition of 0.20 ml of 100 mg/ml In(III) (as  $\text{InCl}_3$ ) as internal standard and 10 times dilution with 3%  $\text{HNO}_3$  (super pure). Standards were prepared using the similar method as samples by dilution of uranium, thorium and chloride standard solutions (purchased from National Institute of Standard technology, USA) with 3%  $\text{HNO}_3$  (super pure). Indium solution, as internal standard, was also added to the standard solution. The concentrations of target analytes (e.g.  $^{238}\text{U}$ ,  $^{235}\text{U}$ ,  $^{232}\text{Th}$  and  $\text{Cl}^-$ ) and internal standard (i.e.  $^{115}\text{In}$ ) in the samples and standards were measured using an inductively coupled plasma mass spectrometry (ICP-MS) system (X Series<sup>II</sup>), Thermo Fisher Scientific, Waltham, MA) equipped with an Xt-skimmer cone and a concentric nebulizer under hot plasma conditions. The concentrations of  $^{235}\text{U}$ ,  $^{238}\text{U}$ ,  $^{232}\text{Th}$  and  $\text{Cl}^-$  in the samples were calculated by comparing with standard and correction for introduction efficiency using indium internal standard. The detection limits calculated as three times of the standard deviation ( $3\sigma$ ) of the processing blank are 0.21 mg/L for  $\text{Cl}^-$ , 1.2 mBq/L, for  $^{232}\text{Th}$ , 0.37mBq/L, for  $^{235}\text{U}$  and 0.95 mBq/L for  $^{238}\text{U}$ . A 0.5 mol/L  $\text{HNO}_3$  solution was used as a washing solution among consecutive assays. No carry-over (memory effect) was observed for consecutive analysis of samples differing in U and Th concentrations up to three orders of magnitude. The accuracy estimate is  $\pm 2.5\%$ , and precision around 0.5%.

The principle of the ICP-MS (Fig. 2.9) is that the elements in their different chemical compounds contained in the sample solution are decomposed into their atomic constituents in an inductively coupled argon plasma at a plasma temperature of approximately 6000–8000 K (about 5700 – 7700 °C) and ionized. This means that the ICP source alters the atoms of the elements into ions, and these ions are then detected by the mass spectrometer. The positively charged ions are extracted from the inductively coupled plasma (at atmospheric pressure) into the high vacuum of the mass spectrometer via an interface (Montaser, 1998). Note that the ions created by the ICP discharge are completely positive ions, thus the elements that form mainly negative ions, are usually not determined via ICP-MS (USGS, 2005). However, in this study  $\text{Cl}^-$  was determined using ICP-MS, where chlorine was injected to the plasma, at a temperature of a few thousands Kelvin in plasma, and the chloride was atomized and then ionized to positive ion, which were separated in the quadrupole and finally measured in the detector. The detection limits of the ICP-MS ranges at  $(0.01 - 0.6) \text{ ng L}^{-1}$  (Becker, 2003), The accuracy estimate is  $\pm 2.5\%$ .



Fig. 2.9 The ICP-MS instrument used for uranium and thorium mass concentrations at the Technical University of Denmark (Center for Nuclear Technologies, Risø campus).

#### **2.4.5 Na<sup>+</sup> and K<sup>+</sup> measurements in groundwater samples**

The analyses of cations (Na<sup>+</sup> and K<sup>+</sup>) were conducted using inductively coupled plasma optical emission spectroscopy (ICP-OES-Varian 715 instrument). A water sample was directly injected into the nebulizer and spectral analysis of each element was standardized using a multi-element standard solution GSC-CAL-8 provided by Inorganic Ventures. The analytical error of all samples is <5%, while the detection limit was in the range of 0.001 to 0.017 mg/l.

#### **2.4.6 <sup>235</sup>U, <sup>238</sup>U and <sup>232</sup>Th measurements in rock samples**

All rock samples were crushed into small pieces by hammer and then powdered using electric molder. The rock samples in general were kept in the molder 30 minutes, while the clay rocks were totally powdered in 10 minutes. From each sample, 0.1-0.2 g of powder was transferred to a teflon beaker 3 ml of HF and 3 mL of HNO<sub>3</sub> were added to the rock powder and mixed, which was refluxed under heating on a hot plate at 100-150 °C. The sample was kept on the hot plate until totally dry, followed by HF and HNO<sub>3</sub> addition in a repeated sequence until no more residue appeared in the solution (Fig 2.10). A 3 ml of super pure HNO<sub>3</sub> was added and the sample was heated on the hot plate until total dryness to remove remaining HF (Lehto & Hou, 2010).



Fig. 2.10 The rock sample with no residue (looks like dry salt) after 3 times repetition of HF and HNO<sub>3</sub> addition.

The residue was then dissolved with 3 ml of 3% HNO<sub>3</sub> and the solution was filtered through a filter paper, and the leachate was transferred to a 20 ml vial, transferred and filtered into the vial. The solution in the vial was treated as the groundwater sample in the previous section for measurements of isotopes of U and Th, using ICP-MS.

#### **2.4.7 <sup>235</sup>U, <sup>238</sup>U and <sup>232</sup>Th measurements in sediment samples**

The sediment samples were dried under the room temperature conditions for three days and were powdered using electric molder. Subsequently, the sediments were heated in the ovens at 500 °C for 8 hours in order to remove the organic matter from the sample. Then 0.1-0.2 g of each sample was put into a

teflon beaker and the steps that were used for the rocks in the previous section were followed.

#### **2.4.8 Major cations measurements in rocks and sediments**

An amount of 0.1 g powdered sample was fused with 0.4 g  $\text{LiBO}_2$  at a temperature of  $1000^\circ\text{C}$  for about 15 minutes in a graphite crucible. The resulting mixture bead was dissolved with 25ml 5%  $\text{HNO}_3$ . The aliquot was measured using inductively coupled plasma sector field mass spectrometry (ICP-SFMS) at the ALS Scandinavia AB, Sweden with a total analytical error at  $< 2\%$ . To calculate level of volatility, in particular  $\text{CO}_2$ , the sample was ignited at  $1000^\circ\text{C}$  (LOI).

#### **2.5 Statistical analyses and mapping**

Statistical analyses were applied to the analytical results to clarify the outputs and build up accurate relations across the observed and predicted parameters in this study. Mapping was also performed to present the variations through radioactivity concentrations and the distribution of the isotopes of the elements in the sampled wells. The Minitab software was used to complete the statistics analyses, while mapping was done by ArcGIS software.

Statistical analyses included calculating the Pearson correlation coefficient as well as the factor analysis. Pearson correlation coefficient (R) measures the linear dependence (correlation) between two variables giving a value between -1 and +1, where -1 is total negative correlation, 0 means no correlation, and

+1 is total positive correlation. A weak correlation is considered if  $0 < |R| < 0.5$ , moderate correlation is assumed if  $0.5 < |R| < 0.8$ , and strong correlation is supposed if  $0.8 < |R| < 1$  (Olea & Olea, 1999). The R value was used to interpret the natural interactions and chemical affinities between the different parameters in this study. On the other hand, factor analysis is defined as grouping comparable variables into groups called factors. Correlated variables usually cluster in a similar position forming a group that is supposed to be controlled by a common factor, i.e. these variables load onto one factor. Therefore, the term “Factor loading” is used to show which variables load into each factor (Kim & Mueller, 1978). In this study, factor analysis was used as a tool for predicting approximately which chemical parameters are related to each other and if one factor or more stands behind the variations among the chemical parameters in different areas.

Creating maps was accomplished by joining an Excel file containing the UTM of each well, as well as the measurement of each chemical parameter in each well. The well was located on the map and then the measurements were quantified relatively using symbols with different sizes where each symbol size defines certain range of concentrations. In this study, each map represents the sampling locations and summarizes the distribution of certain sources of radiation in the UAE. Such a map is helpful to build up an interpretation of the variability in concentrations in terms of geographical location and the well distance from the sea shore.

## 3 RESULTS

### 3.1 General properties of groundwater

The pH, temperature, TDS and concentrations of  $\text{Cl}^-$ ,  $\text{Na}^+$  and  $\text{K}^+$  for the analyzed water samples are presented in Table 3.1. The pH shows a range covering neutral to slightly basic values (7.1–8.8). The temperature of the water varies from about 27.8 °C to 49°C, while TDS values span between 142 mg L<sup>-1</sup> and 12770 mg L<sup>-1</sup> (average: 3394 mg L<sup>-1</sup>). The distribution of groundwater TDS in the investigated areas is illustrated in Fig. 3.1. The TDS concentrations of the groundwater in the emirate of Abu Dhabi (including A-1, A-2 and A-5) are comparable with the concentrations found by the Environment Agency- Abu Dhabi in 2008 presented previously in Fig. 2.3. Variability in  $\text{Cl}^-$  spans between 33 mg L<sup>-1</sup> to 9920 mg L<sup>-1</sup> (average: 2089 mg L<sup>-1</sup>), while the  $\text{Na}^+$  and  $\text{K}^+$  range at (20.9 – 3091.0) mg L<sup>-1</sup> and (0.01 – 86.09) mg L<sup>-1</sup> with averages of 643.9 mg L<sup>-1</sup> and 16.62 mg L<sup>-1</sup>, respectively.

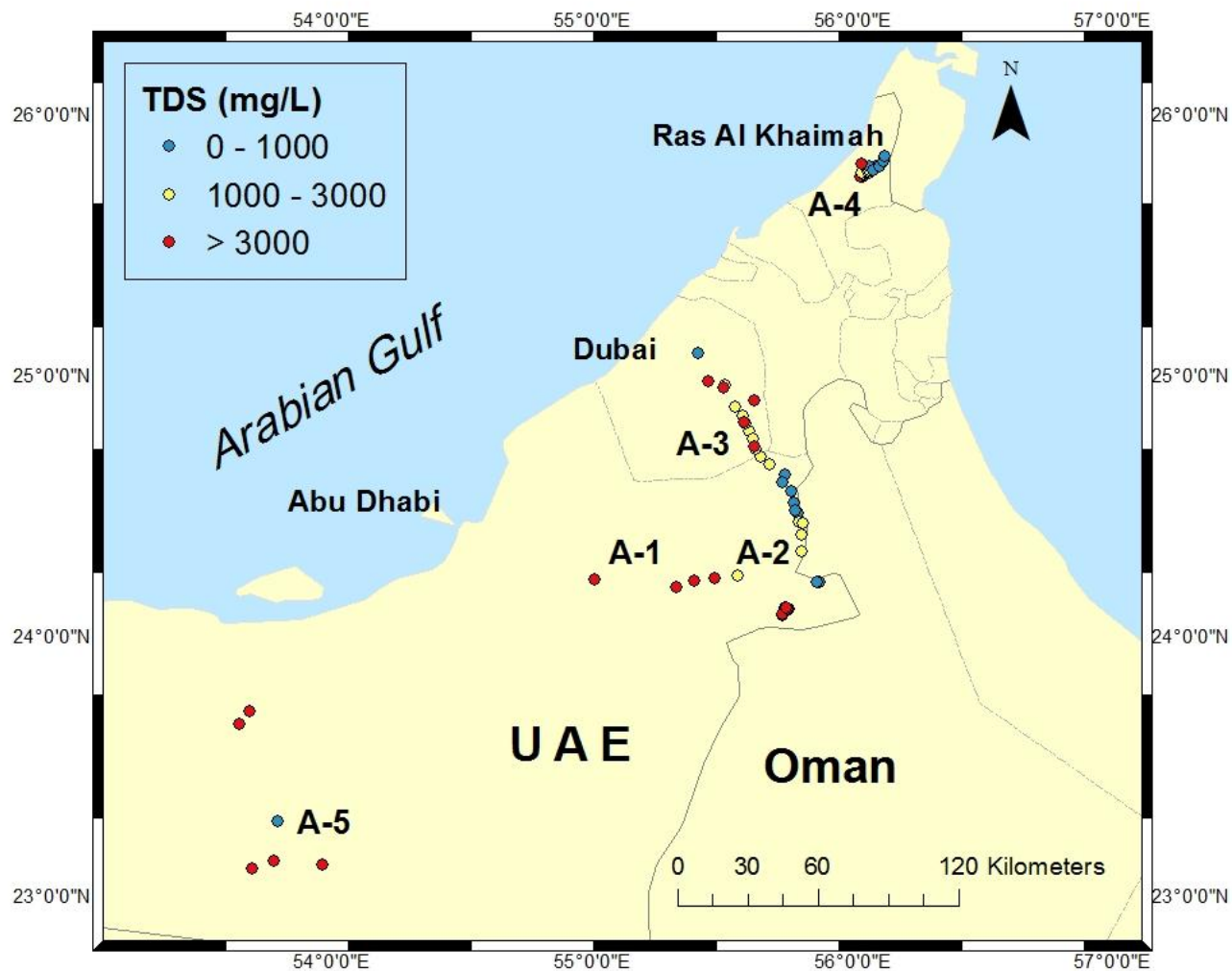


Fig. 3.1 The TDS distribution in the investigated areas.



Table 3.1 Sampling location and groundwater features including pH, temperature, TDS, Cl, Na and K.

Sample #	Sample ID	UTM (E)	UTM (N)	pH	Temperature °C	TDS (mg L <sup>-1</sup> )	Cl <sup>-</sup> (mg L <sup>-1</sup> )	Na <sup>+</sup> (mg L <sup>-1</sup> )	K <sup>+</sup> (mg L <sup>-1</sup> )
<b>A-1</b>	<b>Abu Dhabi-Al Ain road</b>								
1	AD-1	353302	2680076	8.6	32.4	1955	469	411.7	7.71
2	AD-2	344134	2679008	8	35.8	5310	1702	1158.4	37.4
3	AD-3	336559	2678041	8.2	35.3	4270	1218	979.8	20.71
4	AD-4	329139	2675454	8.3	32	4908	988	893.5	13.49
5	AD-6	297385	2679213	7.8	30.9	9890	2449	3091	0.01
<b>A-2</b>	<b>Jabel Hafit</b>								
6	Ma-1	375534	2711071	8.4	35	199	NM	54.7	3.12
7	MO-1	374768	2715691	8.5	34.1	251	NM	73.1	3.13
8	HY-1	372069	2723052	8.2	33.2	326	NM	71.4	4.61
9	Ja-1	371181	2719878	8.2	33.8	326	NM	111.1	5.32
10	SHB-1	376819	2706480	8.1	31.6	481	NM	152.2	11.69
11	EZ-1	376207	2707686	8.1	33.6	745	NM	131.3	6.96
12	MK-1	377423	2702654	7.7	30.8	1299	NM	246	10.39

Sample #	Sample ID	UTM (E)	UTM (N)	pH	Temperature °C	TDS (mg L <sup>-1</sup> )	Cl <sup>-</sup> (mg L <sup>-1</sup> )	Na <sup>+</sup> (mg L <sup>-1</sup> )	K <sup>+</sup> (mg L <sup>-1</sup> )
13	MK-2	379070	2702337	8	34	1480	NM	403.1	9.45
14	FO-1	378277	2690607	7.8	33.4	2084	NM	524	13.13
15	Gh-1	378521	2697207	7.8	32.8	1689	NM	276.8	10.16
16	GWW-58	372788	2665600	8.8	46.9	6080	NM	NM	NM
17	ADD0911078	373094	2665913	8.2	49	6100	NM	NM	NM
18	GWW-47	371506	2666511	8.1	32.5	6940	NM	NM	NM
19	ADD0911076	372277	2666541	8.1	34.6	7040	NM	NM	NM
20	GWW-F1	370885	2663116	8.2	33.4	7200	NM	NM	NM
21	GWW-F	370657	2663966	8	34.8	7300	NM	NM	NM
22	ADD0911080	372642	2665702	8.5	44.9	8700	NM	NM	NM
23	GWW-53	372370	2666667	8.5	34.5	8900	NM	NM	NM
24	GWW-Jaw, 1	385251	2677000	8.8	35.3	354	NM	NM	NM
25	GWW-Jaw, 2	384216	2677310	8.5	33.2	247	NM	NM	NM
<b>A-3</b>	<b>Al Ain-Dubai road</b>								
26	Kh-1	366369	2727640	8.1	32.1	1040	NM	380.1	17.55

Sample #	Sample ID	UTM (E)	UTM (N)	pH	Temperature °C	TDS (mg L <sup>-1</sup> )	Cl <sup>-</sup> (mg L <sup>-1</sup> )	Na <sup>+</sup> (mg L <sup>-1</sup> )	K <sup>+</sup> (mg L <sup>-1</sup> )
27	MQ-1	358665	2741848	8.4	32.1	1190	NM	634.9	14.18
28	FQ-1	362995	2731012	8.1	33.6	1230	NM	820.2	13.86
29	US-1	355953	2748498	8.1	30.4	1250	NM	626.4	16.75
30	GS-1	353131	2751866	8.3	31.8	1320	NM	620.2	12.92
31	Yh-1	359981	2738171	8.4	32.1	1500	NM	844.6	13.44
32	MQ-2	356807	2745234	8.4	30.8	1860	NM	194.8	25.24
33	FQ-2	360970	2733806	8.1	30.6	2610	NM	1329.7	37.2
34	Mm-1	349424	2761392	8.1	30.6	2830	NM	1133.7	24.15
35	LS-1	342825	2763065	7.9	32.8	5840	NM	1501.7	51.12
36	Mgm-1	360766	2754718	7.8	29.1	5920	NM	2265.4	86.09
37	LS-2	348573	2760379	7.8	30.4	3470	NM	1325.9	37.75
38	MQ-3	356337	2745664	8.2	33.4	3640	NM	1297.1	42.3
39	Rw-1	339214	2775281	7.4	28.9	4150	NM	2712.6	36.43
40	FQ-3	360384	2735288	7.7	32.9	4540	NM	1718.1	43.99
41	Bal-1	339078	2775137	8.6	32.5	570	NM	258.3	7.59

Sample #	Sample ID	UTM (E)	UTM (N)	pH	Temperature °C	TDS (mg L <sup>-1</sup> )	Cl <sup>-</sup> (mg L <sup>-1</sup> )	Na <sup>+</sup> (mg L <sup>-1</sup> )	K <sup>+</sup> (mg L <sup>-1</sup> )
<b>A-4</b>	<b>Wadi Al Bih</b>								
42	R-KH01	403711	2850942	8.4	35.4	1510	834	413.6	10.07
43	R-KH02	403589	2849530	7.8	35.7	6600	170	170.6	5.71
44	R-KH03	402635	2849717	7.1	34.6	6400	3834	46.8	31.09
45	R-KH04	403887	2851103	7.6	35.7	1329	887	416.5	10.54
46	R-KH05	404577	2851081	7.5	36.2	1800	994	453.8	11.22
47	R-KH06	404555	2851588	7.2	35	1690	1242	558.4	13.31
48	R-KH07	405098	2851144	7.6	36.8	1596	1278	522.7	11.92
49	R-KH08	408561	2853735	8	33.4	237	46	38	3.45
50	R-KH10	403377	2850866	7.7	36.4	1268	880	398.5	9.76
51	R-KH11	403196	2851429	7.8	35.6	1563	986	475.9	11.53
52	R-KH12	405935	2850976	7.1	36.2	1099	717	347.8	9
53	R-KH13	405233	2851739	7.3	35.2	2730	1491	654	18
54	R-KH14	405789	2852053	7.7	36.5	2200	1420	595.6	13.01
55	R-KH15	406728	2853143	8.1	35.2	310	106	107.1	4.94

Sample #	Sample ID	UTM (E)	UTM (N)	pH	Temperature °C	TDS (mg L <sup>-1</sup> )	Cl <sup>-</sup> (mg L <sup>-1</sup> )	Na <sup>+</sup> (mg L <sup>-1</sup> )	K <sup>+</sup> (mg L <sup>-1</sup> )
56	R-KH16	406153	2853900	7.5	33.6	900	319	162.2	10.33
57	R-KH17	407252	2852160	7.8	35.8	414	156	133.5	5.45
58	R-KH18	409690	2854120	7.5	34.1	142	NM	22.1	2.88
59	R-KH19	411196	2855958	7.9	38.4	155	33	20.9	3.74
60	R-KH20	411668	2858249	7.9	33.9	229	120	77.7	5.03
61	R-KH21	402764	2854872	7.3	32.4	3955	2591	983.4	18.88
A-5	<b>Liwa Oasis</b>								
62	W-1	773125	2624541	NM	27.8	9294	6390	NM	NM
63	W-2	769452	2618721	NM	28.7	12770	9920	NM	NM
64	W-3	784056	2560995	NM	32	10650	7110	NM	NM
65	W-4	775503	2557671	NM	30.8	10300	6700	NM	NM
66	W-5	802838	2559879	NM	29.7	10330	7215	NM	NM
67	W-6	784890	2577879	NM	29.7	933	403	NM	NM

NM: not measured.

### 3.2 $^{235}\text{U}$ and $^{238}\text{U}$ in groundwater

The results of uranium isotopes as activity and mass concentration are presented in Table 3.2. In the five sampling areas, the  $^{235}\text{U}$  and  $^{238}\text{U}$  activity values in groundwater show high variability with ranges of 0.010 – 40.67 mBq L<sup>-1</sup> (average: 4.500 mBq L<sup>-1</sup>) and 0.32- 858.54 mBq L<sup>-1</sup> (average: 95.37 mBq L<sup>-1</sup>) respectively, equivalent to mass concentration ranges of 0.12 - 508.38 ng L<sup>-1</sup> (average: 16.82 ng L<sup>-1</sup>) and 25 – 69237 ng L<sup>-1</sup> (average: 2291 ng L<sup>-1</sup>) respectively. The highest uranium concentration occurs in sample (Rw-1) in A-3, and the lowest exists in sample (GWW-Jaw, 2) in A-2. The variability of uranium concentrations is not restricted to a certain area, but a wide range appears in all the investigated areas (Figs. 3.2 and 3.3). The calculated correlation coefficient (R) between  $^{235}\text{U}$  and  $^{238}\text{U}$  is almost equal to one and the ratio of  $^{235}\text{U} / ^{238}\text{U}$  is around 0.007.

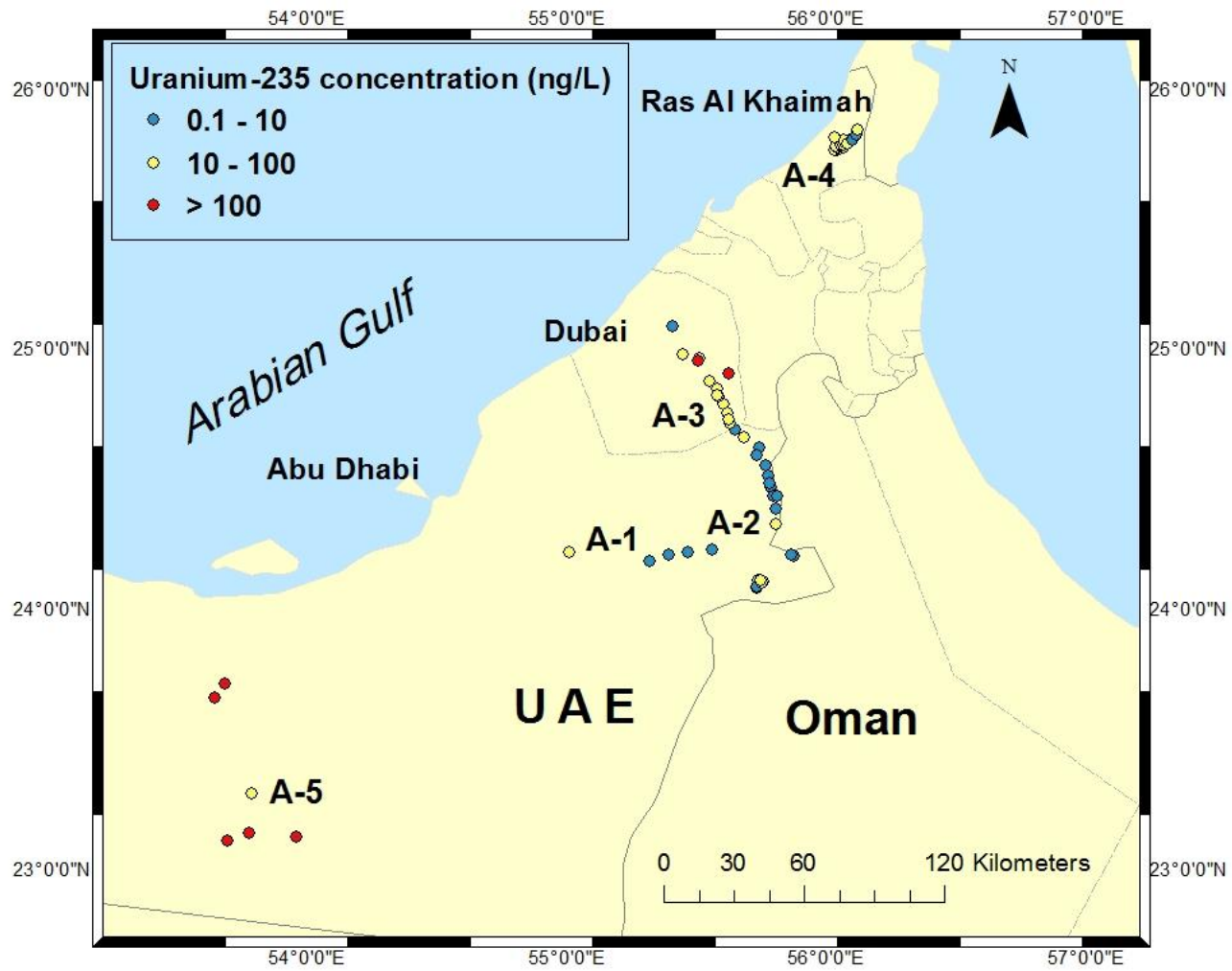


Fig. 3.2 The distribution of  $^{235}\text{U}$  concentration in groundwater of the investigated areas.

Table 3.2 Uranium, thorium, gross  $\beta$  and gross  $\alpha$  concentrations in groundwater samples.

Sample #	Sample ID	<sup>235</sup> U mBq L <sup>-1</sup>	<sup>238</sup> U mBq L <sup>-1</sup>	<sup>232</sup> Th $\mu$ Bq L <sup>-1</sup>	<sup>235</sup> U ng L <sup>-1</sup>	<sup>238</sup> U ng L <sup>-1</sup>	<sup>232</sup> Th ng L <sup>-1</sup>	Gross $\beta$ Bq L <sup>-1</sup>	Gross $\alpha$ Bq L <sup>-1</sup>
<b>A-1</b>	<b>Abu Dhabi-Al Ain road</b>								
1	AD-1	0.19	4.14	NM	2.37	333	NM	2.05	0.17
2	AD-2	0.1	2.02	NM	1.25	162	NM	3.02	0.16
3	AD-3	0.25	5.37	NM	3.12	433	NM	2.93	0.13
4	AD-4	0.32	6.99	NM	4.00	563	NM	2.14	0.16
5	AD-6	5.87	123.56	NM	73.37	9964	NM	6.63	0.53
<b>A-2</b>	<b>Jabel Hafit</b>								
6	Ma-1	0.029	0.62	2.54	0.36	50	0.626	0.3	0.09
7	MO-1	0.039	0.83	40.87	0.49	67	10.066	0.25	0.08
8	HY-1	0.124	2.61	6.32	1.55	210	1.557	0.62	0.08
9	Ja-1	0.122	2.61	4.31	1.52	210	1.061	0.48	0.08
10	SHB-1	0.132	2.84	9.48	1.65	228	2.334	0.82	0.08



Sample #	Sample ID	<sup>235</sup> U mBq L <sup>-1</sup>	<sup>238</sup> U mBq L <sup>-1</sup>	<sup>232</sup> Th μBq L <sup>-1</sup>	<sup>235</sup> U ng L <sup>-1</sup>	<sup>238</sup> U ng L <sup>-1</sup>	<sup>232</sup> Th ng L <sup>-1</sup>	Gross β Bq L <sup>-1</sup>	Gross α Bq L <sup>-1</sup>
11	EZ-1	0.09	1.9	2.29	1.12	153	0.564	0.63	0.08
12	MK-1	0.463	9.81	2.56	5.78	790	0.63	0.95	0.08
13	MK-2	0.232	4.97	1.66	2.90	401	0.409	0.85	0.08
14	FO-1	1.373	29.1	7.2	17.16	2347	1.773	1.04	0.08
15	Gh-1	0.428	9.03	24.27	5.35	728	5.978	1.02	0.08
16	GW-58	0.92	18.3	3050	11.5	1475	751.232	5.23	19.50
17	ADD0911078	0.99	19.55	3370	12.37	1576	830.049	4.22	16.50
18	GW-47	2.54	52.72	<0.04	31.75	4251	<0.01	3.65	1.17
19	ADD0911076	2.60	55.16	<0.04	32.50	4448	<0.01	4.12	4.29
20	GW-F1	0.28	5.32	<0.04	3.50	429	<0.01	3.84	5.60
21	GW-F	0.29	6.51	<0.04	3.62	525	<0.01	4.88	10.50
22	ADD0911080	1.24	25.32	10270	15.50	2041	2529	5.81	12.80
23	GW-53	3.12	64.72	8810	39.00	5219	2169	3.51	3.76
24	GW-Jaw, 1	0.03	0.68	<0.04	0.37	54	<0.01	0.23	0.01

Sample #	Sample ID	<sup>235</sup> U mBq L <sup>-1</sup>	<sup>238</sup> U mBq L <sup>-1</sup>	<sup>232</sup> Th μBq L <sup>-1</sup>	<sup>235</sup> U ng L <sup>-1</sup>	<sup>238</sup> U ng L <sup>-1</sup>	<sup>232</sup> Th ng L <sup>-1</sup>	Gross β Bq L <sup>-1</sup>	Gross α Bq L <sup>-1</sup>
25	GWJW-Jaw, 2	0.01	0.32	<0.04	0.12	25	<0.01	0.33	0.01
<b>A-3</b>	<b>Al Ain-Dubai road</b>								
26	Kh-1	1.10	22.79	NM	13.75	1837	NM	0.67	0.09
27	MQ-1	1.36	28.65	NM	17.00	2310	NM	2.3	0.17
28	FQ-1	0.61	13.14	NM	7.62	1059	NM	2.13	0.22
29	US-1	2.56	53.46	NM	32.00	4311	NM	2.33	0.24
30	GS-1	1.44	29.49	NM	18.00	2378	NM	0.33	0.03
31	Yh-1	1.57	33.13	NM	19.62	2671	NM	2.22	0.19
32	MQ-2	4.26	88.22	NM	53.25	7114	NM	2.68	0.22
33	FQ-2	2.01	42.19	NM	25.12	3402	NM	3.15	0.2
34	Mm-1	3.12	64.19	NM	39.00	5176	NM	2.85	0.19
35	LS-1	2.23	44.45	NM	27.87	3584	NM	0.71	0.09
36	Mgm-1	27.26	572.52	NM	340.75	46170	NM	3.45	0.28
37	LS-2	15.50	324.31	NM	193.75	26154	NM	1.12	0.08

Sample #	Sample ID	<sup>235</sup> U mBq L <sup>-1</sup>	<sup>238</sup> U mBq L <sup>-1</sup>	<sup>232</sup> Th μBq L <sup>-1</sup>	<sup>235</sup> U ng L <sup>-1</sup>	<sup>238</sup> U ng L <sup>-1</sup>	<sup>232</sup> Th ng L <sup>-1</sup>	Gross β Bq L <sup>-1</sup>	Gross α Bq L <sup>-1</sup>
38	MQ-3	5.96	123.61	NM	74.50	9968	NM	1.37	0.12
39	Rw-1	40.67	858.54	NM	508.38	69237	NM	1.99	0.03
40	FQ-3	4.23	85.76	NM	52.87	6916	NM	1.35	0.08
41	Bal-1	0.43	8.57	NM	5.37	691	NM	0.21	0.33
<b>A-4</b>	<b>Wadi Al Bih</b>								
42	R-KH01	1.477	31.1	21.81	18.46	2508	5.372	1.08	0.18
43	R-KH02	1.63	34.31	22.82	20.37	2766	5.621	0.56	0.13
44	R-KH03	1.711	35.85	16.99	21.39	2891	4.185	0.23	0.01
45	R-KH04	1.594	34.01	3.35	19.93	2742	0.825	1.08	0.18
46	R-KH05	1.603	33.84	2.55	20.03	2729	0.628	0.98	0.16
47	R-KH06	3.072	65.64	2.21	38.39	5293	0.544	1.22	0.16
48	R-KH07	1.782	37.82	1.49	22.27	3050	0.367	1.00	0.20
49	R-KH08	0.859	18.26	1.08	10.74	1472	0.266	0.23	0.08
50	R-KH10	1.534	32.26	0.96	19.17	2601	0.236	0.71	0.1

Sample #	Sample ID	<sup>235</sup> U mBq L <sup>-1</sup>	<sup>238</sup> U mBq L <sup>-1</sup>	<sup>232</sup> Th μBq L <sup>-1</sup>	<sup>235</sup> U ng L <sup>-1</sup>	<sup>238</sup> U ng L <sup>-1</sup>	<sup>232</sup> Th ng L <sup>-1</sup>	Gross β Bq L <sup>-1</sup>	Gross α Bq L <sup>-1</sup>
51	R-KH11	1.497	31.78	0.96	18.71	2563	0.236	1.12	0.12
52	R-KH12	1.615	34.27	23.68	20.19	2764	5.832	0.83	0.17
53	R-KH13	6.875	146.3	19.27	85.94	11798	4.746	0.30	0.10
54	R-KH14	6.941	147.75	10.89	86.76	11915	2.682	1.40	0.50
55	R-KH15	1.547	32.78	3.79	19.33	2643	0.933	0.4	0.08
56	R-KH16	2.275	48.32	60.38	28.44	3897	14.87	0.99	0.17
57	R-KH17	1.677	35.72	1.87	20.96	2881	0.46	0.58	0.11
58	R-KH18	0.370	7.79	1.11	4.63	628	0.273	0.23	0.04
59	R-KH19	0.526	11.09	10.87	6.57	894	2.677	0.16	0.08
60	R-KH20	1.187	25.3	1.06	14.84	2040	0.261	0.33	0.09
61	R-KH21	3.659	77.68	1.83	45.74	6264	0.451	0.25	0.08
<b>A-5</b>	<b>Liwa Oasis</b>								
62	W-1	11.306	241.47	2862.00	141.34	19473	705	1.71	0.2
63	W-2	23.592	507.26	1583.00	294.91	40908	390	2.65	0.33

Sample #	Sample ID	<sup>235</sup> U mBq L <sup>-1</sup>	<sup>238</sup> U mBq L <sup>-1</sup>	<sup>232</sup> Th μBq L <sup>-1</sup>	<sup>235</sup> U ng L <sup>-1</sup>	<sup>238</sup> U ng L <sup>-1</sup>	<sup>232</sup> Th ng L <sup>-1</sup>	Gross β Bq L <sup>-1</sup>	Gross α Bq L <sup>-1</sup>
64	W-3	33.408	716.48	1177.00	417.6	57780	290	2.65	0.55
65	W-4	35.798	771.88	933.80	447.48	62248	230	3.75	0.79
66	W-5	16.168	346.17	568.40	202.1	27917	140	2.71	0.50
67	W-6	1.745	37.24	203.00	21.81	3003	50	0.55	0.14

NM: not measured.

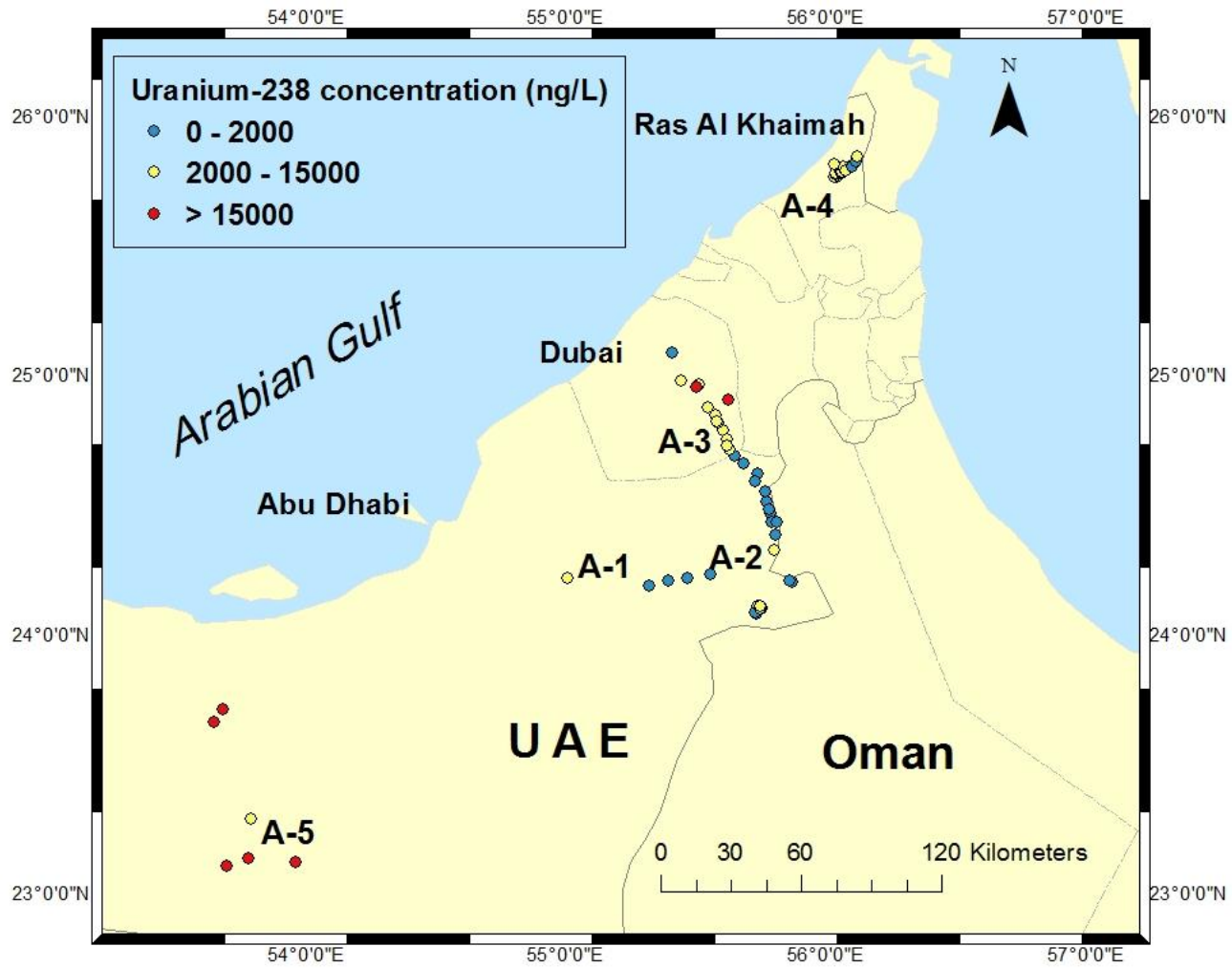


Fig. 3.3 The distribution of  $^{238}\text{U}$  concentration in groundwater of the investigated areas.

### 3.3 $^{232}\text{Th}$ in the groundwater

$^{232}\text{Th}$  was measured in three (A-2, A-4 and A-5) out of the five investigated areas, i.e. 46 samples out of 67 samples (Fig. 3.4). The  $^{232}\text{Th}$  activity spans between  $0.96 \mu\text{Bq L}^{-1}$  and  $10270 \mu\text{Bq L}^{-1}$  (average:  $828.4 \mu\text{Bq L}^{-1}$ ).  $^{232}\text{Th}$  mass concentration ranges between  $0.236 \text{ ng L}^{-1}$  and  $2529 \text{ ng L}^{-1}$  (average  $204 \text{ ng L}^{-1}$ ). The highest thorium concentration occurs in sample (ADD0911080) in A-2, and the lowest is found in sample (R-KH10 & R-KH11) in A-4.  $^{232}\text{Th}$  was below the detection limit in 6 samples in A-2.

### 3.4 Gross $\beta$ and gross $\alpha$ in groundwater

Gross  $\beta$  and gross  $\alpha$  were measured for all water samples for the purpose of future referencing rather than sample screening. Gross  $\beta$  ranges between  $0.16 \text{ Bq L}^{-1}$  to  $6.63 \text{ Bq L}^{-1}$  (average:  $1.73 \text{ Bq L}^{-1}$ ), while gross  $\beta$  is found at its highest activity in sample (AD-6) in A-1 and lowest activity in sample (R-KH19) in A-4 (Fig. 3.5). On the other hand, gross  $\alpha$  varies from  $0.01 \text{ Bq L}^{-1}$  to  $19.5 \text{ Bq L}^{-1}$  (average:  $1.25 \text{ Bq L}^{-1}$ ), with highest activity in sample (GWW-58) in A-2 and lowest activity in samples (GWW-Jaw, 1) and (GWW-Jaw, 2) in A-2 too (Fig. 3.6).

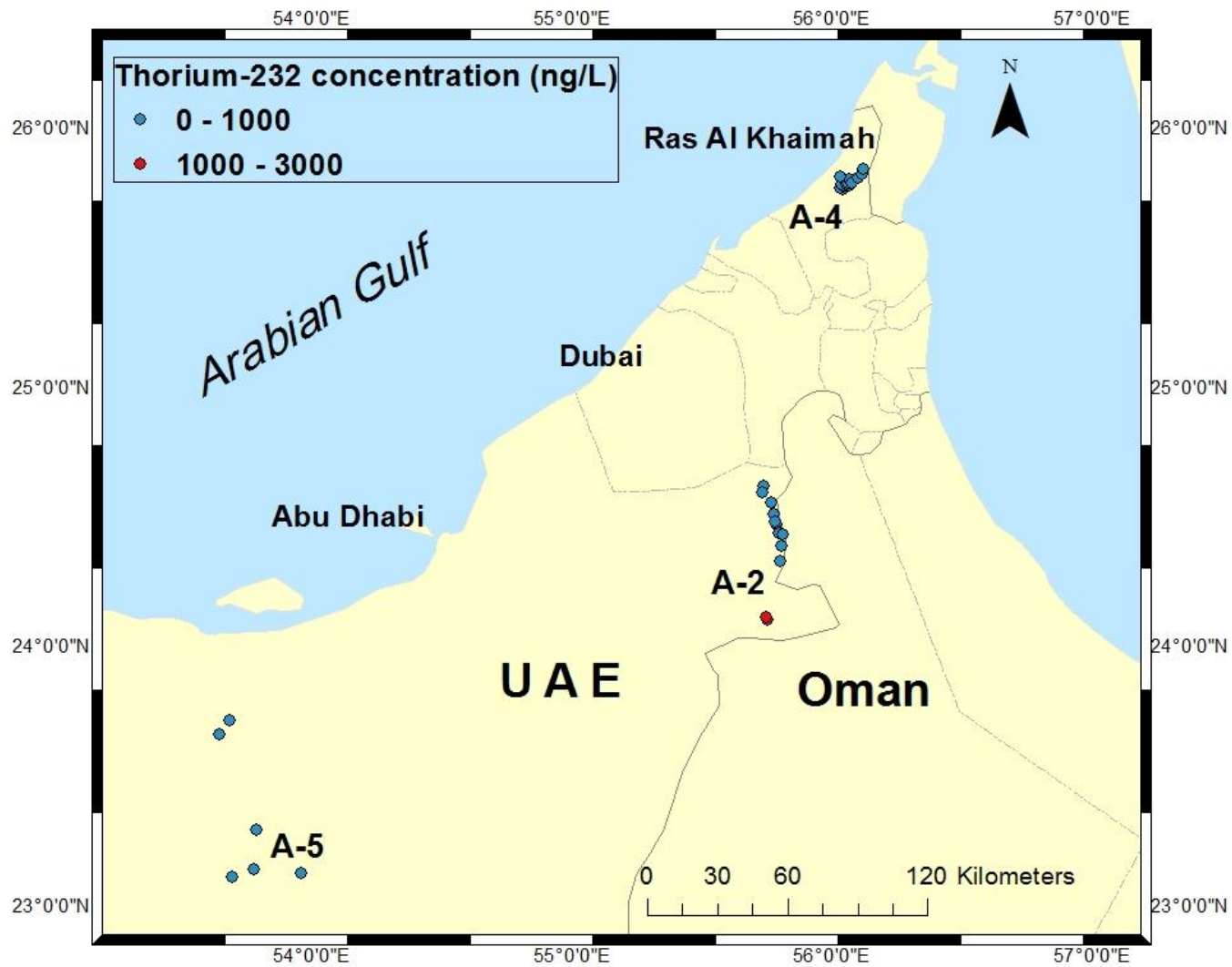


Fig. 3.4 The distribution of the  $^{232}\text{Th}$  concentration in groundwater from A-2, A-4 and A-5.



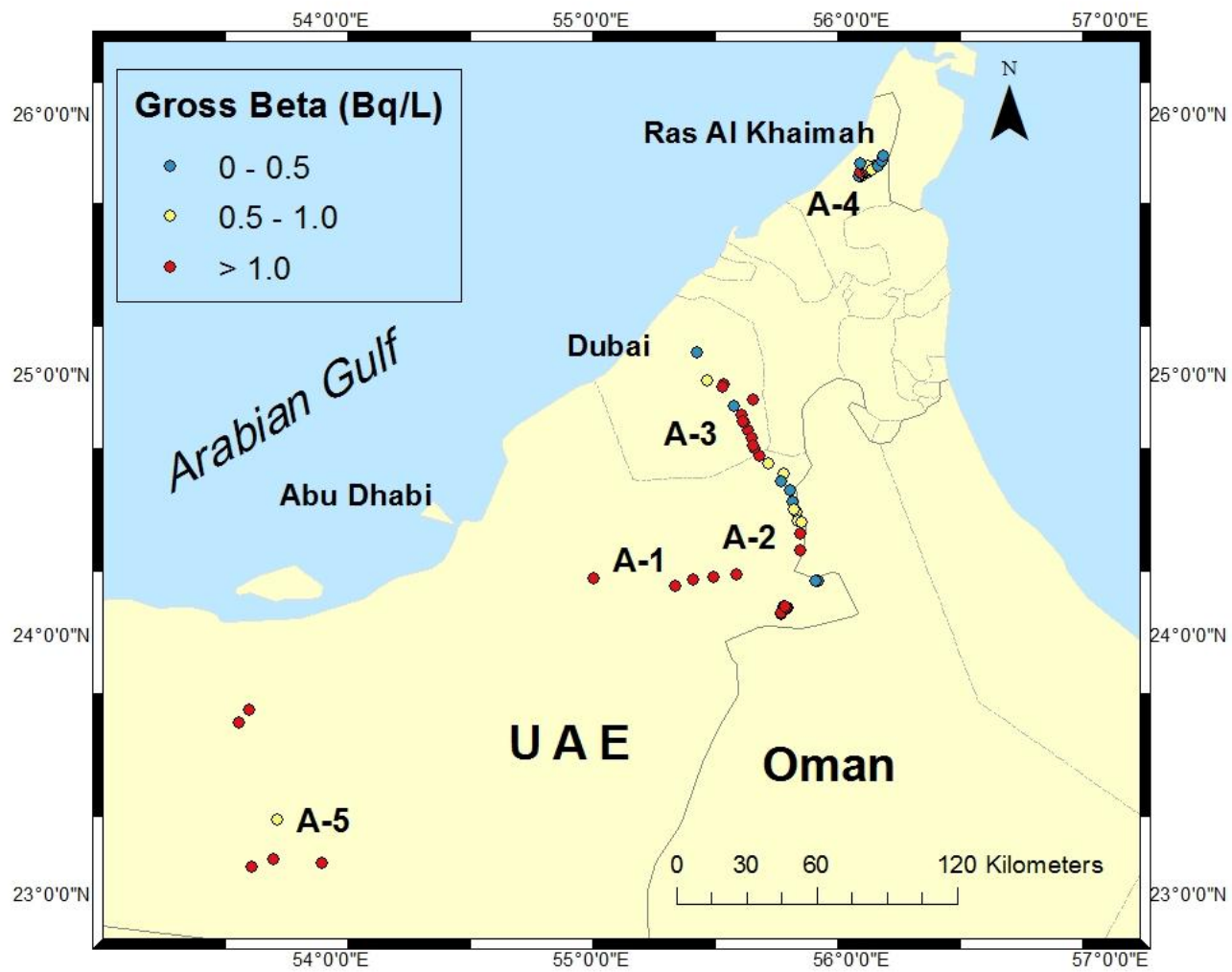


Fig. 3.5 Gross  $\beta$  distribution in the study areas.

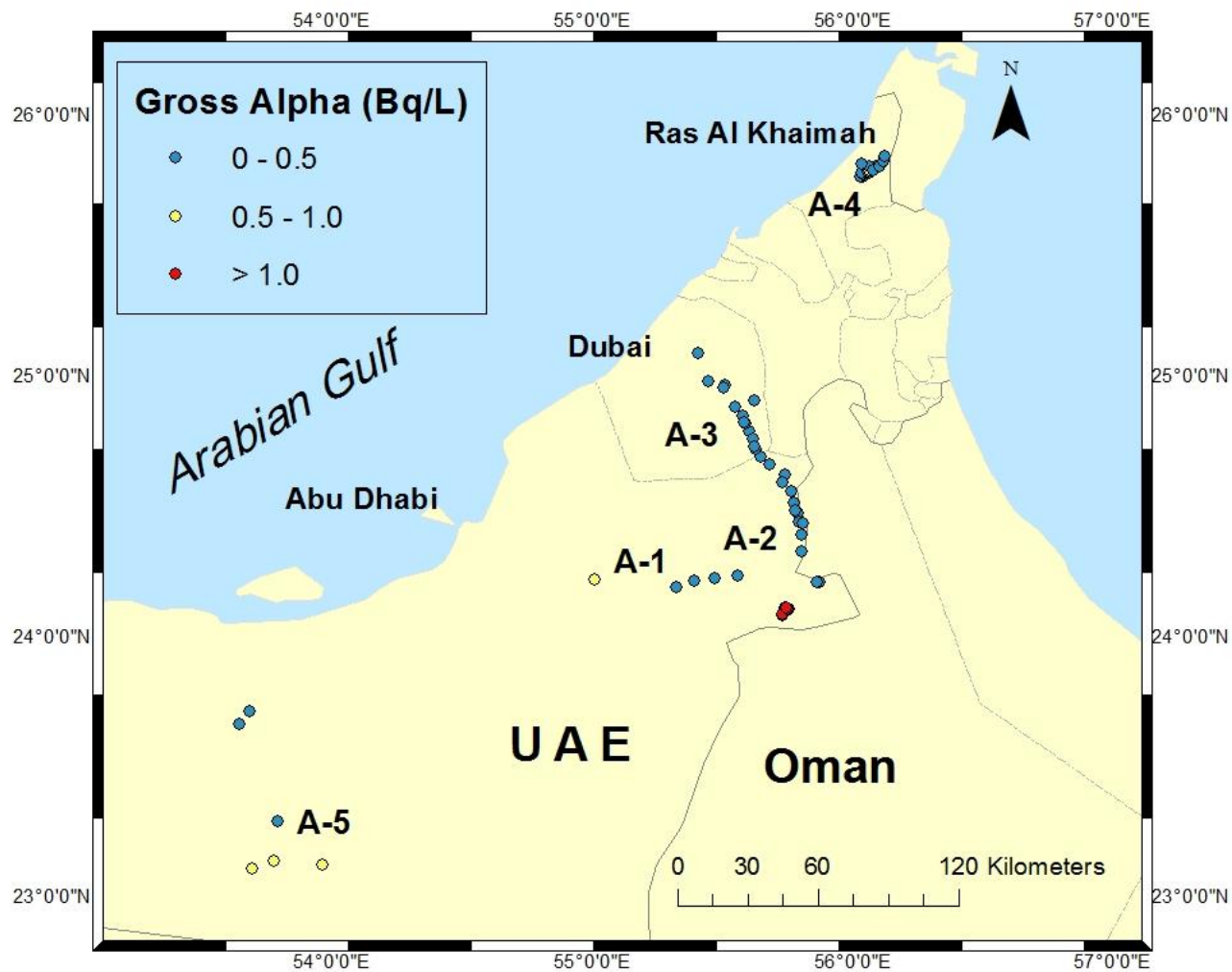


Fig. 3.6 Gross  $\alpha$  distribution in the study areas.

### 3.5 Major element chemistry of rocks and sediments

The results of major elements in selected rocks and sediments are presented in Table 3.3. The elemental composition of the rocks is dominated by  $\text{SiO}_2$  and  $\text{CaO}$  which are major indicators of rock type either sandstone or carbonate.  $\text{SiO}_2$  and  $\text{CaO}$  range in the rock samples at (0.12 – 7.6%), averages 1.6%, and (29.6 – 60.2%), averages 36.7%, respectively (some measurements were below detection limits and are excluded from ranges and averages). The highest  $\text{SiO}_2$  was found in sample (JH-2) in Jabal Hafit location in A-2. The highest  $\text{CaO}$  was measured also in A-2 in sample JH-1. The  $\text{Al}_2\text{O}_3$ ,  $\text{Fe}_2\text{O}_3$  and  $\text{K}_2\text{O}$  are indicators of mainly non-carbonate minerals, and they range at (0.04-0.58%), (0.16 – 0.31%) and (0.11 – 0.99%) respectively. The averages of  $\text{Al}_2\text{O}_3$ ,  $\text{Fe}_2\text{O}_3$  and  $\text{K}_2\text{O}$  in the sediment samples are 0.25%, 0.24% and 0.17%, respectively. The  $\text{MgO}$  might relate to the dolomite and ranges at (0.24 – 22.38%) with average 16.6%. The  $\text{MnO}_2$  ranges at (0.003 – 0.13%) and has an average of 0.007%. The  $\text{Na}_2\text{O}$  was below the detection limit in the rocks and the  $\text{P}_2\text{O}_5$  in the rocks occur in very small amounts ranging from 0.008% to 0.022% (average: 0.012%).

Table 3.3 Major elemental composition of rocks and sediments samples.

Sample ID	Sample type	SiO <sub>2</sub> %	CaO%	Al <sub>2</sub> O <sub>3</sub> %	Fe <sub>2</sub> O <sub>3</sub> %	MgO %	K <sub>2</sub> O %	MnO <sub>2</sub> %	Na <sub>2</sub> O%	P <sub>2</sub> O <sub>5</sub> %	LOI (Loss On Ignition) %	Sum of all oxides and LOI %
<b>A-2</b>	<b>Jabel Hafit</b>											
JH-1	rock	0.18	60.2	0.04	<0.1	0.24	<0.1	0.003	<0.06	<0.009	43.6	104
JH-2	rock	7.60	51.9	0.58	0.31	0.52	0.19	0.003	<0.06	0.022	39.8	100
<b>A-4</b>	<b>Wadi Al Bih</b>											
r-3	rock	<0.08	31.3	0.04	<0.1	20.22	<0.1	0.009	<0.06	<0.009	46.5	98.0
r-8	rock	0.49	32.4	0.26	0.16	21.55	0.11	0.007	<0.06	<0.009	46.5	101
r-15	rock	2.18	29.6	0.46	0.27	21.55	0.23	0.013	<0.06	0.013	45.8	100
r-20	rock	0.18	31.3	0.08	<0.1	21.88	<0.1	0.008	<0.06	0.008	46.6	99.9
r-23	rock	0.35	31.8	0.15	<0.1	21.05	<0.1	0.005	<0.06	0.0129	46.6	99.9
r-26	rock	0.12	32.1	0.09	<0.1	22.38	<0.1	0.010	<0.06	0.010	46.7	101
r-30	rock	1.84	29.6	0.52	0.23	20.55	0.20	0.006	<0.06	0.0122	45.7	98.6

Sample ID	Sample type	SiO <sub>2</sub> %	CaO%	Al <sub>2</sub> O <sub>3</sub> %	Fe <sub>2</sub> O <sub>3</sub> %	MgO %	K <sub>2</sub> O %	MnO <sub>2</sub> %	Na <sub>2</sub> O%	P <sub>2</sub> O <sub>5</sub> %	LOI (Loss On Ignition) %	Sum of all oxides and LOI %
F1 10-20	sediment	19.74	36.3	3.2	1.4	3.79	0.53	0.035	0.35	0.056	33.5	98.4
F1 20-30	sediment	18.43	37.7	2.8	1.4	3.53	0.46	0.032	0.32	0.046	34.4	98.3
F2 10-20	sediment	25.45	30.6	2.5	1.1	4.51	0.55	0.028	0.30	0.038	31.5	96.5
F2 20-30	sediment	22.03	32.1	2.8	1.2	6.23	0.53	0.029	0.29	0.039	33.0	98.0
F3 10-20	sediment	25.88	28.3	5.7	2.5	3.87	0.84	0.053	0.35	0.071	28.9	95.5
F3 20-30	sediment	28.23	24.4	6.7	2.9	3.49	0.99	0.060	0.41	0.087	26.0	93.0

Note: All the measurements were done as elemental, and then converted to oxides. Some iron oxides of hematite were not included as well as structural water was not calculated. Thus, the summation in the last column was a bit far from 100% in some samples.

In the sediment/soil samples the SiO<sub>2</sub> and CaO range at (18.4 - 28%) and (24.4 - 37%) with averages of 23.08% and 31.4%, respectively. The Al<sub>2</sub>O<sub>3</sub>, Fe<sub>2</sub>O<sub>3</sub>, MgO and K<sub>2</sub>O range at (2.5 – 6.7%), (1.1 – 2.9%), (3.5 – 6.2%) and (0.46 – 0.99%) with averages of 3.95%, 1.75%, 4.2% and 0.65%, subsequently. The MnO<sub>2</sub> ranges from 0.028% to 0.06% with average of 0.039%. The Na<sub>2</sub>O is almost ten times as the MnO<sub>2</sub> where it ranges from 0.29% to 0.4% with average of 0.33%. Finally, the P<sub>2</sub>O<sub>5</sub> in sediments varies from 0.03% to 0.087% with average of 0.054%.

### 3.6 <sup>235</sup>U, <sup>238</sup>U and <sup>232</sup>Th in rocks and sediments

The <sup>235</sup>U, <sup>238</sup>U and <sup>232</sup>Th were measured in 42 rocks and sediments samples and are presented in Table 3.4. Three rocks from A-2, thirty rocks from A-4 and nine sediments samples from A-4. The sediments were sampled from three different depths: 10, 20 and 30 cm from surface, particularly from farms which are irrigated by the sampled wells in A-4. In rocks, the <sup>235</sup>U, <sup>238</sup>U and <sup>232</sup>Th activities range at (111 - 2603) mBq g<sup>-1</sup>, (2321 - 55227) mBq g<sup>-1</sup> and (53.8 – 5551.1) mBq g<sup>-1</sup>, as well as the averages of <sup>235</sup>U, <sup>238</sup>U and <sup>232</sup>Th are: 1068 mBq g<sup>-1</sup>, 22639 mBq g<sup>-1</sup> and 619.1 mBq g<sup>-1</sup>, respectively. Equivalent ranges of mass concentrations of <sup>235</sup>U, <sup>238</sup>U and <sup>232</sup>Th are: (1.4 – 32.5) ng g<sup>-1</sup>, (187 - 4453) ng g<sup>-1</sup> and (13.2 – 1367.2) ng g<sup>-1</sup> with averages of 13.36 ng g<sup>-1</sup>, 1825 ng g<sup>-1</sup> and 152.5 ng g<sup>-1</sup>, respectively. The sediments have much higher activity values than the rocks, where the <sup>235</sup>U, <sup>238</sup>U and <sup>232</sup>Th values range at (370.1 – 1401.1) mBq g<sup>-1</sup>, (7832 - 29837) mBq g<sup>-1</sup> and (103.9 – 3246.4) mBq g<sup>-1</sup> with averages of 744.8 mBq g<sup>-1</sup>, 15784 mBq g<sup>-1</sup> and 940 mBq g<sup>-1</sup>, respectively. Ranges of mass concentrations of

$^{235}\text{U}$ ,  $^{238}\text{U}$  and  $^{232}\text{Th}$  in the sediments are: (4.6 – 17.5)  $\text{ng g}^{-1}$ , (631 - 2406)  $\text{ng g}^{-1}$  and (25.6 – 799.6)  $\text{ng g}^{-1}$  with averages at 9.3  $\text{ng g}^{-1}$ , 1272  $\text{ng g}^{-1}$  and 231.5  $\text{ng g}^{-1}$ , respectively.

Table 3.4 Uranium and thorium concentrations in rocks and sediments samples.

Sample ID	Sample type	<sup>235</sup> U mBq g <sup>-1</sup>	<sup>238</sup> U mBq g <sup>-1</sup>	<sup>232</sup> Th mBq g <sup>-1</sup>	<sup>235</sup> U ng g <sup>-1</sup>	<sup>238</sup> U ng g <sup>-1</sup>	<sup>232</sup> Th ng g <sup>-1</sup>
<b>A-2</b>	<b>Jabel Hafit</b>						
JH-1	rock	197.6	4168	<40	2.5	336.2	<10
JH-2	rock	691.9	14602	319.9	8.6	1177	78.8
JH-3	rock	111.0	2321	55.9	1.4	187	13.8
<b>A-4</b>	<b>Wadi Al Bih</b>						
r-1	rock	653.7	13884	253.4	8.2	1119	62.4
r-2	rock	1077.0	23062	53.80	13.5	1859	13.2
r-3	rock	1259.4	26979	148.3	15.7	2175	36.5
r-4	rock	729.6	15466	5551.1	9.1	1247	1367.2
r-5	rock	210.8	4398	90.7	2.6	354	22.3
r-6	rock	1781.5	37574	965.9	22.3	3030	237.9



Sample ID	Sample type	<sup>235</sup> U	<sup>238</sup> U	<sup>232</sup> Th	<sup>235</sup> U	<sup>238</sup> U	<sup>232</sup> Th
		mBq g <sup>-1</sup>	mBq g <sup>-1</sup>	mBq g <sup>-1</sup>	ng g <sup>-1</sup>	ng g <sup>-1</sup>	ng g <sup>-1</sup>
r-7	rock	1543.4	32664	225.4	19.3	2634	55.5
r-8	rock	1832.9	39093	178.6	22.9	3152	43.9
r-9	rock	1057.7	22408	217.0	13.2	1807	53.4
r-10	rock	262.9	5521	418.7	3.3	445	103.1
r-11	rock	430.1	9068	854.2	5.4	731	210.4
r-12	rock	437.1	9223	1150.0	5.5	743	283.3
r-13	rock	430.0	9044	771.7	5.4	729	190.1
r-14	rock	1049.9	22025	601.4	13.1	1776	148.1
r-15	rock	357.3	7392	1314.7	4.5	596	323.8
r-16	rock	641.7	13475	404.1	8.0	1086	99.5
r-17	rock	616.6	13018	<40	7.7	1049	<10
r-18	rock	842.8	17807	178.8	10.5	1436	44.0

Sample ID	Sample type	<sup>235</sup> U	<sup>238</sup> U	<sup>232</sup> Th	<sup>235</sup> U	<sup>238</sup> U	<sup>232</sup> Th
		mBq g <sup>-1</sup>	mBq g <sup>-1</sup>	mBq g <sup>-1</sup>	ng g <sup>-1</sup>	ng g <sup>-1</sup>	ng g <sup>-1</sup>
r-19	rock	2460.4	52383	288.4	30.8	4224	71.0
r-20	rock	785.7	16602	<40	9.8	1338	<10
r-21	rock	1729.0	36464	679.3	21.6	2940	167.3
r-22	rock	2391.0	50786	354.2	29.9	4095	87.2
r-23	rock	944.0	19983	595.9	11.8	1611	146.8
r-24	rock	1941.4	40976	207.4	24.3	3304	51.1
r-25	rock	912.3	19282	549.5	11.4	1555	135.3
r-26	rock	1403.2	29386	129.4	17.5	2369	31.9
r-27	rock	2139.5	45621	304.1	26.7	3679	74.9
r-28	rock	2602.9	55227	344.2	32.5	4453	84.8
r-29	rock	563.7	11943	1398.5	7.0	963	344.5
r-30	rock	737.4	15543	336.6	9.2	1253	82.9

Sample ID	Sample type	<sup>235</sup> U	<sup>238</sup> U	<sup>232</sup> Th	<sup>235</sup> U	<sup>238</sup> U	<sup>232</sup> Th
		mBq g <sup>-1</sup>	mBq g <sup>-1</sup>	mBq g <sup>-1</sup>	ng g <sup>-1</sup>	ng g <sup>-1</sup>	ng g <sup>-1</sup>
F1 0-10	sediment	1199.5	25577	966.3	14.9	2062	238.0
F1 10-20	sediment	1401.1	29837	3246.4	17.5	2406	799.6
F1 20-30	sediment	370.1	7832	103.9	4.6	631	25.6
F2 0-10	sediment	417.1	8721	143.9	5.2	703	35.5
F2 10-20	sediment	759.5	16054	798.5	9.5	1294	196.7
F2 20-30	sediment	593.8	12407	706.2	7.4	1000	173.9
F3 0-10	sediment	708.3	15051	485.6	8.9	1213	119.6
F3 10-20	sediment	583.3	12479	778.9	7.3	1006	191.8
F3 20-30	sediment	671.2	14102	1231.4	8.4	1137	303.3

### 3.7 Groundwater in Oman

Thirteen groundwater samples were collected from Oman since the mountains of Oman recharge the UAE aquifer at precipitation times. The samplings were in three different regions: along the borders between UAE and Oman, near Muscat, and between these two regions (Fig. 2.5). Groundwater properties and concentrations of the radioactive elements are presented in Table 3.5, including the measurements of the pH, temperature, TDS, chloride, uranium, thorium, radon, radium, gross  $\beta$  and gross  $\alpha$ . The pH shows a range covering acidic to basic values (6.9–9.7). Temperature of the water varies from about 30 °C to 62 °C, while TDS values span between 152 mg L<sup>-1</sup> and 890 mg L<sup>-1</sup>. Variability of Cl<sup>-</sup> spans between 40 mg L<sup>-1</sup> and 850 mg L<sup>-1</sup>. The radionuclides <sup>235</sup>U, <sup>238</sup>U, <sup>232</sup>Th, <sup>222</sup>Rn and <sup>226</sup>Ra range at (0.02 – 10.40) ng L<sup>-1</sup>, (3.17 - 1450) ng L<sup>-1</sup>, (0.004 – 0.013) mBq L<sup>-1</sup>, (1.4 – 120) Bq L<sup>-1</sup> and (0.005 – 0.111) Bq L<sup>-1</sup>, respectively. The majority of gross  $\alpha$  and gross  $\beta$  measurements are below the detection limits and do not exceed 0.3 Bq L<sup>-1</sup>.

Table 3.5 Groundwater properties and radioactivity in Oman. All samples were taken from wells except sample 13.

Sample #	Sample ID	UTM(E)	UTM(N)	pH	Temp. °C	TDS mg L <sup>-1</sup>	Cl <sup>-</sup> mg L <sup>-1</sup>	<sup>235</sup> U ng L <sup>-1</sup>	<sup>238</sup> U ng L <sup>-1</sup>	<sup>232</sup> Th mBq L <sup>-1</sup>	<sup>222</sup> Rn Bq L <sup>-1</sup>	<sup>226</sup> Ra Bq L <sup>-1</sup>	Gross β Bq L <sup>-1</sup>	Gross α Bq L <sup>-1</sup>
1	FO-1	396405	2676095	8.7	31	152	40	0.02	3.17	0.013	4.2	0.005	<0.1	<0.01
2	FO-2	396200	2675528	8.6	30	274	101	0.24	31.69	0.008	4.6	0.007	<0.1	<0.01
3	FO-3	396170	2677751	8.5	30	222	83	0.02	3.17	0.004	4.4	0.026	<0.1	<0.01
4	FO-4	394551	2679009	8.4	31	256	82	0.39	50.70	0.004	1.4	0.033	<0.1	<0.01
5	FO-5	394199	2679883	8.3	31	297	135	0.26	38.02	<0.004	16.8	0.026	<0.1	<0.01
6	FO-6	396818	2681377	8.5	33	170	47	0.06	7.39	<0.004	3.6	0.017	<0.1	<0.01
7	FO-7	394421	2681094	8.6	31	871	190	0.44	59.15	<0.004	<0.36	0.023	<0.1	<0.01
8	FO-8	396256	2681552	8.4	39	509	77	0.49	66.54	<0.004	3.1	0.021	<0.1	<0.01
9	FO-9	396695	2681806	8.3	32	643	89	0.11	12.67	<0.004	13.1	0.034	<0.1	<0.01
10	FO-10	394919	2681355	8.5	34	857	850	1.99	265.10	<0.004	7.1	0.035	<0.1	<0.01
11	102/72	537665	2545410	9.7	35	425	NM	<0.06	<0.3	NM	0.1	<0.001	<0.1	0.07
12	WD-1	530082	2556732	7.4	32.	750	NM	8.24	1103.00	NM	1.5	0.006	<0.1	0.03
13	MO-1	641243	2692779	6.8	62	890	NM	10.40	1425.00	NM	120.0	0.111	0.3	0.3

## 4 DISCUSSION

### 4.1 Uranium and thorium variations in groundwater and environmental impact

The World Health Organization (WHO) recommended permissible levels for some radionuclides in drinking water in 2008, and these levels were updated by 2011. These levels were based on the possible impact on human health and were corroborated by experimental work on mammals. Consideration of THE effects on human health is calculated on the assumption that annually each person consumes 730 liters of water and has an Individual Dose Criterion (IDC) of 0.1 mSv. The United States Environmental Protection Agency (EPA) also has standardized limits for some ionizing radiations (Table 4.1). The WHO permissible levels of  $^{235}\text{U}$ ,  $^{238}\text{U}$ ,  $^{232}\text{Th}$  concentration in drinking water are  $1 \text{ Bq L}^{-1}$ ,  $10 \text{ Bq L}^{-1}$  and  $1 \text{ Bq L}^{-1}$ , respectively. It is important to keep in mind that these activity values may add up and also further activity in groundwater can exist from the products (daughter nuclides) of the uranium and thorium series chain decay as well as  $^{40}\text{K}$ . However, from a chemical point of view, the uranium is taken as a total mass content rather than separated isotopes based on its chemical toxicity. The permissible level of total uranium mass concentration is  $60 \mu\text{g L}^{-1} \sim 60000 \text{ ng L}^{-1}$ . Apparently, the activity concentration of  $^{235}\text{U}$ ,  $^{238}\text{U}$ ,  $^{232}\text{Th}$  in the investigated groundwater here are below the proposed WHO permissible level of each isotope (Table 3.2), but when mass concentration is considered then uranium exceeds the permissible limits in some samples. Out of the 67 samples, five have total

uranium concentration  $>30000$  ng/L (exceeding EPA permissible limits), and two of them  $> 60000$  ng L<sup>-1</sup> (exceeding WHO permissible limits). Three of these high concentration samples occur in area A-5.

A relatively good correlation between uranium and TDS is found for the groundwater samples with measured TDS. This feature implies that the uranium behaves conservatively in groundwater with high TDS (Fig. 4.1 a, b, e).

Alternatively, in the highly variable or with low TDS groundwater, the uranium-TDS relationship is weak (Figs. 4.1 c, d). This finding of U-TDS agrees well with previous reports, which showed strong linear relationship between uranium and highly saline water (Dunk et al., 2002); however, this relationship is not validated for brackish water (Porcelli et al., 1997, 2001; Andersson et al., 1995, 1998; Andersen et al., 2007; Not et al., 2012). This means if a linear relationship was found in the low TDS water in carbonates aquifer, it might be explained as a result of natural dissolution of uranium-rich limestone and shales (Swarzenski et al., 1995).

As the groundwater is extensively used for a variety of human purposes, it is likely that people and animals could be exposed to the radionuclides through direct (drinking) and indirect ways (food crops grown in the areas). There are significant differences in the uptake of long-lived radionuclides among different plant species (Chen et al., 2005). In the different studied areas in this dissertation, most of the harvests are grasses and hay for animal feed; therefore the health risk is indirect through human consumption of meat and dairy produce (Makoti et al., 2012).

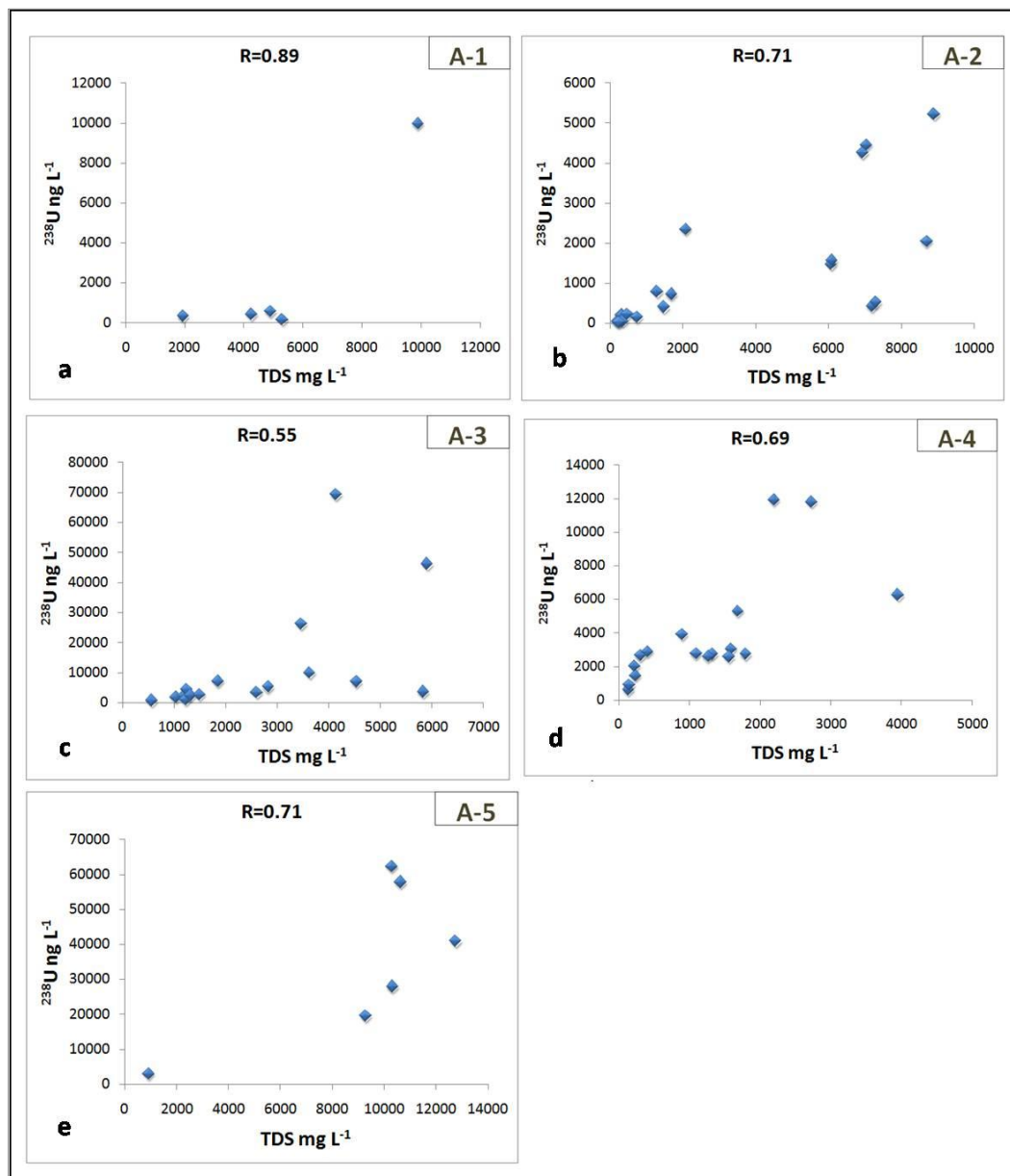


Fig. 4.1 Correlation between  $^{238}\text{U}$  and TDS in groundwater from 5 investigation areas.



Table 4.1 Permissible limits for radioactivity level in groundwater recommended by the World Health Organization (WHO) and US Environmental Protection Agency (EPA).

Component	WHO permissible limits (2011)	EPA permissible limits (2012)
<b>Gross <math>\alpha</math></b>	0.5 Bq/L	0.5 Bq/L
<b>Gross <math>\beta</math></b>	1 Bq/L	4 mrem/year (40 $\mu$ Sv/year)
<sup>235</sup> U	1 Bq/L	–
<sup>238</sup> U	10 Bq/L	–
Total U	60 $\mu$ g/L (60000 ng/L)	30 $\mu$ g/L (30000 ng/L)
<sup>232</sup> Th	1 Bq/L	–
<sup>222</sup> Rn	100 Bq/L	11 Bq/L
<sup>226</sup> Ra	1 Bq/L	–

However, a study in the Mediterranean region confirms the preferential uptake of grass to uranium daughter (<sup>226</sup>Ra) in contrast to uranium and thorium isotopes (Vera Tome et al., 2003). Thus, the occurrence of elevated concentrations of uranium and thorium influence the food chain indirectly through their decay products. Another work had been conducted (EPA, 2011) in the USA in the years 2000 to 2010 to investigate transfer of radionuclides and anions through irrigation from water and soil to plant through irrigation and concluded that only one lb out of 622 lbs of uranium contained in irrigation water was transferred to 480 tons of hay in 2002 (note that the uranium concentrations in hay were fairly similar in 1999 and 2010), which means that less than 1% of the uranium that was supplied to the field in 2002 was removed by the hay. Using this

approach, the uranium tolerable daily intake (TDI) estimated by WHO (60  $\mu\text{g}$  per kilogram of body weight) was compared to the highest  $^{238}\text{U}$  concentration reported here in the irrigational groundwater ( $69237 \text{ ng L}^{-1} = 69.237 \mu\text{g L}^{-1}$ ) represented by sample (Rw-1) (Table 3.2). The estimation indicates about 1% of the  $^{238}\text{U}$  ( $0.69237 \mu\text{g}$ ) may be taken by hay and grasses, and this is much less than the WHO TDI. Broadly speaking, in contrast to contamination from fallout sources, the risk of root uptake of uranium and thorium is negligible in grass, since roots act as a natural barrier preventing the transfer of numerous trace metals - including radionuclides - to upper plant parts (Shtangeeva, 2010). Also, it has been mentioned in several publications that concentrations of uranium and thorium in roots are much higher than in leaves (Shtangeeva & Ayrault, 2004; Chang et al., 2005). In the case of plant species and uranium uptake by roots, Shahandeh and Hossner found in their study in 2002 that grass and wheat had the lowest uranium concentrations in their roots, while sunflower and Indian mustard had highest root uranium. In this dissertation, the tested groundwater is used mainly for irrigating grasses (alfalfa), so it is expected that the roots uptake of uranium is relatively low. Thus, the use of groundwater for agricultural purpose is considered acceptable in terms of uranium and thorium, but further evaluation based on time series data and of decay products such as  $^{226}\text{Ra}$  needs to be determined for accurate assessment of radiological impact assessment and quality assurance.

Despite the variability of uranium concentration in the different climatic regions, all the averaged values examined here are far below the WHO

permissible limits (Figs. 4.2 and 4.3). The activity concentrations of  $^{238}\text{U}$  and  $^{232}\text{Th}$  in the studied areas in the UAE are comparable with other countries in the arid regions (Fig. 4.3; Table 4.4). The uranium and thorium concentrations in countries included in Figs. 4.2 and 4.3, and Tables 4.2 and 4.3 are shown on the world map (Figs. 4.4, 4.5 and 4.6). Uranium is shown in the world map in both activities and mass concentrations because of the consideration of its chemical toxicity.

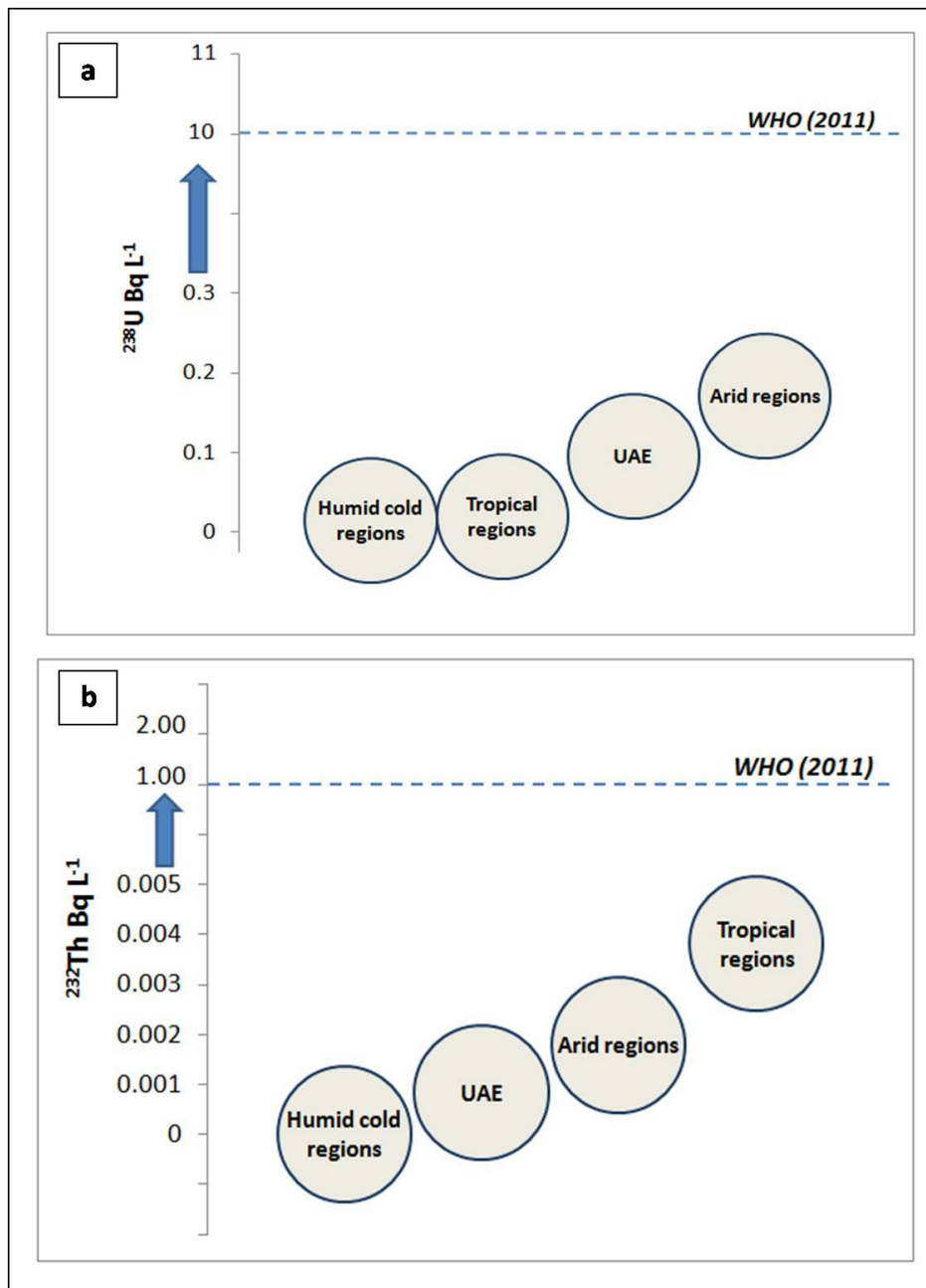


Fig. 4.2 Average concentrations of (a)  $^{238}\text{U}$  (b)  $^{232}\text{Th}$  in the different climatic regions, details are in Table 4.2 and Table 4.3 compared with the WHO (2011) permissible limit (dashed line).

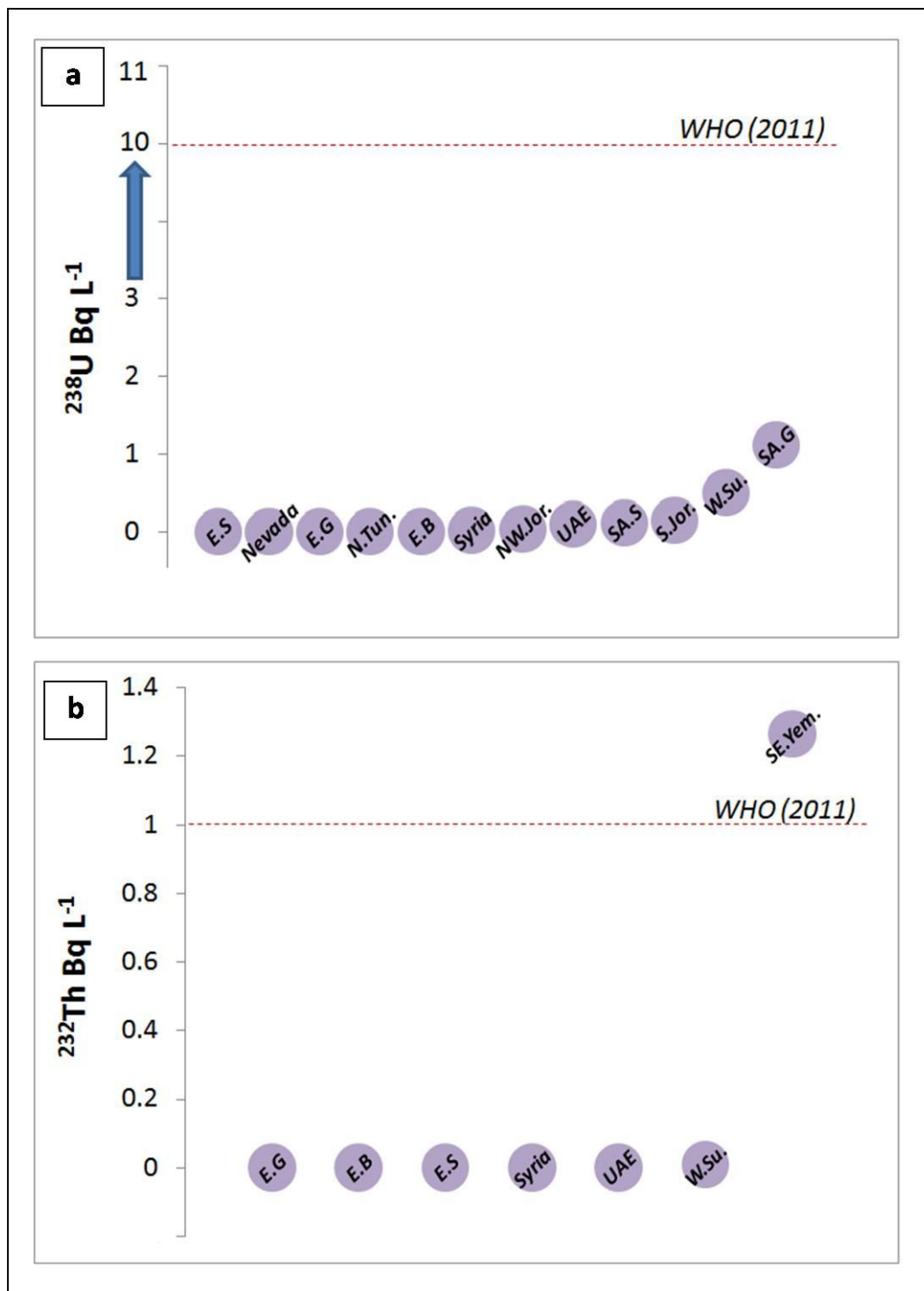


Fig. 4.3 The concentration of (a)  $^{238}\text{U}$  and (b)  $^{232}\text{Th}$  in some arid and semi-arid countries compared with WHO (2011) permissible limits (dashed line). The countries abbreviations and  $^{238}\text{U}$  and  $^{232}\text{Th}$  concentrations are illustrated in Table 4.4.

Table 4.2 Comparison of uranium concentration (in Bq L<sup>-1</sup> and in ng L<sup>-1</sup>), measured in UAE and Oman with those in other regions reported in the literatures.

Country	U Bq L <sup>-1</sup> (Average)	U ng L <sup>-1</sup> (Average)	U ng L <sup>-1</sup> (range)	Reference
Egypt	0.002	175	1.19 – 519	Dabous et al., 2002
United States (Nevada)	0.00003	2.9	0.17 – 9.87	Cizdziel et al., 2005
Tunisia (North)	0.004	354	4.83 – 709	Added et al., 2005
Syria	0.026	2096	240 – 3420	Abdul-Hadi et al., 2001
Jordan	0.032	2629	2233 – 2685	Al-Amir et al., 2012
<b>United Arab Emirates</b>	<b>0.09</b>	<b>7685</b>	<b>25.8 – 69237</b>	<b>This work</b>
Saudi Arabia	0.6	49927	322 – 39113	Shabana et al., 1999
Sudan	0.5	40403	1298 – 138709	Osman et al., 2008
Sweden	0.01	900	900 – 445000	Skeppström & Olofsson, 2007
Finland (Nordic countries)	0.001	107	4.9 – 56200	Frengstad et al., 2010
France	0.005	457	177 – 466	Hubert et al., 2006
United States (Florida)	0.019	1600	Data not available	Brown et al., 2007
Germany	0.003	258	56.4 – 25806	Beyerman et al., 2010
Slovenia	0.01	823	Data not available	Benedik & Jeran, 2012
United States (Tennessee)	0.007	626	59.6 – 4296	Hileman & Lee, 1993
Greece	0.036	2958	330 – 7660	Samaropoulos et al., 2012
Brazil (Rio de Janerio)	0.01	1201	10 – 3720	Lauria et al., 2004
Brazil (Parana)	0.004	368	2.5 – 7229	Bonotto, 2011
India	0.068	5532	7193 – 123709	Aleissa & Islam, 2008
China	0.17	14354	10 – 162000	Min et al., 2007

<b>Country</b>	<b>U Bq L<sup>-1</sup> (Average)</b>	<b>U ng L<sup>-1</sup> (Average)</b>	<b>U ng L<sup>-1</sup> (range)</b>	<b>Reference</b>
Turkey	0.78	62943	Data not available	Kabadaıı & Gümüő, 2012
Italy	0.02	1725	16 – 8306	Guogang et al., 2009
Kazakhstan	0.22	18266	507 – 70750	Kawabata et al., 2008
<b>Oman</b>	<b>0.017</b>	<b>842</b>	<b>0.3 – 1425</b>	<b>This study</b>

Table 4.3 Comparison of thorium concentration in groundwater measured in this work with those in other regions reported in the literatures.

Country	Th Bq L <sup>-1</sup> (Average)	Th Bq L <sup>-1</sup> (range)	Reference
Egypt	$1.5 \times 10^{-6}$	$4.06 \times 10^{-8} - 9.7 \times 10^{-7}$	Dabous et al., 2002
Syria	$7.2 \times 10^{-4}$	$5 \times 10^{-4} - 1.2 \times 10^{-3}$	Abdul-Hadi et al., 2001
<b>United Arab Emirates</b>	<b>0.000828</b>	<b><math>9.6 \times 10^{-7} - 0.01</math></b>	<b>This study</b>
United States (Idaho)	$5.5 \times 10^{-6}$	$4 \times 10^{-7} - 4.6 \times 10^{-5}$	Luo et al., 2000
Sudan	0.009	0.0001 – 0.039	Osman et al., 2008
Finland (Nordic countries)	$6.4 \times 10^{-6}$	$1.2 \times 10^{-6} - 4 \times 10^{-5}$	Frengstad et al., 2010
France	$6 \times 10^{-7}$	$4.7 \times 10^{-8} - 4.3 \times 10^{-6}$	Hubert et al., 2006
Brazil (Rio de Janerio)	0.0005	$1.6 \times 10^{-4} - 1 \times 10^{-3}$	Lauria et al., 2004
Turkey	1.05	Data not available	Kabadayi & Gümüş, 2012
Italy	$1.3 \times 10^{-6}$	$7 \times 10^{-7} - 2.7 \times 10^{-6}$	Guogang et al., 2009
Yemen	1.2	0.3 – 2.9	El-Majeed et al., 2013



Table 4.4 Data used to build up Fig. 4.3; countries' abbreviations and radionuclide concentrations.

Country	Abbreviations	$^{238}\text{U Bq L}^{-1}$	$^{232}\text{Th Bq L}^{-1}$
<b>Egypt: Central Eastern Desert Sedimentary aquifer</b>	(E.S)	$3.3 \times 10^{-5}$	$3.8 \times 10^{-6}$
<b>Nevada</b>	Nevada	$3.6 \times 10^{-5}$	Data not available
<b>Egypt: Central Eastern Desert Granitic aquifer</b>	(E.G)	$1.4 \times 10^{-4}$	$4.3 \times 10^{-7}$
<b>Northern Tunisia</b>	(N.Tun.)	$4.4 \times 10^{-3}$	Data not available
<b>Egypt: Central Eastern Desert Bostonitic aquifer</b>	(E.B)	$6.4 \times 10^{-3}$	$4.1 \times 10^{-7}$
<b>Syria</b>	Syria	$2.6 \times 10^{-2}$	$7.2 \times 10^{-4}$
<b>North western Jordan; Sweileh area</b>	(NW.Jor.)	$3.3 \times 10^{-2}$	Data not available
<b>UAE</b>	UAE	$9.5 \times 10^{-2}$	$8.3 \times 10^{-4}$
<b>Southern Jordan; Aqaba area</b>	(S.Jor.)	$15 \times 10^{-2}$	Data not available
<b>Central Saudi Arabia Sedimentary aquifer</b>	(SA.S)	$31 \times 10^{-2}$	Data not available
<b>West central Sudan</b>	(W.Su.)	$50 \times 10^{-1}$	$9.2 \times 10^{-3}$
<b>North western Saudi Arabia Granitic aquifer</b>	(SA.G)	1.1	Data not available
<b>Soth Eastern Yemen</b>	(SE.Yem.)	Data not available	1.2

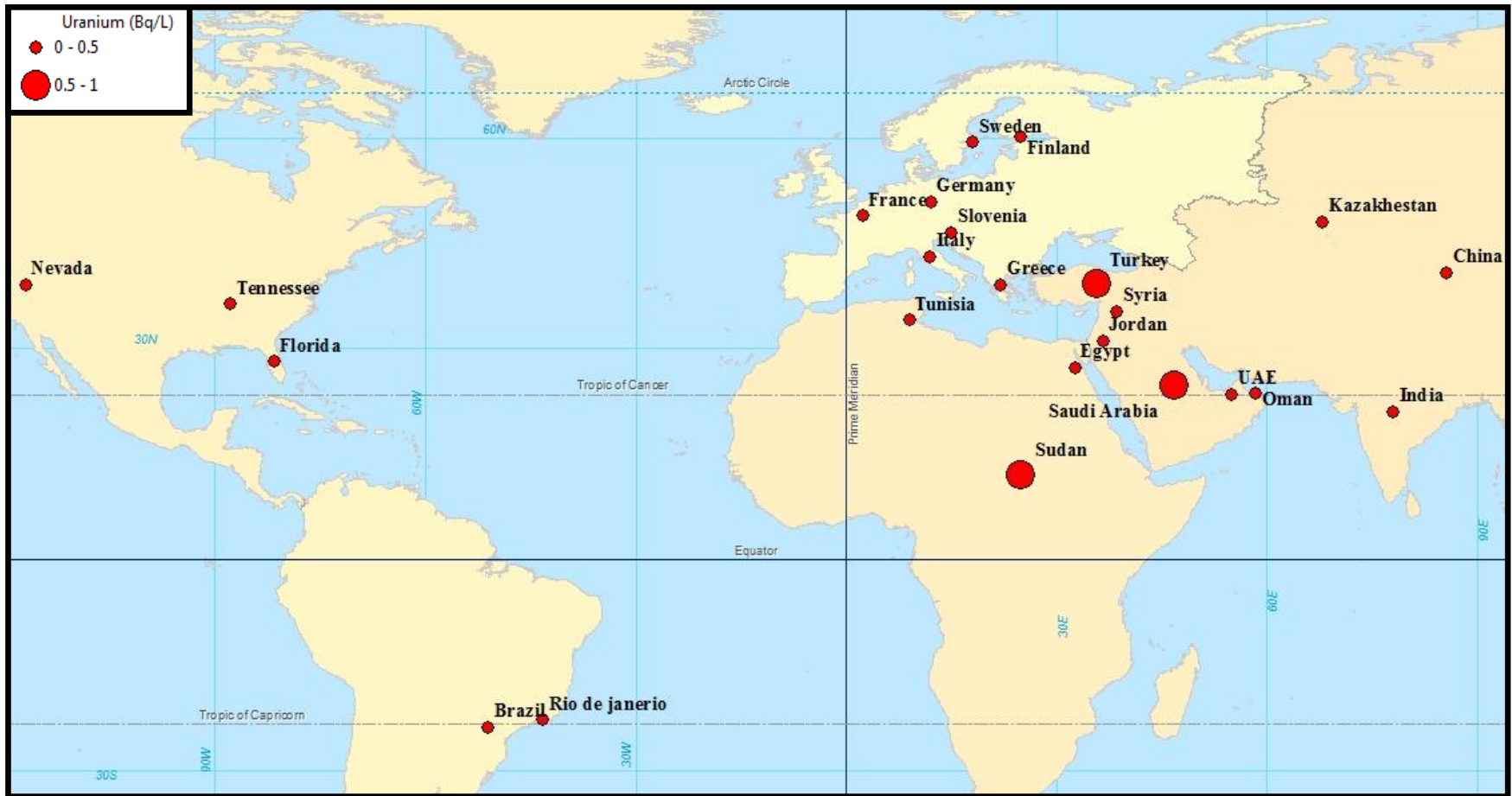


Fig. 4.4 The concentration of uranium in groundwater over the world (references are in Table 4.2).

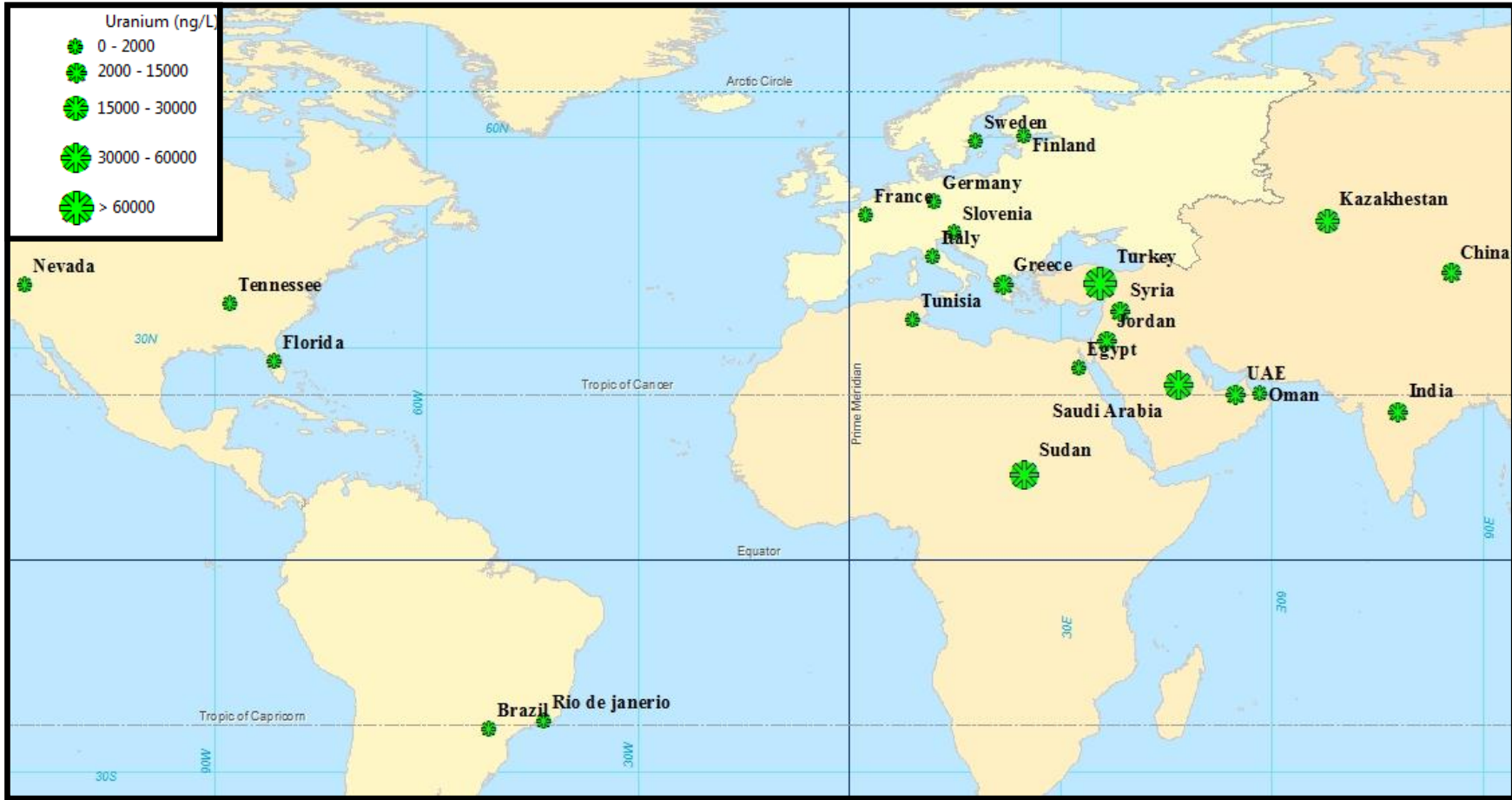


Fig. 4.5 The uranium concentration in groundwater all over the world (references are in Table 4.2).

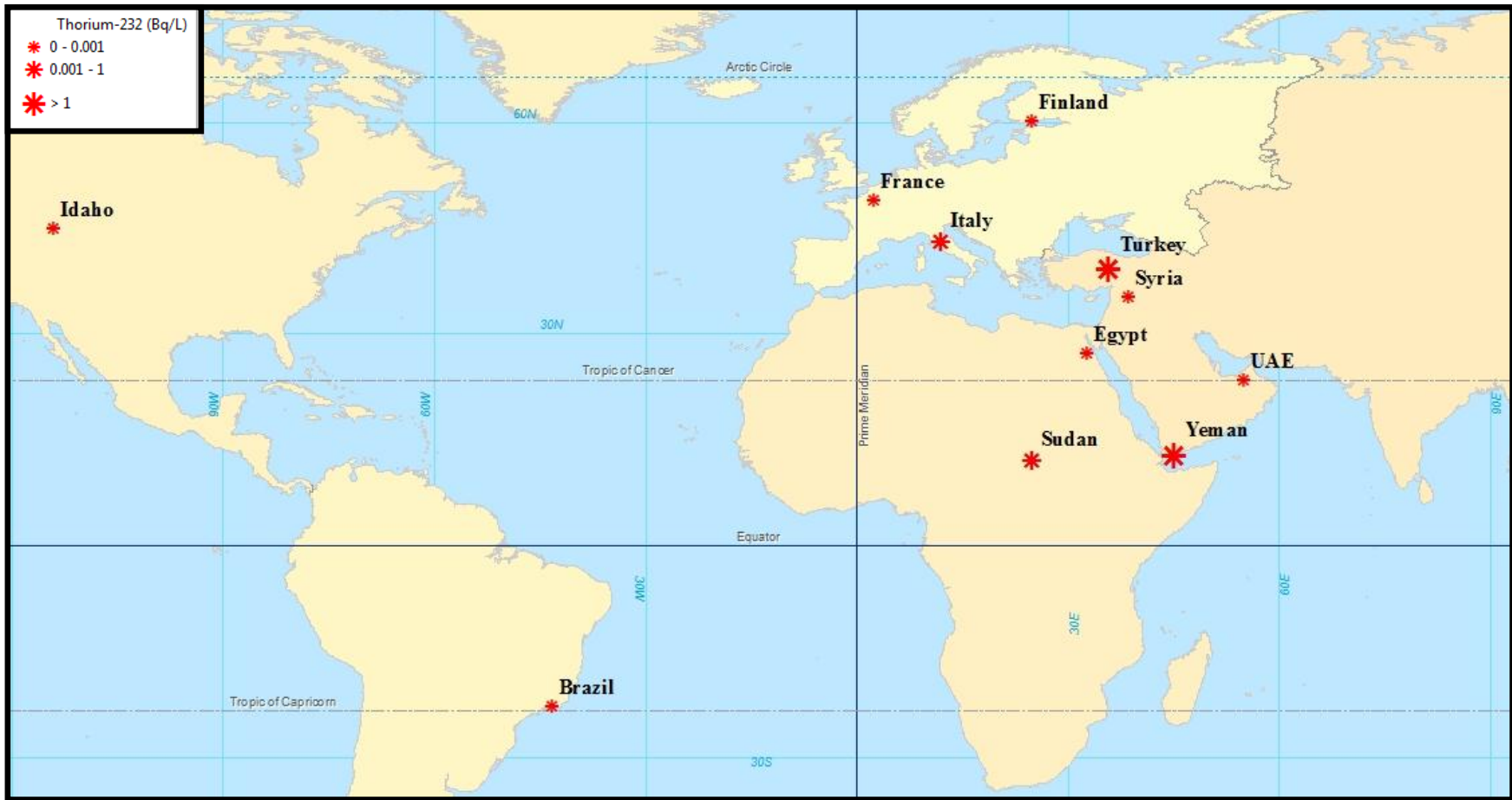


Fig. 4.6 The  $^{232}\text{Th}$  concentration in groundwater in some areas in the world (references are in Table 4.3).

Gross  $\beta$  and gross  $\alpha$  measurements are good indicators of radioactivity level in the groundwater. Gross- $\beta$  activity is mostly related to  $^{40}\text{K}$  as well as  $^{228}\text{Ra}$  and  $^{210}\text{Pb}$  (Zorer et al., 2013). Gross- $\alpha$  activity in groundwater is, to a large extent, the result of uranium isotopes ( $^{234}\text{U}$ ,  $^{235}\text{U}$ ,  $^{238}\text{U}$ ) and  $^{232}\text{Th}$  and their progeny upon decay (Osmond & Ivanovich, 1992). The gross  $\beta$  and gross  $\alpha$  measurements are quite simple and straightforward, and so they are used as a first survey in study areas. In this study, it was found that some gross  $\beta$  and gross  $\alpha$  values exceed the WHO permissible limits for drinking water (52 samples out of 67 exceed gross  $\beta$  permissible limit and 8 samples exceed gross  $\alpha$ ). Thus, relating to WHO permissible limits, a calculation of the additional contribution (from each radionuclide) to the IDC is needed in order make sure if this water is suitable for drinking in terms of radioactivity. If neither gross  $\beta$  nor gross  $\alpha$  values are exceeded, the IDC of 0.1 mSv/year (WHO, 2011) will also not be exceeded, but in our study IDC is expected to exceed this value in some samples, according to the violations in both gross  $\beta$  and  $\alpha$ . The calculation formula of the contribution to the IDC is shown in equation (1) below:

$$\Sigma_i = C_i / GL_i \dots \dots \dots (1)$$

Where:

**i:** radionuclide

**C<sub>i</sub>:** the measured activity concentration of radionuclide i

**GL<sub>i</sub>**: the WHO permissible limit (Table 4.5) of radionuclide *i*, which is based on drinking of 2 liters/day for one year and will result in an effective dose of 0.1 mSv/year.

The outcome of this additive equation should not exceed unity if all the radionuclides are below the permissible limit. If the value of either gross  $\beta$  or gross  $\alpha$  in a water sample exceeds the WHO permissible limit (1 Bq/L for gross  $\beta$  and 0.5 Bq/L for gross  $\alpha$ ), then the output of equation (1) will be  $>1$  which means that the IDC of 0.1 mSv/year might be exceeded too. This will be true only if the ingestion of the polluted water was continuous for a complete year. Such a result does not alone mean that the water is not suitable for consumption. In this study, the additive formula was applied to all water samples even for those with acceptable gross  $\beta$  and gross  $\alpha$  activity (Table 4.5). Also it is useful to mention that only  $^{235}\text{U}$ ,  $^{238}\text{U}$  and  $^{232}\text{Th}$  were included in the summation formula and the results did not exceed unity although screening levels of  $\beta$  and  $\alpha$  were above permissible limit in some samples. This means that high levels of gross  $\beta$  and gross  $\alpha$  were sourced from other radionuclides, such as  $^{226}\text{Ra}$  and  $^{40}\text{K}$ .

Table 4.5 Ranges and averages of dose contribution estimated by applying the additive formula on all samples by including  $^{235}\text{U}$ ,  $^{238}\text{U}$  and  $^{232}\text{Th}$  and their permissible limit in equation (1).

Sampled area	Range of the contribution to IDC (mSv)	Average of the contribution to IDC (mSv)
A-1	$0.03 \times 10^{-2} - 0.01$	$0.04 \times 10^{-1}$
A-2	$0.04 \times 10^{-3} - 0.18 \times 10^{-1}$	$0.03 \times 10^{-1}$
A-3	$0.01 \times 10^{-1} - 0.12$	0.02
A-4	$0.01 \times 10^{-1} - 0.02$	$0.06 \times 10^{-1}$
A-5	$0.05 \times 10^{-1} - 0.11$	$0.65 \times 10^{-1}$

The highest obtained value of IDC (0.12) in Table 4.5 was found in sample Rw-1 in A-3, which also has the highest measured  $^{238}\text{U}$  concentration ( $858.54 \text{ mBq L}^{-1} = 69237 \text{ ng L}^{-1}$ ). The  $^{238}\text{U}$  concentration in this sample is below the permissible limit in terms of radioactivity, which is 10000 mBq/L and higher than permissible limit in terms of chemical toxicity, which is 60000 ng/L. Thus, concern should be paid to the chemical toxicity of uranium rather than only radioactivity. In A-2 area, 18 out of the total 20 groundwater samples are within carbonate rocks aquifers, and the two other samples are within alluvial sediments aquifers. Even though gross  $\alpha$  values exceed the permissible limit of 1 Bq/L in the 9 samples, the calculation using equation 1 (for uranium and thorium) did not expose these samples as radiologically hazardous. This feature indicates that some other radionuclides contribute to the gross  $\alpha$  activity especially in A-2 area where data on other radionuclides (Radium and Radon) were reported (Murad et al.,

2014). More time series data are needed to resolve the different sources of radioactivity.

#### **4.2 Groundwater discharge inventory for uranium and thorium**

Most of the sampled wells in the studied areas are used intensively for agriculture, and thus radiological quality assurance is significant for safe water use and environmental impact. To partly elucidate the possible effects, we carried out a simple model calculation of the amount of uranium and thorium that can accumulate in the soils and sediments from the pumped groundwater. For this calculation, the chosen farms use mainly groundwater for irrigation and also the irrigated area can be estimated and a good example is found in A-4 area. In general, the thickness of soil/sediment layers in these farms is about 1 m. It has been assumed that all uranium and thorium in the groundwater are remained in the soil/sediment layers without further infiltration to the groundwater. This assumption is reasonable knowing that groundwater level in these areas is more than 5 m deep. Also, the fact that uranium and thorium show significant retention at the surface of different soils is due to several processes such as adsorption, and ion exchange or their combination (Allard et al., 1984). Uranium and thorium present more retention to soil in the presence of clays and organic matter (hydrocarbons) because of adsorption. The calculated values of inventory are referred to as groundwater access inventory as shown in Table 4.6 because there is also primary mineralogically-linked concentrations in the soil/sediment and unknown anthropogenic addition from fertilizers. The amount of groundwater which was daily used for irrigation had been estimated to be between 5 to 10 m<sup>3</sup>.



Depending on that, the calculations were worked out for the accumulated  ${}^T\text{U}$  and  ${}^{232}\text{Th}$  in soil loaded from groundwater, in annual base, and then an estimate of the cumulative inventory after twenty years was estimated on specific agricultural area.

Table 4.6 Accumulation of uranium and thorium in soil loaded from groundwater by irrigation in the cases of 5 m<sup>3</sup> or 10 m<sup>3</sup> daily irrigation.

Sample #	Sample ID	Farm area (km <sup>2</sup> )	Annual load from groundwater		20 years load from groundwater	
			Daily irrigation is 5 m <sup>3</sup> or (10 m <sup>3</sup> )			
			<sup>235</sup> U (g/ m <sup>2</sup> )	<sup>232</sup> Th (g/ m <sup>2</sup> )	<sup>235</sup> U (g/ m <sup>2</sup> )	<sup>232</sup> Th (g/ m <sup>2</sup> )
<b>A-4</b>	<b>Wadi Al Bih</b>					
<b>49</b>	R-KH08	0.25	1.08 *10 <sup>-5</sup> (2.16 *10 <sup>-5</sup> )	2.00 *10 <sup>-9</sup> (4.00 *10 <sup>-9</sup> )	2.15 *10 <sup>-4</sup> (4.32 *10 <sup>-4</sup> )	3.60 *10 <sup>-8</sup> (7.60 *10 <sup>-8</sup> )
<b>56</b>	R-KH16	0.25	2.85 *10 <sup>-5</sup> (5.71 *10 <sup>-5</sup> )	1.08 *10 <sup>-7</sup> (2.16 *10 <sup>-7</sup> )	5.71 *10 <sup>-4</sup> (1.14 *10 <sup>-3</sup> )	2.16 *10 <sup>-6</sup> (4.32 *10 <sup>-6</sup> )
<b>58</b>	R-KH18	0.25	4.61 *10 <sup>-6</sup> (9.22 *10 <sup>-6</sup> )	1.60 *10 <sup>-9</sup> (4.00 *10 <sup>-9</sup> )	9.22 *10 <sup>-5</sup> (1.84 *10 <sup>-4</sup> )	3.60 *10 <sup>-8</sup> (7.60 *10 <sup>-8</sup> )
<b>61</b>	R-KH21	5.00	2.29 *10 <sup>-6</sup> (4.59 *10 <sup>-6</sup> )	1.60 *10 <sup>-10</sup> (2.00 *10 <sup>-10</sup> )	4.59 *10 <sup>-5</sup> (9.19 *10 <sup>-5</sup> )	3.20 *10 <sup>-9</sup> (6.60 *10 <sup>-9</sup> )

The load of  ${}^T\text{U}$  and  ${}^{232}\text{Th}$  to the soil from groundwater is  $1.14 \times 10^{-3}$  g (1.14 mg) and  $4.32 \times 10^{-6}$  g (4.32  $\mu\text{g}$ ) respectively after twenty years if the daily irrigation is at its maximum amount ( $10 \text{ m}^3$ ). However, despite these concentrations, the transfer of uranium and thorium into crops is not readily. In addition, even when uranium is consumed, only a tiny fraction of the element is directly absorbed into the body and more than 90% is eliminated through the digestion process (Ebbs et al., 1998; Food Standards Agency, 2001). Therefore, apparently the added uranium and thorium from the groundwater to the soil is relatively small and environmentally less hazardous.

#### **4.3 Factors affecting the concentrations of ${}^{235}\text{U}$ , ${}^{238}\text{U}$ and ${}^{232}\text{Th}$ in groundwater**

The average total uranium ( ${}^T\text{U}$ ) concentration of the studied groundwater areas in the UAE with annual rainfall average in each area shows a negative correlation ( $R = -0.71$ ; Fig. 4.7a), which indicates that uranium concentrations are largely inversely proportional to rainfall input. A possible explanation for the negative correlation of uranium with rainfall is the dilution of uranium concentration in the groundwater because the major source of groundwater is the recharge from rainfall in the investigated areas. Note that in the study areas in the UAE, the highest rainfall average occurs in A-2 and A-4 regions (the carbonate aquifers). Despite the lithological carbonate composition of A-2 and A-4 aquifers, the relatively higher rainfall would dilute the uranium in the groundwater of A-2 and A-4 region, which might be the reason for obliterating the effect of the carbonate rocks as a source of uranium in groundwater. Table 4.7 compares the

uranium concentrations and rainfall in the study areas with those in other regions in global scale. Here, the extremely high uranium concentrations caused by lithological composition of the aquifer were excluded. The comparison between uranium concentration and rainfall shows  $R = -0.71$  when the UAE study areas are only included (Fig. 4.7a), while for France, Northern Tunisia, Germany, Nordic countries together with UAE study areas,  $R = -0.53$  (Fig. 4.7b). The correlation coefficient  $R$  was reduced in the latter case due to the uranium dilution by heavy rainfall in shallow aquifers. The rainfall may eliminate the effect of lithology, like the case in A-2, A-4 as well as some shallow granite aquifers in the Nordic countries (Table 4.7). Although the rainfall average in A-5 area is greater than A-3 area, the uranium concentration in A-5 area is more than A-3 area. This probably relates to the sabkha geological composition in A-5 area which has higher affinity to conserve uranium.

These outcomes reflect the effect of climatic conditions on the availability of uranium in groundwater. In the same context, a comparison was made in this study to examine the effect of climate on the uranium and thorium concentrations in groundwater around the world. The regions were divided into three groups according to their climatic zone (humid cold, arid and tropical) and compared to UAE groundwater data (Fig. 4.2 and Tables 4.2 and 4.3). The concentrations of each radionuclide (uranium and thorium) in each climatic zone were averaged and illustrated in Fig. 4.2. It can be observed that the uranium concentration decreases with increasing rainfall.

The distribution of  $^{232}\text{Th}$  concentrations in different climatic regions and those studied here is comparable with the concentrations in arid regions. Unlike the uranium, thorium is apparently not sensitive to climatic conditions since it is less soluble in water (Dinh Chau et al., 2011).

Table 4.7 A comparison between the uranium concentrations and average annual rainfall in the study areas and other countries. The rainfall averages in the study areas in the UAE are taken from the website of National Center of Meteorology and Seismology as averages from 2003 to 2011. Rainfall in the other regions obtained from the US National Oceanographic and Atmospheric Agency (NOAA) and World Meteorological Organization (Retrieved in October, 2013).

<b>Study area</b>	<b>Annual rainfall (mm/year)</b>	<b><math>^{238}\text{U}</math> concentration in ground water, ng L<sup>-1</sup> average</b>	<b>Aquifer Type</b>
<b>A-1</b>	82.9	2307	Sandstone
<b>A-2</b>	95.3	1270	Carbonate
<b>A-3</b>	27.5	12150	Sandstone
<b>A-4</b>	95.9	3744	Carbonate
<b>A-5</b>	40.8	35475	Sandstone
<b>France</b>	649.0	457	Chalk
<b>Tunisia (North)</b>	510.0	354	Sandstone
<b>Germany</b>	570.0	258	Sandstone
<b>Nordic countries</b>	650.0	107	Mainly granite

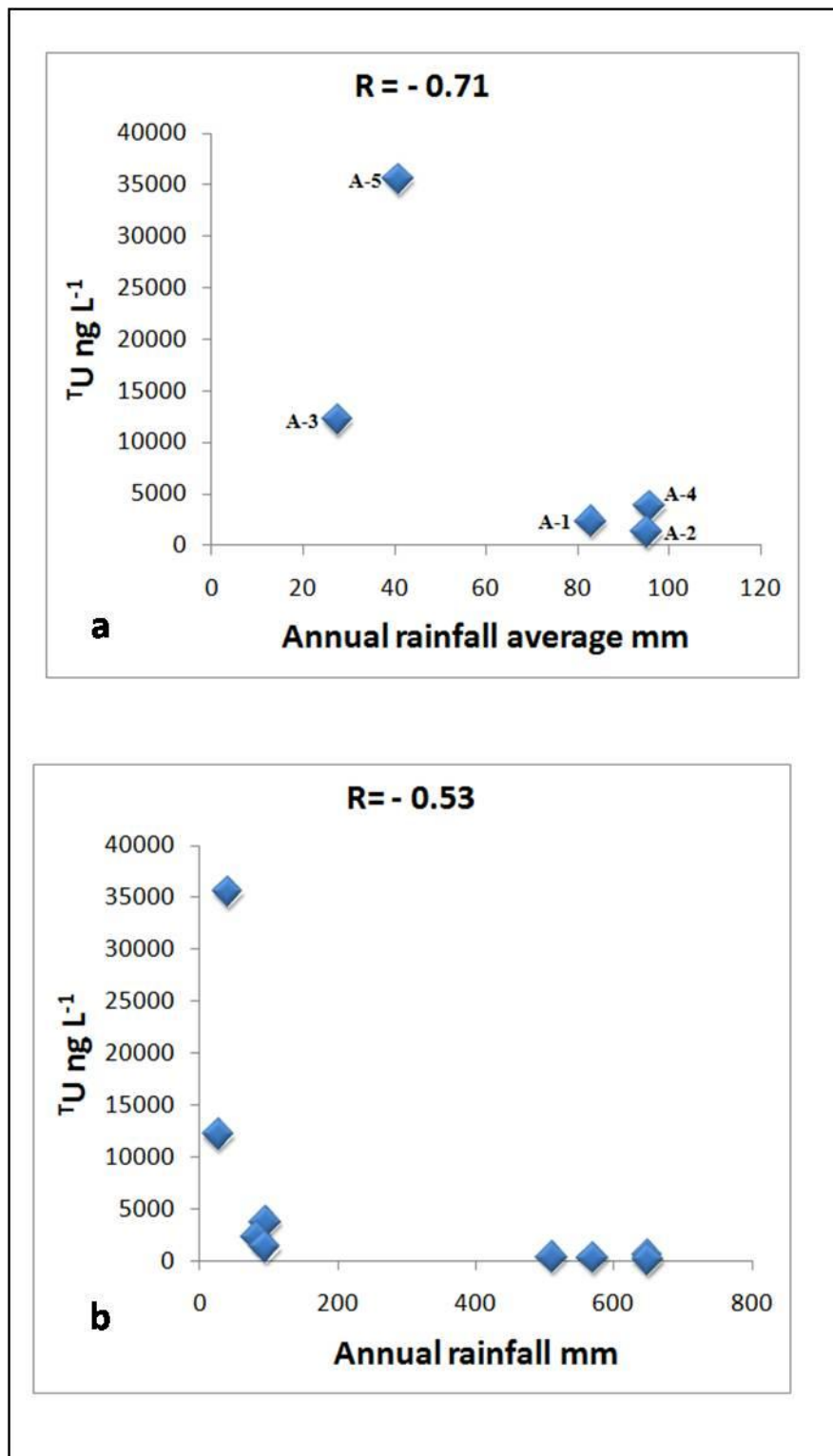


Fig. 4.7 Annual rainfall average versus total uranium <sup>T</sup>U (a) in the study areas in the UAE (b) in the study areas in the UAE and other regions mentioned in Table 4.7.

Uranium and thorium are common trace components of most rocks and sediments that make up the aquifer system in the studied areas. Generally, the highest thorium concentrations occur in granites, while with uranium the maximum concentrations are found in shales (Faure, 1998). Also, elevated concentrations of uranium in groundwater are frequently observed in coastal aquifers suggesting a probability of marine intrusion (Hadj et al., 2010). Similar to other arid regions, groundwater quality patterns in the UAE are complex because of many different water sources (rainfall, seawater intrusion, and anthropogenic sources such as wastewater, domestic use and irrigation return flow) as well as water-rock interaction. In the analyzed groundwater samples, five out of 67 contain  $^{238}\text{U} > 30000 \text{ ng L}^{-1}$ , while all  $^{232}\text{Th}$  concentrations fall within the acceptable range according to WHO permissible limits (Tables 3.2 and 4.1). Since thorium is not a major groundwater contaminant, more focus will be on uranium sources in this section. In the presence of carbonate aquifers, uranium forms highly soluble complexes, which can be transported for large distances in groundwater (Dinh Chau et al., 2011). Areas A-2 and A-4 studied here are both far away from each other, but are dominated by aquifers made up of carbonates intercalated with shale and mudstones of different ages (carbonates in A-2 are Paleogene to Neogene and in A-4 are Upper Triassic to Lower Cretaceous) (Rizk et al., 2007; El-Saiy & Jordan, 2007). Factor analysis shows that uranium in water has different loading than uranium in rocks (Fig. 4.8), which means an unclear relationship between the rocks and groundwater uranium concentrations. Factor analysis is a statistical process for grouping variables in a way that depends

on the degree of correlation between the variables (Mardia et al., 1979; Khattree & Naik, 2000). In Fig. 4.8 the "U in water" and "TDS" are associated with the horizontal axis "First Factor", whereas the "U in rocks" is associated with the vertical axis "Second Factor". Moreover, the trend of the "U in water" and "TDS" is negative with respect to the second loading factor and positive to the first loading factor. The trend of "U in rocks" extends, however, from positive to negative values with respect to both factors. This feature may give indications that uranium concentration in water and the TDS are probably sourced from a common origin in general but the stronger negative loading of the second factor suggests contribution of additional source to the TDS. This source might be agricultural loading which could also contribute to the uranium in the groundwater. The different sources of uranium can be aquifer rocks, particularly carbonates, intrusion of seawater and agricultural practices. The data on uranium from these different sources are meager and thus, only inferences on the of each factor are discussed below.

The interaction between aquifer body, i.e. rocks and sediments, can be a possible source of uranium in the groundwater, particularly in the carbonate rocks where groundwater contains a higher concentration of uranium than the alluvial plain. For example, the samples (GWW-Jaw, 1) and (GWW-Jaw, 2) are from alluvial deposits aquifer and have very low  $^{238}\text{U}$  concentrations compared with the majority of carbonate aquifer samples. Another possible source of uranium in groundwater is intrusion from deep-seated reservoirs and seawater. The later may be of special concern when dealing with coastal aquifers. In many near coastal



areas in the UAE, extensive pumping rates permit sea-water invasion to the aquifers (Wetzelhuetter, 2013).

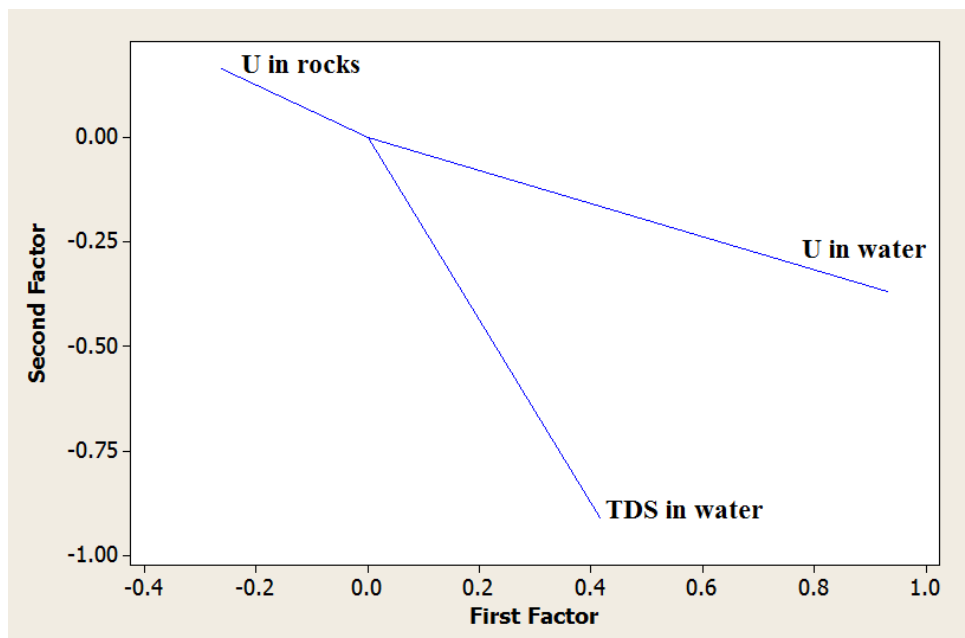


Fig. 4.8 Loading plot of factor analysis using the parameters of uranium in rocks, uranium in water and TDS in water, details in Appendix-B.

However, most of the sampled wells used here are far from the sea and only a few wells (five in area A-3 and four wells in area A-4) are located close to the sea and may have some seawater intrusion effect. In this study, as A-3 is near to coast and A-5 is located in Abu Dhabi interdunal sabkha (El-Sayed, 2000), groundwater in both areas show elevated salinity (TDS) values. The interdunal sabkha, area A-5, contains brine water (TDS average =  $9046 \text{ mg L}^{-1}$ ). Coastal sabkha can affect nearby aquifers through development of evaporitic minerals (e.g. gypsum and halite) that can hold uranium and would easily be dissolved and transported to the groundwater during storm rainfall. Also, the factor analysis (Fig. 4.8) illustrates that uranium and TDS probably have a common source.

Besides this, the correlation coefficient (R) between uranium and TDS are moderate to strong ranging from 0.55 to 0.89 (Fig. 4.1). The correlations in A-1, A-2, A-3, A-4 and A-5 are: 0.89, 0.71, 0.55, 0.69 and 0.71 respectively. In A-4 the samples R-KH1, R-KH2 and R-KH3 are outliers and so were excluded from the correlations. Moreover, a moderate value of correlation ( $R = 0.84$ ) was obtained between the total uranium (total uranium  $^T\text{U}$  concentration is calculated here as the sum of  $^{235}\text{U}$  and  $^{238}\text{U}$  and sometimes considered as  $^{238}\text{U}$  alone due to its high abundance in nature) and chloride, which supports the idea of seawater intrusion (Fig. 4.9). In some samples, however, high chloride may originate from deep seated sources such as brine water of hydrocarbon reservoirs (Kelly et al., 2012).

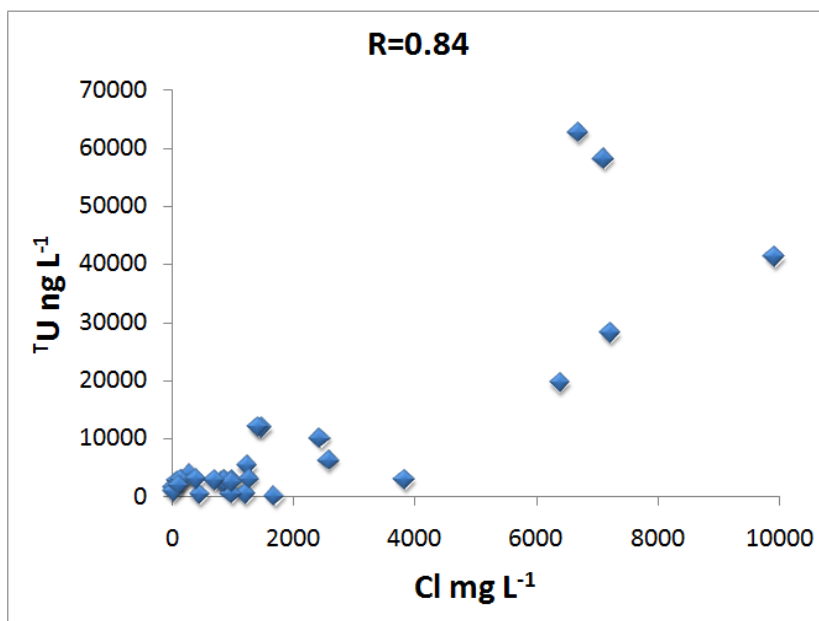


Fig. 4.9 Correlation between total uranium and chloride anion among 30 groundwater samples, showing moderate linear relationship ( $R=0.84$ ).

Factor analysis indicates that both  $^{235}\text{U}$  and  $^{238}\text{U}$  have the same source reflecting natural abundance of the isotopes, since they are almost overlapped in the loading plot (Fig. 4.10). Despite that all the trends (TDS, Cl and uranium) indicate common grouping and as they are likely to have similar sources, the partition of TDS and Cl supports additional sources such as agricultural practices and intrusion of seawater. It is clear that more uranium data from wells situated near to coastlines and time series data on groundwater and fertilizers uses are needed to better connect the relationship between groundwater and sources.

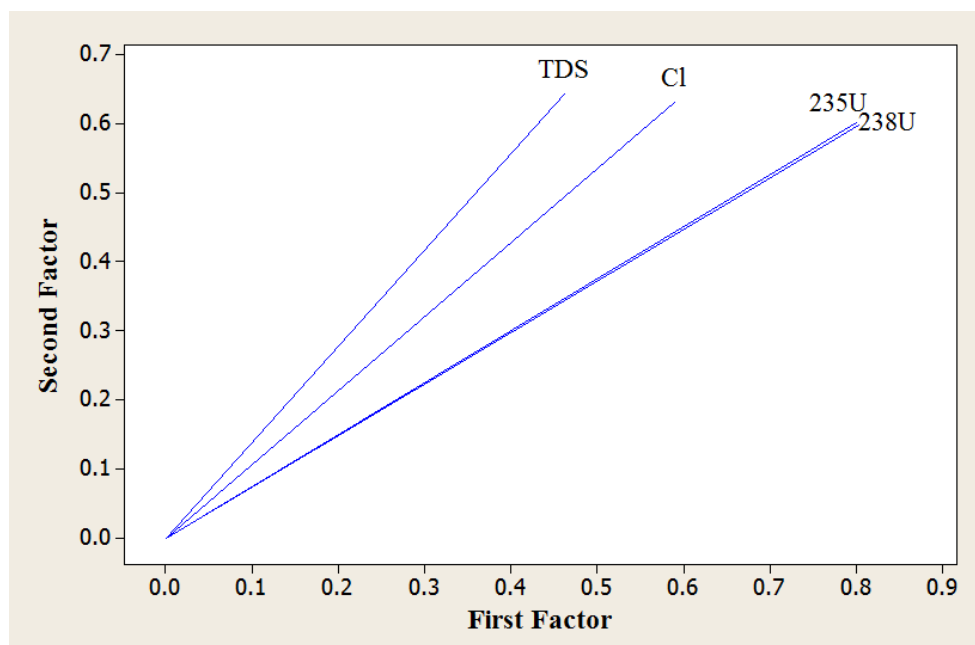


Fig. 4.10 Factor analysis using  $^{235}\text{U}$ ,  $^{238}\text{U}$ , TDS and  $\text{Cl}^-$  as loadings, details in Appendix-C.

Uranium might enter the hydrological system through the agricultural activities that regularly use phosphate fertilizers commonly containing some uranium and thorium (Roselli, 2009). In the UAE, fertilizers are mainly NPK

type (Nitrate, Phosphate and Potassium) that are known to have an appreciable concentration of uranium varying from 0.337 Bq/g to 4.823 Bq/g (EPA, 2009; Khater, 2012). Upon irrigation, uranium in the fertilizer might be dissolved and infiltrate the groundwater aquifers. The amount of fertilizer-related uranium is difficult to estimate in the studied groundwater samples, as most of the wells are rather deep (>10 m). However, caution should be taken when dealing with groundwater at a shallow level (the saturated zone near to the Earth's surface as is the case in central Europe) as the possible infiltration of uranium to the groundwater is more effective (Lienert et al., 1994). Even with no clear idea about the fertilizers in the study areas, the uranium concentration in water and the uranium content in soil (sediments) show a good correlation coefficient ( $R = 0.71$ ). The soil samples were collected from farms irrigated by the sampled groundwater in A-4. It is, however, anticipated that the fertilizers infiltrate shallow aquifers and provide a source of uranium in the water.

In contrast to uranium, thorium is almost insoluble in water, and so the mass of leached thorium from soil will be much lower than uranium. Despite its weak solubility, thorium is strongly adsorbed on iron hydroxides and clays (Nash & Choppin, 1980; Hunter et al., 1988; Murphy et al., 1999). This fact was clearly observed in the rocks collected, where the correlation coefficient between the  $^{232}\text{Th}$  and  $\text{Fe}_2\text{O}_3$  was moderately strong ( $R = 0.85$ ), indicating that the thorium was selectively adsorbed on the iron oxides. Also, the correlation coefficient between the  $^{232}\text{Th}$  in water samples and  $\text{Fe}_2\text{O}_3$  in rocks was extremely strong ( $R = 0.92$ ) (Fig. 4.11). The  $^{232}\text{Th}$  average concentration in groundwater is below 1000

ng L<sup>-1</sup> in 65 out of 67 groundwater samples in this study (Table 3.2). The variations in <sup>232</sup>Th concentrations are probably controlled by the availability of sulfate salt rocks (like gypsum) interacting with thorium and forming soluble thorium compounds (Weast, 1988). This process might be the major source of thorium in the groundwater investigated here, where gypsum is a common component in most rocks and sediments investigated here.

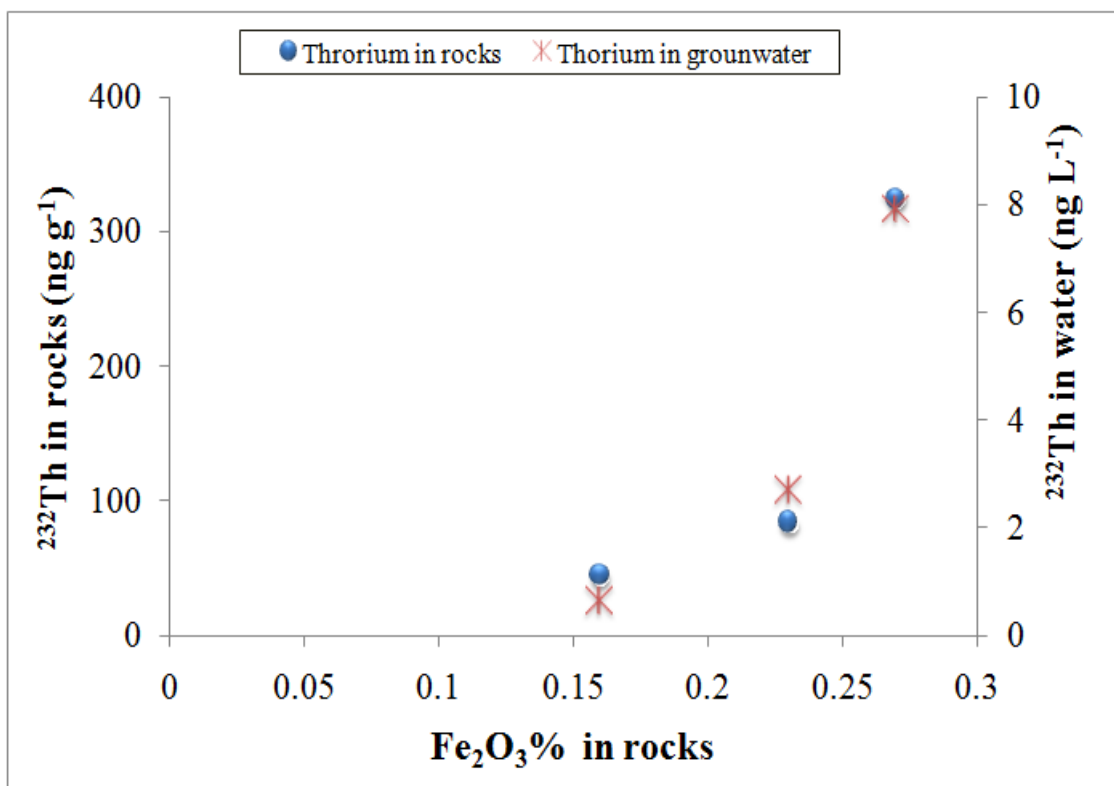


Fig. 4.11 The correlation between thorium in rocks and in groundwater versus iron oxides has the values of  $R = 0.85$  and  $0.92$  respectively.

It is worth to mentioning that rocks and sediments/soils contains different types of oxides as found by the chemical analysis (Table 3.3). The analysis

elucidates that the soil/sediment samples from A-2 area are mainly limestone showing high content of CaO. Sample (JH-2) in particular has high content of SiO<sub>2</sub> than other samples, which is related to chertification (silicification) in this part of the rock section. In A-4 area, the chemistry of the rocks points out dolomitization of the limestone or even dominantly dolomite rock as shown by the relatively high content of MgO (20%) in these samples. The Al<sub>2</sub>O<sub>3</sub> and Fe<sub>2</sub>O<sub>3</sub> are used as indicators of phyllosilicates (mainly clay, such as illite and chlorite) minerals, in addition to iron oxides, and thus they have higher concentrations in mudstones and siltstones such as samples r-15 and r-30 (Table 2.1). The concentration of K<sub>2</sub>O, MnO<sub>2</sub>, Na<sub>2</sub>O and P<sub>2</sub>O<sub>5</sub> were rather low in the investigated rocks and relatively high in sediments. This may reflect the effect of weathering and interference from NPK fertilizers contents.

#### **4.4 Groundwater in Oman**

Some groundwater samples were collected from Oman to compare the radioactivity level with those investigated in the UAE since both countries are arid and located in a similar geographic region. The groundwater quality of samples from Oman seems to be good in terms of acidity (pH), salinity, and radiations activity. Oman water could be considered as fresh neutral water that is suitable for drinking. The pH of water has no direct health impact and so the WHO has not established a permissible limit for the pH (WHO, 2011). The pH affects the taste of water, and the range of pH in Oman samples (6.9 – 9.7) is acceptable in terms of taste. The TDS in all water samples in Oman are below 1000 mg L<sup>-1</sup> which fall under the fresh water type. The highest <sup>238</sup>U

concentration is  $1425 \text{ ng L}^{-1}$  in sample (MO-1) occurring in fractured ophiolite-carbonate aquifer and is far below the WHO permissible limit for uranium ( $60000 \text{ ng L}^{-1}$ ). The uranium concentrations in the alluvial deposits water samples in Oman (FO-1 to FO-10) are comparable with the alluvial deposits water samples in the UAE (GWW-Jaw, 1 and GWW-Jaw, 2). On the other hand, a noticeable variation occurs between the uranium concentrations in Oman (WD-1 and MO-1) and UAE (A-2 and A-4) carbonate water samples, due the effect of higher rains in Oman ( $275 \text{ mm/ year}$ ) (NOAA, 2013).

At local level, a marked difference is observed between the uranium concentrations in the alluvial deposits (FO-1 to FO-10) and carbonates (WD-1 and MO-1) in Oman, suggesting different recharge sources or ages as well as interaction with the aquifer body. This age difference, together with the much higher porosity and permeability in the alluvial deposits, might result in short residence time for the rainfall-dominated recharge to react and include more radionuclides than the carbonates aquifers (Murad et al., 2014). However, the uranium concentration in carbonate aquifers in Oman is relatively low compared to the UAE carbonate aquifers in A-2 and A-4 area. This could be due to dilution by rainfall in Oman, where the annual rain average is about  $275 \text{ mm/year}$  (Charabi and Al-Hatrushi, 2010), almost triple the rainfall in the UAE.

The highest concentrations of both  $^{222}\text{Rn}$  and  $^{226}\text{Ra}$  occur in sample (MO-1) at  $120 \text{ Bq L}^{-1}$  and  $0.111 \text{ Bq L}^{-1}$  respectively. Also, the highest water temperature ( $62 \text{ }^\circ\text{C}$ ) occurs in the sample (MO-1), while all the other samples have similar temperatures in the ranges of  $30.2 - 39.8 \text{ }^\circ\text{C}$ . The high temperature in

sample MO-1 might be linked to the relatively high radioactivity of the  $\alpha$  emitters:  $^{238}\text{U}$ ,  $^{222}\text{Rn}$  and  $^{226}\text{Ra}$  (Gundersen and Wanty, 1992), but it may also be due to tectonic instability and intrusion of water from deep-seated sources in contact with a hydrothermal source. Six out of thirteen groundwater samples have  $^{232}\text{Th}$  below the detection limit, and the highest concentration is  $0.013 \text{ mBq L}^{-1}$  in sample (FO-1). Gross  $\beta$ , gross  $\alpha$ , uranium, thorium, radon and radium are all below the WHO permissible limits in Oman water samples. These results confirm the relatively low radioactivity in the sampled Oman groundwater and may again suggest rainfall and extensive recharge as a possible factor affecting concentration of radioactive elements in groundwater of arid regions.



## 5 CONCLUSIONS AND RECOMMENDATIONS

### 5.1 Concluding summary

Based on the investigation results and discussion above, the following main conclusions can be drawn:

1. The  $^{235}\text{U}$ ,  $^{238}\text{U}$  and  $^{232}\text{Th}$  concentrations in the investigated groundwater (in the UAE) are below the WHO permissible limits for drinking water in most of the groundwater analyzed here.
2. The  $^{235}\text{U}$  and  $^{238}\text{U}$  concentrations in the investigated groundwater are comparable with other countries in arid regions, and are slightly lower than concentrations in groundwater of countries located in humid regions.
3. The  $^{232}\text{Th}$  concentrations in the investigated groundwater here are below the WHO permissible limits for drinking water, and this is expected due to the low solubility of natural thorium in water.
4. Gross  $\beta$  and gross  $\alpha$  activity values in the groundwater in this work were found to exceed the WHO permissible limits for drinking water in some locations. The activity of  $^{235}\text{U}$ ,  $^{238}\text{U}$  and  $^{232}\text{Th}$  does not account for all the measured gross- $\alpha$  and thus progeny radionuclides of isotopes of uranium and thorium such as  $^{226}\text{Ra}$  might be the possible sources of elevated gross  $\alpha$  activity level, while  $^{40}\text{K}$ ,  $^{228}\text{Ra}$  and  $^{210}\text{Pb}$ , which are not measured in this

investigation, might contribute to the elevated level of gross  $\beta$  activity in these samples.

5. Uranium concentrations in groundwater seem to decrease by dilution with increasing rainfall, as shown by regional and worldwide comparison.
6. Uranium in the groundwater of the UAE is mainly sourced from aquifer geochemical interaction as well as the fertilized soils. Effects from seawater intrusion are not clearly fingerprinted.
7. Thorium is mainly sourced from the aquifers' geochemical interaction, and the concentration increases in groundwater as the iron oxides and particulate materials increase.
8. The  $^{235}\text{U}$ ,  $^{238}\text{U}$  and  $^{232}\text{Th}$  concentrations in Oman alluvial deposits groundwater are comparable with the UAE alluvial water; however, uranium concentrations in Oman carbonate aquifers are much less than the UAE due to the increased rainfall in Oman.
9. The concentration of  $^{235}\text{U}$ ,  $^{238}\text{U}$  and  $^{232}\text{Th}$  in groundwater sampled from Oman are about one order of magnitude lower than in the UAE. This might be attributed to higher precipitation rate and consequent dilution of aquifers water.
10. The activity of  $^{222}\text{Rn}$  and  $^{226}\text{Ra}$  in the groundwater from Oman are one to three orders of magnitude lower than the WHO permissible

limits. Dilution of groundwater by relatively high rainfall can be a possible reason. However, the  $^{222}\text{Rn}$  in the spring hot water sample (120 Bq/L) is slightly higher than the WHO permissible limit (100 Bq/L).

11. Calculation of IDC from  $^{235}\text{U}$ ,  $^{238}\text{U}$  and  $^{232}\text{Th}$  in the studied areas in the UAE suggests that the radiation in the groundwater will not add a sufficient amount to the highest permissible annual dose to human in general.

## **5.2 Prospect for future research**

The results of this investigation suggest several issues for future studies that will expand our understanding of the distribution of natural radioactivity in the UAE surface environment. Among these issues, an investigation of all UAE groundwater aquifers radioactivity is essential. Another vital issue for future investigation is conducting a systematic sampling of soil, in particular the agricultural areas, in order to fingerprint the differences between natural and artificial signals of radioactivity. The third issue is to do as much as possible analysis of aquifer rock samples from outcrops and drilled wells for the accurate estimation of rock-water interaction and subsequent thermodynamic modeling. Finally, the establishment of a soil-to-plant transfer factor for the arid regions, which is presently missing due to the absence of data, on plant radioactivity for proper environmental impact assessments.

## 6 REFERENCES

- Abdul-Hadi, A., Alhassanieh, O., & Ghafar, M. (2001). Disequilibrium of uranium isotopes in some Syrian groundwater. *Applied Radiation and Isotopes*, 55(1), 109-113.
- Adamiec, G., & Aitken, M. J. (1998). Dose-rate conversion factors: update. *Ancient tL*, 16(2), 37-50.
- Added, A., Ben Mammou, A., Fernex, F., Rezzoug, S., & Bernat, M. (2005). Distribution of uranium and radium isotopes in an aquifer of a semi-arid region (Manouba-Essijoumi, Northern Tunisia). *Journal of environmental radioactivity*, 82(3), 371-381.
- Åkerblom, G. (1994). Radon i vatten (Radon in water). *Borrsvängen*, 3(94), 16-21.
- Al-Aasm, I., Sirat, M., Morad, S., AlDahan, A., & Al-Jallad, O. (2013, April). Fracturing and carbonate mineralization in Palaeogene carbonate rocks from the United Arab Emirates: A record of fluid flow. In *EGU General Assembly Conference Abstracts* (Vol. 15, p. 12085).
- Al-Amir, S. M., Al-Hamarneh, I. F., Al-Abed, T., & Awadallah, M. (2012). Natural radioactivity in tap water and associated age-dependent dose and lifetime risk assessment in Amman, Jordan. *Applied Radiation and Isotopes*, 70(4), 692-698.
- Aldahan, A., & Possnert, G. (2003). Geomagnetic and climatic variability reflected by  $^{10}\text{Be}$  during the Quaternary and late Pliocene. *Geophysical research letters*, 30(6).
- Aleissa, K. A., & Islam, M. S. (2008). Evaluation of the extractive procedure for determination of  $^{238}\text{U}$   $^{234}\text{U}$  in groundwater and comparison with traditional  $\alpha$ -spectro.
- Allard, B., Olofsson, U., & Torstenfelt, B. (1984). Environmental actinide chemistry. *Inorganica chimica acta*, 94(4), 205-221.
- Alpen, E. L. Radiation biophysics, 1998.
- Alshamsi, D. M., Murad, A. A., Aldahan, A., & Hou, X. (2013). Uranium isotopes in carbonate aquifers of arid region setting. *Journal of Radioanalytical and Nuclear Chemistry*, 298(3), 1899-1905.
- Alsharhan, A. S., Rizk, Z. A., Nairn, A. E. M., Bakhit, D. W., & Alhajari, S. A. (Eds.). (2001). *Hydrogeology of an Arid Region: The Arabian Gulf and Adjoining Areas: The Arabian Gulf and Adjoining Areas*. Elsevier.

- Andersen, M. B., Stirling, C. H., Porcelli, D., Halliday, A. N., Andersson, P. S., & Baskaran, M. (2007). The tracing of riverine U in Arctic seawater with very precise  $^{234}\text{U}$ / $^{238}\text{U}$  measurements. *Earth and Planetary Science Letters*, 259(1), 171-185.
- Andersson, P. S., Porcelli, D., Wasserburg, G. J., & Ingri, J. (1998). Particle transport of  $^{234}\text{U}$ - $^{238}\text{U}$  in the Kalix River and in the Baltic Sea. *Geochimica et cosmochimica acta*, 62(3), 385-392.
- Andersson, P. S., Wasserburg, G. J., Chen, J. H., Papanastassiou, D. A., & Ingri, J. (1995).  $^{238}\text{U}$ - $^{234}\text{U}$  and  $^{232}\text{Th}$ - $^{230}\text{Th}$  in the Baltic Sea and in river water. *Earth and Planetary Science Letters*, 130, 217-234.
- Asikainen, M. (1982). *Natural radioactivity of ground and drinking water in Finland* (Vol. 39). Institute of Radiation Protection.
- ATSDR (Agency for Toxic Substances and Disease Registry) (2012) Toxicological Profiles. <http://www.atsdr.cdc.gov/toxprofiles/tp147-c5.pdf>. Retrieved 2014-03-17.
- Banks, D., Røyset, O., Strand, T., & Skarphagen, H. (1995). Radioelement (U, Th, Rn) concentrations in Norwegian bedrock groundwaters. *Environmental geology*, 25(3), 165-180.
- Becker, J. S. (2003). Review: Mass spectrometry of long-lived radionuclides. Elsevier, *Spectrochimica Acta Part B*; 58:1757-1784.
- Benedik, L., & Jeran, Z. (2012). Radiological of natural and mineral drinking waters in Slovenia. *Radiation protection dosimetry*, 151(2), 306-313.
- Beyermann, M., Bünger, T., Schmidt, K., & Obrikat, D. (2010). Occurrence of natural radioactivity in public water supplies in Germany:  $^{238}\text{U}$ ,  $^{234}\text{U}$ ,  $^{235}\text{U}$ ,  $^{228}\text{Ra}$ ,  $^{226}\text{Ra}$ ,  $^{222}\text{Rn}$ ,  $^{210}\text{Pb}$ ,  $^{210}\text{Po}$  and gross  $\alpha$  activity concentrations. *Radiation protection dosimetry*, 141(1), 72-81.
- Bishop, M. (2010). Heat. Retrieved from <http://www.eoearth.org/view/article/153460>.
- Bleise, A., Danesi, P. R., & Burkart, W. (2003). Properties, use and health effects of depleted uranium (DU): a general overview. *Journal of Environmental Radioactivity*, 64(2), 93-112.
- Bonotto, D. M. (2011). Natural radionuclides in major aquifer systems of the Paraná sedimentary basin, Brazil. *Applied Radiation and Isotopes*, 69(10), 1572-1584.
- Breesch, L., Swennen, R., Vincent, B., Ellison, R., & Dewever, B. (2010). Dolomite cementation and recrystallisation of sedimentary breccias along

the Musandam Platform margin (United Arab Emirates). *Journal of Geochemical Exploration*, 106(1), 34-43.

- Brenner, D. J., Doll, R., Goodhead, D. T., Hall, E. J., Land, C. E., Little, J. B., ... & Zaider, M. (2003). Cancer risks attributable to low doses of ionizing radiation: assessing what we really know. *Proceedings of the National Academy of Sciences*, 100(24), 13761-13766.
- Brook, M. C., Al Houqani, H., Darawsha, T., & Achary, M. A. A. S. (2006). Groundwater Resources: Development & Management in the Emirate of Abu Dhabi, United Arab Emirates. *Arid Land Hydrogeology: In search of a Solution to a Threatened Resource*. Taylor and Francis, Balkema, Netherlands, 15-34.
- Brown, C. J., Jurgens, B. C., Katz, B. G., Landon, M. K., & Eberts, S. M. (2007, March). Arsenic and uranium in four aquifer settings: occurrence, distribution, and mechanisms for transport to supply wells. In *Proceedings of the 2007 National Groundwater Association Naturally Occurring Contaminants Conference: Arsenic, Radium, Radon, and Uranium*, Charleston, South Carolina (p. 15).
- Burchfield, L. A. (2009). *Radiation safety: Protection and management for homeland security and emergency response*. John Wiley & Sons.
- Chang, P., Kim, K. W., Yoshida, S., & Kim, S. Y. (2005). Uranium accumulation of crop plants enhanced by citric acid. *Environmental geochemistry and health*, 27(5-6), 529-538.
- Charabi, Y., & Al-Hatrushi, S. (2010). Synoptic aspects of winter rainfall variability in Oman. *Atmospheric Research*, 95(4), 470-486.
- Chen, S. B., Zhu, Y. G., & Hu, Q. H. (2005). Soil to plant transfer of  $^{238}\text{U}$ ,  $^{226}\text{Ra}$  and  $^{232}\text{Th}$  on a uranium mining-impacted soil from southeastern China. *Journal of Environmental radioactivity*, 82(2), 223-236.
- Chkir, N., Guendouz, A., Zouari, K., Hadj Ammar, F., & Moulla, A. S. (2009). Uranium isotopes in groundwater from the continental intercalaire aquifer in Algerian Tunisian Sahara (Northern Africa). *Journal of environmental radioactivity*, 100(8), 649-656.
- Cizdziel, J., Farmer, D., Hodge, V., Lindley, K., & Stetzenbach, K. (2005).  $^{234}\text{U}/^{238}\text{U}$  isotope ratios in groundwater from Southern Nevada: a comparison of alpha counting and magnetic sector ICP-MS. Elsevier, *Science of the Total Environment*, 350 (1), 248– 260.
- Clarkson, M.O., Richoz, S., Wood, R.A., Maurer, F., Krystyn, L., McGurty, D.J., & Astratti, D. (2013). A new high-resolution  $\delta^{13}\text{C}$  record for the Early

Triassic: Insights from the Arabian Platform. *Gondwana research*, 24 (1) 233-242.

- Cothern, C. R. (1996). An overview of environmental risk decision making: Values, perceptions, and ethics. *Handbook for Environmental Risk Decision Making: Values, Perceptions, and Ethics*, 37-67.
- Da Conceição, F. T., Bonotto, D. M., Jiménez-Rueda, J. R., & Roveda, J. A. F. (2009). Distribution of <sup>226</sup>Ra, <sup>232</sup>Th and <sup>40</sup>K in soils and sugar cane crops at Corumbataí river basin, São Paulo State, Brazil. *Applied Radiation and Isotopes*, 67(6), 1114-1120.
- Dabous, A. A., Osmond, J. K., & Dawood, Y. H. (2002). Uranium/Thorium isotope evidence for ground-water history in the Eastern Desert of Egypt. *Journal of Arid Environments*, 50(2), 343-357.
- Dahlkamp, F. J. (1993). Uranium ore deposits.
- Dalrymple, G. B. (2001). The age of the Earth in the twentieth century: a problem (mostly) solved. *Geological Society, London, Special Publications*, 190(1), 205-221.
- Darby, S., Hill, D., & Doll, R. (2001). Radon: a likely carcinogen at all exposures. *Annals of Oncology*, 12(10), 1341-1351.
- Dawoud, M. A. (2008). Water resources in Abu Dhabi emirate, United Arab Emirates. Environmental Agency Abu Dhabi (EAD). <http://www.agedi.ae/Pages/pdf/4%20Water%20Resources.pdf>.
- Department of Environmental Services (2007). Radium, Radon, and Uranium: Health Information Summary: *Environmental factsheet; ARD-EHP-22*. New Hampshire, USA.
- Dinh Chau, N., Dulinski, M., Jodlowski, P., Nowak, J., Rozanski, K., Slezniak, M., & Wachniew, P. (2011). Natural radioactivity in groundwater—a review. *Isotopes in environmental and health studies*, 47(4), 415-437.
- Drissi, S. H., Refait, P., Abdelmoula, M., & Génin, J. M. R. (1995). The preparation and thermodynamic properties of Fe (II) & Fe (III) hydroxide-carbonate (green rust 1); Pourbaix diagram of iron in carbonate-containing aqueous media. *Corrosion science*, 37(12), 2025-2041.
- Dunk, R. M., Mills, R. A., & Jenkins, W. J. (2002). A reevaluation of the oceanic uranium budget for the Holocene. *Chemical Geology*, 190(1), 45-67.
- Ebbs, S. D., Brady, D. J., & Kochian, L. V. (1998). Role of uranium speciation in the uptake and translocation of uranium by plants. *Journal of experimental botany*, 49(324), 1183-1190.

- El-Mageed, A. I. A., El-Kamel, A. E. H., Abbady, A. E. B., Harb, S., & Saleh, I. I. (2013). Natural radioactivity of ground and hot spring water in some areas in Yemen. *Desalination*, 321, 28-31.
- El-Saiy, A. K., & Jordan, B. R. (2007). Diagenetic aspects of tertiary carbonates west of the Northern Oman Mountains, United Arab Emirates. *Journal of Asian Earth Sciences*, 31(1), 35-43.
- El-Sayed, M. I. (2000). The nature and possible origin of mega-dunes in Liwa, Ar Rub'Al Khali, UAE. *Sedimentary Geology*, 134(3), 305-330.
- Emsley & John (2001). "Uranium". *Nature's Building Blocks: An A to Z Guide to the Elements*. Oxford University Press. pp. 476–482. ISBN 0-19-850340-7.
- Erhard, A. (2013). Non-destructive Evaluation. In *Handbook of Technical Diagnostics* (pp. 161-174). Springer Berlin Heidelberg.
- ESRI 2011. ArcGIS Desktop: Release 10.1. Redlands, CA: Environmental Systems Research Institute.
- Fano U. (1964). Penetration of protons, alpha particles, and mesons<sup>12</sup>. *Studies in Penetration of Charged Particles in Matter*, (39), 287.
- Faure, G. (1998). *Principles and applications of geochemistry* (Vol. 2). Upper Saddle River, NJ: Prentice-Hall.
- Faure, G., & Mensing, T. M. (2005). *Isotopes: principles and applications*. John Wiley & Sons Inc.
- Finch, R., & Murakami, T. (1999). Systematics and paragenesis of uranium minerals. *Reviews in Mineralogy and Geochemistry*, 38(1), 91-179.
- Flynn, J., & MacGregor, D. G. (2002). *Low Dose Risk, Decisions, and Risk Communication* (No. EMSP-69904). Decision Research, Eugene, Oregon (US).
- Food Standards Agency, UK (2001) Uranium-238 in the 2001 Total Diet Study. FSA library, FSIS 56/04.
- Forsberg, C. W., & Lewis, L. C. (1999). Uses for Uranium-233: What Should Be Kept for Future Needs?. *ORNL*, 6952.
- Foutes, C. S., Elliot, G., Shankar, L., Brian, M., Schultheisz, J., Daniel, S., & Mark, S. L. (2006). Technologically Enhanced Naturally Occurring Radioactive Materials From Uranium Mining "Mining and Reclamation Background". US Environmental Protection Agency Office of Radiation



and Indoor Air Radiation Protection Division. Washington, D.C., pp. 1–8 to 1–9.

- Freeze, A. O., & Cherry, J. A. (1979) Groundwater (Edition 1), Prentice-Hall.
- Frengstad, B. S., Lax, K., Tarvainen, T., Jæger, Ø., & Wigum, B. J. (2010). The chemistry of bottled mineral and spring waters from Norway, Sweden, Finland and Iceland. *Journal of Geochemical Exploration*, 107(3), 350-361.
- Fried, S., Friedman, A. M., Callis, E., Schreiner, F., Hines, J., Orlandini, K., ... & Olsen, E. (1985). Enrichment of  $^{235}\text{U}$  and the concentration of  $^{239}\text{Pu}$  in volcanic samples.
- Garba, M. L., Arabi, A. S., & Adeyemo, D. J. (2013). Assessment of Gross Alpha and Beta Radioactivity in Groundwater by Liquid Scintillation. *J. Appl. Environ. Biol. Sci*, 3(7), 1-5.
- Gundersen, L. C., & Wanty, R. B. (1993). *Field studies of radon in rocks, soils, and water*. CRC Press.
- Gunter Faure. Principles and applications of geochemistry. Second edition (1998). Upper saddle river, New Jersey, USA: Prentice hall.
- Guogang, J., Torri, G., & Magro, L. (2009). Concentrations of  $^{238}\text{U}$ ,  $^{234}\text{U}$ ,  $^{235}\text{U}$ ,  $^{232}\text{Th}$ ,  $^{230}\text{Th}$ ,  $^{228}\text{Th}$ ,  $^{226}\text{Ra}$ ,  $^{228}\text{Ra}$ ,  $^{224}\text{Ra}$ ,  $^{210}\text{Po}$ ,  $^{210}\text{Pb}$  and  $^{212}\text{Pb}$  in drinking water in Italy: reconciling safety standards based on measurements of gross  $\alpha$  and  $\beta$ . *Journal of Environmental Radioactivity*, 100(11), 941-949.
- Hadj Ammar, F., Chkir, N., Zouari, K., & Azzouz-Berriche, Z. (2010). Uranium isotopes in groundwater from the “Jeffara coastal aquifer”(southeastern Tunisia). *Journal of environmental radioactivity*, 101(9), 681-691.
- Hammond, C. R. (2004). *The Elements, in Handbook of Chemistry and Physics 81st edition*. CRC press.
- Hanks, P., et al. (Eds.). (2003). Collins pocket English dictionary. London, England: Collins.
- Health Physics Society Specialists in Radiation Safety (2011) Depleted uranium. Retrieved from [http://hps.org/documents/URANIUM\\_fact\\_sheet.pdf](http://hps.org/documents/URANIUM_fact_sheet.pdf).
- Hileman, G. E., & Lee, R. W. (1993). *Geochemistry of and radioactivity in ground water of the Highland Rim and Central Basin aquifer systems, Hickman and Maury Counties, Tennessee*. US Department of the Interior, US Geological Survey.

- Hou, X., & Roos, P. (2008). Critical comparison of radiometric and mass spectrometric methods for the determination of radionuclides in environmental, biological and nuclear waste samples. *Analytica Chimica Acta*, 608(2), 105-139.
- HPS (Health Physics Society Specialists in Radiation Safety) (2010) Factsheet: Uranium. Retrieved from <http://hps.org/documents/dufactsheet.pdf>.
- Hubert, A., Bourdon, B., Pili, E., & Meynadier, L. (2006). Transport of radionuclides in an unconfined chalk aquifer inferred from U-series disequilibria. *Geochimica et cosmochimica acta*, 70(22), 5437-5454.
- Hunter, K. A., Hawke, D. J., & Choo, L. K. (1988). Equilibrium adsorption of thorium by metal oxides in marine electrolytes. *Geochimica et Cosmochimica Acta*, 52(3), 627-636.
- Hyde, E. K. (1960). NAS-NS 3004. *The Radiochemistry of Thorium*, 6.
- Ignasi, P. (2004). Hydra/Medusa Chemical Equilibrium Database and Plotting Software, KTH Royal Institute of Technology, freely downloadable software at University of Bath & Western Oregon University. Retrieved in 2014 from: [http://en.wikipedia.org/wiki/Pourbaix\\_diagram](http://en.wikipedia.org/wiki/Pourbaix_diagram).
- International Commission on Radiation Units and Measurements (1970). Linear Energy Transfer. Washington D.C. ISBN 978-0913394090. ICRU report 16. Retrieved in December 2012.
- Janković, M. M., Todorović, D. J., Todorović, N. A., & Nikolov, J. (2012). Natural radionuclides in drinking waters in Serbia. *Applied Radiation and Isotopes*, 70(12), 2703-2710.
- Kabadayi, Ö., & Gümüş, H. (2012). Natural activity concentrations in bottled drinking water and consequent doses. *Radiation protection dosimetry*, 150(4), 532-535.
- Kawabata, Y., Aparin, V., Nagai, M., Yamamoto, M., Shiraishi, K., & Katayama, Y. (2008). Uranium and thorium isotopes from Kazakhstan. *Journal of radioanalytical and nuclear chemistry*, 278(2), 459-462.
- Kelly, W. R., Panno, S. V., & Hackley, K. (2012). The Sources, Distribution, and Trends of Chloride in the Waters of Illinois. Retrieved from <http://www.isws.illinois.edu/pubdoc/B/ISWSB-74.pdf>.
- Khater, A. E. (2012). Uranium and trace elements in phosphate fertilizers—Saudi Arabia. *Health physics*, 102(1), 63-70.
- Khattree, R., & Naik, D. N. (2000). *Multivariate data reduction and discrimination with SAS software*. Sas Institute.

- Kim, J. O., & Mueller, C. W. (Eds.). (1978). *Factor analysis: Statistical methods and practical issues* (Vol. 14). Sage.
- Kim, J. O., & Mueller, C. W. (Eds.). (1978). *Introduction to factor analysis: What it is and how to do it* (No. 13). Sage.
- Kónya, J., & Nagy, N. M. (2012). *Nuclear and Radiochemistry*. Elsevier.
- Kozinski, J., Szabo, Z., Zapecza, O. S., & Barringer, T. H. (1993). Natural radioactivity in, and inorganic chemistry of, ground water in the Kirkwood-Cohansey aquifer system, southern New Jersey, 1983-89.
- Krupka, K. M., & Serne, R. J. (2002). Geochemical factors affecting the behavior of antimony, cobalt, europium, technetium, and uranium in vadose sediments. *Report PNNL, 14126*.
- Lauria, D. C., Almeida, R. M., & Sracek, O. (2004). Behavior of radium, thorium and uranium in groundwater near the Buena Lagoon in the Coastal Zone of the State of Rio de Janeiro, Brazil. *Environmental Geology, 47*(1), 11-19.
- Lehto, J., & Hou, X. (2010). *Chemistry and analysis of radionuclides: laboratory techniques and methodology*. John Wiley & Sons.
- Lienert, C., Short, S. A., & Gunter, H. R. V. (1994) Uranium infiltration from a river to shallow groundwater. *Geochimica et Cosmochimica Acta, 58* (24), 5455–5463.
- Luo, S., Ku, T. L., Roback, R., Murrell, M., & McLing, T. L. (2000). In-situ radionuclide transport and preferential groundwater flows at INEEL (Idaho): decay-series disequilibrium studies. *Geochimica et Cosmochimica Acta, 64*(5), 867-881.
- Makoti, C. A., Marwa, E. M., & Kaaya, A. K. (2012). Determination of uranium concentration in selected agriculture soils of Bah district in Tanzania and its uptake by food crops. Third RUFORUM Biennial Meeting 24 - 28 September 2012, Entebbe, Uganda.
- Mardia, K., Kent, J. T., & Bibby, J. M. 1979. *Multivariate Analysis*.
- Martin, P. (2003). Uranium and thorium series radionuclides in rainwater over several tropical storms. *Journal of environmental radioactivity, 65*(1), 1-18.
- Maurer, F., Rettori, R., & Martini, R. (2008). Triassic stratigraphy, facies and evolution of the Arabian shelf in the northern United Arab Emirates. *International Journal of Earth Sciences, 97*(4), 765-784.

- Merkel, B. J., Planer-Friedrich, B., & Nordstrom, D. K. (2005). *Groundwater geochemistry*. Springer-Verlag.
- Min, M., Peng, X., Zhou, X., Qiao, H., Wang, J., & Zhang, L. (2007). Hydrochemistry and isotope compositions of groundwater from the Shihongtan sandstone-hosted uranium deposit, Xinjiang, NW China. *Journal of Geochemical Exploration*, 93(2), 91-108.
- Ministry of Energy in the United Arab Emirates (2006) Initial National Communication to the United Nations Framework Convention on Climate Change. <http://unfccc.int/resource/docs/natc/arenc1.pdf>.
- Minitab Inc. (2010) Minitab (Version 16) [Software] LEAD Technologies Inc.
- Mohr, P. J., Taylor, B. N., & Newell, D. B. (2008). CODATA recommended values of the fundamental physical constants: 2006a). *Journal of Physical and Chemical Reference Data*, 37(3), 1187-1284.
- Montaser, A. (Ed.). (1998). *Inductively coupled plasma mass spectrometry*. Wiley-Vch.
- Moody, D. W. (1986). National water summary 1985: hydrologic events and surface-water resources. *Geological Survey water-supply paper*.
- Murad, A., Alshamsi, D., Hou, X. L., Al Shidi, F., Al Kendi, R., & Aldahan, A. (2014). Radioactivity in groundwater along the borders of Oman and UAE. *Journal of Radioanalytical and Nuclear Chemistry*, 299(3), 1653-1660.
- Murphy, R. J., Lenhart, J. J., & Honeyman, B. D. (1999). The sorption of thorium (IV) and uranium (VI) to hematite in the presence of natural organic matter. *Colloids and surfaces A: physicochemical and engineering aspects*, 157(1), 47-62.
- Nash, K. L., & Choppin, G. R. (1980). Interaction of humic and fulvic acids with Th (IV). *Journal of Inorganic and Nuclear Chemistry*, 42(7), 1045-1050.
- National Center of Meteorology and Seismology, Retrieved from <http://new.ncms.ae/arabic/climate.html>, 2014-01-28.
- National Geographic Education (2014) Geothermal energy. Retrieved from [http://education.nationalgeographic.com/education/encyclopedia/geothermal-energy/?ar\\_a=1](http://education.nationalgeographic.com/education/encyclopedia/geothermal-energy/?ar_a=1).
- National Institute of Standards and Technology. "Radionuclide Half-Life Measurements". Retrieved in 2011-11-07.

- National Nuclear Data Center (NNDC) (2009). Chart Nuclides by the National Nuclear Data Center . Retrieved from <http://www.nndc.bnl.gov/chart/>.
- National Oceanic and Atmospheric Administration (NOAA). Retrieved from <http://www.noaa.gov/wx.html>.
- Not, C., Brown, K., Ghaleb, B., & Hillaire-Marcel, C. (2012). Conservative behavior of uranium vs. salinity in Arctic sea ice and brine. *Marine Chemistry*, *130*, 33-39.
- O'Neil, M. J., Smith, A., & Heckelman, P. E. (2006). The Merck Index. Whitehouse Station, NJ: Merck & Co.
- OECD Nuclear Energy Agency (2003). Nuclear Energy Today. *OECD Publishing (964)*, 25. ISBN 9789264103283.
- Olea, R. A., & Olea, R. A. (1999). Geostatistics for engineers and earth scientists.
- Osman, A. A., Salih, I., Shaddad, I. A., El Din, S., Siddeeg, M. B., Eltayeb, H., ... & Yousif, E. H. (2008). Investigation of natural radioactivity levels in water around Kadugli, Sudan. *Applied Radiation and Isotopes*, *66*(11), 1650-1653.
- Osmond, J. K., & Ivanovich, M. (1992). Uranium-series mobilization and surface hydrology. *Uranium-Series Disequilibrium: Application to Earth, Marine, and Environmental Sciences*, Oxford Sciences Publications, Oxford, 259-289.
- Porcelli, D., Andersson, P. S., Baskaran, M., & Wasserburg, G. J. (2001). Transport of U-and Th-series nuclides in a Baltic Shield watershed and the Baltic Sea. *Geochimica et Cosmochimica Acta*, *65*(15), 2439-2459.
- Porcelli, D., Andersson, P. S., Wasserburg, G. J., Ingri, J., & Baskaran, M. (1997). The importance of colloids and mires for the transport of uranium isotopes through the Kalix River watershed and Baltic Sea. *Geochimica et Cosmochimica Acta*, *61*(19), 4095-4113.
- Puigdomenech, I. (2010). Hydra/Medusa Chemical Equilibrium Database and Plotting Software 2004. *KTH Royal Institute of Technology, freely downloadable software at <http://www.kemi.kth.se/medusa>. accessed in March.*
- Rizk, Z. S., Alsharhan, A. S., & Wood, W. W. (2007). Sources of dissolved solids and water in Wadi Al Bih aquifer, Ras Al Khaimah Emirate, United Arab Emirates. *Hydrogeology journal*, *15*(8), 1553-1563.
- Rogers, J. J. W., & Adams, J. A. S. (1969). Uranium, Handbook of Geochemistry. *KH Wedepohl, Springer, Berlin II/3, Section, 92.*

- Roselli, C., Desideri, D., & Meli, M. A. (2009). Radiological characterization of phosphate fertilizers: comparison between alpha and gamma spectrometry. *Microchemical Journal*, 91(2), 181-186.
- Samaropoulos, I., Efstathiou, M., Pashalidis, I., & Ioannidou, A. (2012). Determination of uranium concentration in ground water samples of Northern Greece. In *EPJ Web of Conferences* (Vol. 24, p. 03005). EDP Sciences.
- Satake, M. (1997). *Environmental toxicology*. Discovery Publishing House.
- Shabana, E. I., & Al-Hobaib, A. S. (1999). Activity concentrations of natural radium, thorium and uranium isotopes in ground water of two different regions. *Radiochimica Acta*, 87(1-2), 41-46.
- Shahandeh, H., & Hossner, L. R. (2002). Role of soil properties in phytoaccumulation of uranium. *Water, air, and soil pollution*, 141(1-4), 165-180.
- Shtangeeva, I. (2010). Uptake of uranium and thorium by native and cultivated plants. *Journal of environmental radioactivity*, 101(6), 458-463.
- Shtangeeva, I., & Ayrault, S. (2004). Phytoextraction of thorium from soil and water media. *Water, air, and soil pollution*, 154(1-4), 19-35.
- Skeppström, K., & Olofsson, B. (2007). Uranium and radon in groundwater. *European Water*, 17(18), 51-62.
- Stellman, J. M. (Ed.). (1998). *Encyclopaedia of occupational health and safety* (Vol. 1). International Labour Organization.
- Swarzenski, P. W., McKee, B. A., & Booth, J. G. (1995). Uranium geochemistry on the Amazon shelf: chemical phase partitioning and cycling across a salinity gradient. *Geochimica et Cosmochimica Acta*, 59(1), 7-18.
- Taylor, D. M., & Taylor, S. K. (1997). Environmental uranium and human health. *Reviews on environmental health*, 12(3), 147-158.
- Templeton, D. M., Ariese, F., Cornelis, R., Danielsson, L. G., Muntau, H., van Leeuwen, H. P., & Lobinski, R. (2000). Guidelines for terms related to chemical speciation and fractionation of elements. Definitions, structural aspects, and methodological approaches (IUPAC Recommendations 2000). *Pure and Applied Chemistry*, 72(8), 1453-1470.
- Titayeva, N. A., & Titayeva, N. A. (1994). *Nuclear geochemistry*. Mir.
- Tripathi, R. M., Sahoo, S. K., Mohapatra, S., Lenka, P., Dubey, J. S., & Puranik, V. D. (2013). Study of uranium isotopic composition in groundwater and

deviation from secular equilibrium condition. *Journal of Radioanalytical and Nuclear Chemistry*, 295(2), 1195-1200.

Turhan, Ş., Özçitak, E., Taşkın, H., & Varinlioğlu, A. (2013). Determination of natural radioactivity by gross alpha and beta measurements in ground water samples. *Water research*, 47(9), 3103-3108.

Union of Concerned Scientist in the USA (UCSUSA) (2014) How Geothermal Energy Works. Retrieved from [http://www.ucsusa.org/clean\\_energy/our-energy-choices/renewable-energy/how-geothermal-energy-works.html](http://www.ucsusa.org/clean_energy/our-energy-choices/renewable-energy/how-geothermal-energy-works.html).

United Nations Scientific Committee on the Effects of Atomic Radiation UNSCEAR 2008 Report (2008). Retrieved from [www.unscear.org](http://www.unscear.org).

United States Nuclear Regulatory Commission (U.S.NRC) (2013) Uranium enrichment. Retrieved from <http://www.nrc.gov/materials/fuel-cycle-fac/ur-enrichment.html>.

US Environmental Protection Agency (EPA) (2011) Grants Reclamation Project Evaluation of Years 2000 Through 2010 Irrigation with Alluvial Ground Water.

US Environmental Protection Agency (EPA) (2013). A Citizen's Guide to Radon. Retrieved from <http://www.epa.gov/radon/pubs/citguide.html>.

US Environmental Protection Agency (EPA) and US Department of Energy (2012) <http://www.epa.gov/rpdweb00/understand/equilibrium.html>.

US Environmental Protection Agency (EPA) and US Department of Energy (2009) Radiation Protection:Fertilizer and Fertilizer Production Wastes. Retrieved from <http://www.epa.gov/rpdweb00/glossary/termuvwxyz.html#uranium> February 2, 2010.

US National Library of Medicine (2014) Radium, radioactive. Retrieved from <http://webwiser.nlm.nih.gov/>.

USGS (1999) Radium in Ground Water from Public-Water Supplies in Northern Illinois. Factsheet 137-99.

VanLoon, G. W. & Duffy, S. J. (2011). *Environmental Chemistry - a global perspective* (3rd ed.). Oxford University Press.

Veeramani, H., Alessi, D. S., Suvorova, E. I., Lezama-Pacheco, J. S., Stubbs, J. E., Sharp, J. O., ... & Bernier-Latmani, R. (2011). Products of abiotic U (VI) reduction by biogenic magnetite and vivianite. *Geochimica et Cosmochimica Acta*, 75(9), 2512-2528.

- Veeramani, H., Alessi, D., Suvorova, E., Lezama-Pacheco, J., Stubbs, J., Sharp, J., Dippon, U., Kappler, A., Bargar, J., & Bernier-Latmani, R. (2011). Products of abiotic U(VI) reduction by biogenic magnetite and vivianite. *Geochim. Cosmochim. Acta*, 75(9):2512–2528.
- Vera Tome, F., Blanco Rodriguez, M. P., & Lozano, J. C. (2003). Soil-to-plant transfer factors for natural radionuclides and stable elements in a Mediterranean area. *Journal of Environmental radioactivity*, 65(2), 161-175.
- Vonberg, D., Vanderborght, J., Cremer, N., Pütz, T., Herbst, M., & Vereecken, H. (2014). 20 years of long-term atrazine monitoring in a shallow aquifer in western Germany. *Water research*, 50, 294-306.
- Weast, R. C. (1988). CRC HANDBOOK OF CHEMISTRY AND PHYSICS, 1988-1989.
- Wetzelhuetter, C. (2013). *Groundwater in the Coastal Zones of Asia-Pacific* (Vol. 7). Springer.
- Wickleder, M. S., Fourest, B., Dorhourt, P. K. (2006). "Thorium". In Morss, Lester R.; Edelstein, Norman M.; Fuger, Jean. *The Chemistry of the Actinide and Transactinide Elements* (3rd ed.). Springer Science+Business Media. ISBN 1-4020-3555-1.
- Wolf Ruth E. (2005) What is ICP-MS and more importantly, what can it do. USGS/Central Region/Crustal Imaging & Characterization Team. [http://crustal.usgs.gov/laboratories/icpms/What\\_is\\_ICPMS.pdf](http://crustal.usgs.gov/laboratories/icpms/What_is_ICPMS.pdf).
- Wood, W. W., & Alsharhan, A. S. (Eds.). (2003). *Water Resources Perspectives: Evaluation, Management and Policy: Evaluation, Management and Policy*. Elsevier.
- World Health Organization (2011) Guidelines for Drinking-water Quality, fourth edition. WHO Library Cataloguing-in-Publication Data.
- World Meteorological Organization (2011) World Weather Information Service - Rio de Janeiro. Retrieved April 12, 2013. <http://www.worldweather.org/>.
- World Nuclear Association (2010) Geology of uranium deposits. Retrieved from <http://www.world-nuclear.org/info/Nuclear-Fuel-Cycle/Uranium-Resources/Geology-of-Uranium-Deposits/>.
- World Nuclear Association (2013) World uranium mining production. Retrieved from <http://www.world-nuclear.org/info/Nuclear-Fuel-Cycle/Mining-of-Uranium/World-Uranium-Mining-Production/>. 2014-02-09



- World Nuclear Association (2014) Uranium and depleted uranium.  
<http://www.world-nuclear.org/info/Nuclear-Fuel-Cycle/Uranium-Resources/Uranium-and-Depleted-Uranium/>.
- [www.holiday-weather.com/tunis/averages](http://www.holiday-weather.com/tunis/averages), retrieved 2014-01-30.
- Zapeczka, O. S., & Szabo, Z. (1988). Natural radioactivity in ground water--a review. *Geological survey-water supply paper*, 1988.
- Zhongbo Yu, Yuyu Lin, Karen Johannesson, Amy J. Smiecinski, Klaus J. Stetzenbach (2007) Geochemical modeling of solubility and speciation of uranium, neptunium, and plutonium. University of Nevada, Las Vegas. Available at: [http://digitalscholarship.unlv.edu/yucca\\_mtn\\_pubs/66](http://digitalscholarship.unlv.edu/yucca_mtn_pubs/66).
- Zielinski, J. M. & Jiang, H. (2007) World Radon map by continent. Samuel McLaughlin Centre for Population Health Risk Assessment, Institute of population health. Retrieved in 2014-02-19 from [http://www.mclaughlincentre.ca/research/map\\_radon/Index.htm](http://www.mclaughlincentre.ca/research/map_radon/Index.htm).
- Zorer, Ö. S., Şahan, T., Ceylan, H., Doğru, M., & Şahin, S. (2013). 238U and 222Rn activity concentrations and total radioactivity levels in lake waters. *Journal of Radioanalytical and Nuclear Chemistry*, 295(3), 1837-1843.

## 7 APPENDICES

### Appendix-A

Published papers:

- I. Alshamsi, D. M., Murad, A. A., Aldahan, A., & Hou, X. (2013). Uranium isotopes in carbonate aquifers of arid region setting. *Journal of Radioanalytical and Nuclear Chemistry*, 298(3), 1899-1905.
- II. Murad, A., Alshamsi, D., Hou, X. L., Al Shidi, F., Al Kendi, R., & Aldahan, A. (2014). Radioactivity in groundwater along the borders of Oman and UAE. *Journal of Radioanalytical and Nuclear Chemistry*, 299(3), 1653-1660.
- III. Murad, A., Zhou, X. D., Yi, P., Alshamsi, D., Aldahan, A., Hou, X. L., & Yu, Z. B. (2014). Natural radioactivity in groundwater from the south-eastern Arabian Peninsula and environmental implications. *Environmental Monitoring and Assessment*, 1-11.

## Appendix-B

### Unrotated Factor Loadings and Communalities

Variable	Factor1	Factor2	Communality
TDS in water	0.834	-0.551	1.000
U in water	0.983	0.181	1.000
U in rocks	-0.309	0.000	0.096
Variance	1.7590	0.3367	2.0957
% Var	0.586	0.112	0.699

### Rotated Factor Loadings and Communalities

#### Varimax Rotation

Variable	Factor1	Factor2	Communality
TDS in water	0.415	-0.910	1.000
U in water	0.930	-0.369	1.000
U in rocks	-0.262	0.164	0.096
Variance	1.1048	0.9909	2.0957
% Var	0.368	0.330	0.699

### Factor Score Coefficients

Variable	Factor1	Factor2
TDS in water	-0.532	-1.341
U in water	1.313	0.598
U in rocks	0.000	-0.000

## Appendix-C

### Unrotated Factor Loadings and Communalities

Variable	Factor1	Factor2	Communality
235U	0.985	0.174	1.000
238U	0.984	0.178	1.000
TDS	0.785	-0.102	0.627
Cl	0.863	-0.000	0.746
Variance	3.3002	0.0720	3.3722
% Var	0.825	0.018	0.843

### Rotated Factor Loadings and Communalities Varimax Rotation

Variable	Factor1	Factor2	Communality
235U	0.799	0.601	1.000
238U	0.802	0.598	1.000
TDS	0.462	0.643	0.627
Cl	0.590	0.631	0.746
Variance	1.8428	1.5293	3.3722
% Var	0.461	0.382	0.843

### Sorted Rotated Factor Loadings and Communalities

Variable	Factor1	Factor2	Communality
238U	0.802	0.598	1.000
235U	0.799	0.601	1.000
TDS	0.462	0.643	0.627
Cl	0.590	0.631	0.746
Variance	1.8428	1.5293	3.3722
% Var	0.461	0.382	0.843

### Factor Score Coefficients

Variable	Factor1	Factor2
235U	-147.318	197.644
238U	148.118	-197.045
TDS	-0.000	0.000
Cl	-0.000	0.000